ARSENIC REMOVAL AND STABILIZATION BY SYNTHESIZED PYRITE

A Dissertation

by

JIN KUN SONG

Submitted to the Office of Graduate Studies of
Texas A&M University
in partial fulfillment of the requirements for the degree of

DOCTOR OF PHILOSOPHY

December 2008

Major Subject: Civil Engineering

ARSENIC REMOVAL AND STABILIZATION BY SYNTHESIZED PYRITE

A Dissertation

by

JIN KUN SONG

Submitted to the Office of Graduate Studies of
Texas A&M University
in partial fulfillment of the requirements for the degree of

DOCTOR OF PHILOSOPHY

Approved by:

Chair of Committee,	Bill Batchelor
Committee Members,	Robin Autenrieth
	Richard Loeppert
	Bruce Herbert
Head of Department,	David Rosowsky

December 2008

Major Subject: Civil Engineering

ABSTRACT

Arsenic Removal and Stabilization by Synthesized Pyrite. (December 2008)

Jin Kun Song, B.S., Soongsil University;

M.E., University of Florida

Chair of Advisory Committee: Dr. Bill Batchelor

Arsenic is ubiquitous whether it is naturally occurring or produced by humans. It is found at sites on the National Priority List and at sites operated by DOE, where it is the second most commonly found contaminant. More wastes containing arsenic will be produced due to the lowering of the Maximum Contaminant Level (MCL) for arsenic in drinking water which will result in more treatment facilities for arsenic removal that will generate residuals. Furthermore, arsenic can be released from such wastes under the reduced conditions that are found in landfills. Pyrite (FeS_2) is believed to be a compound that has a high affinity for arsenic and is stable under anoxic conditions.

The first task of this research was to develop a method for making pyrite crystals of defined size with minimal reaction time and at high yield. Effects on the synthesis of pyrite particles of pH, the ratio of Fe/S, temperature and reaction time were investigated in batch reactor systems. Pyrite was synthesized within 24 hours at pH values ranging from pH 3.6 through pH 5.6, and at a ratio of Fe/S of 0.5. X-ray diffraction and scanning electron microscopy were used to size and characterize the pyrite particles. Experimental and analytical procedures developed for this work, included a hydride generation atomic absorption spectrometry method for measuring arsenic species (As(III), As(V)). The synthesized pyrite was applied to remove arsenic and its maximum capacity for arsenic

removal was measured in batch adsorption experiments to be 3.23 μmol/g for As(III) and 113 μmol/g for As(V). Information obtained on the characteristics of chemical species before and after the reaction with arsenic showed that iron and sulfur were oxidized. Last, how strongly arsenic was bound to pyrite was investigated and it was determined that release of arsenic from As(III)-pyrite is not affected by pH, but release from As(V)-pyrite is affected by pH with minimum release in the range pH 5 to pH 8.

DEDICATION

To my wife, Jihye Han, my daughter June, and my son John
for their love and patience
To my parents and parents-in-law, for always being there and having faith in me

ACKNOWLEDGEMENTS

I would like to thank Dr. Bill Batchelor, whose immeasurable support and advice enabled me to complete this study. His scientific and personal advice and encouragement have carried me through difficult times, and his tremendous efforts to guide me and insightful advice have made all my research possible. I have enjoyed working with him very much. Having him as my advisor is a very significant turning point in my science career and life.

Special thanks are extended to the rest of the members of my dissertation committee, Dr. Robin Autenrieth, Dr. Richard Loeppert, and Dr. Bruce Herbert, who have made significant contributions to my professional experience during my graduate study. Their comments and encouragement are greatly appreciated. I would like to thank Dr. Mike Pendleton in the Department of Biology and Yulia Vasilyeva in the Department of Chemical Engineering for their technical support in this project.

I would like to extend sincere gratitude to all of Dr. Batchelor's group members for their collaboration. Specially, I want to give very special thanks to Mr. Dongsuk (Shane) Han, Sunghyuk Park, Eunjung Kim, Bhanu Vellanki, Sanjay Tewari, and Adi Desai for their opinion in projects as well as friendships.

Lastly, I would like to thank my parents and parents-in-law for their love, support, encouragement, and prayer. Most of all, I am deeply indebted to my wife, Jihye Han, who tolerated and advised me through the years of my doctoral study. I deeply appreciate her patience, love, and prayer. Above all, I greatly thank my God for giving me all these opportunities and precious people in Aggieland.

TABLE OF CONTENTS

Page

CHAPTER Page

LIST OF TABLES

Page

LIST OF FIGURES

Page

Page

CHAPTER I

INTRODUCTION

1.1 PROBLEM STATEMENT

It is a fact that a children's playground has been closed and that groundwater cannot be consumed, because they have been found to be contaminated by arsenic. Arsenic has been a long lasting problem throughout human history. Arsenic is a poisonous metalloid and the twentieth most abundant element in the earth's crust (Mandal and Suzuki 2002). Elemental arsenic occurs naturally, but it is usually found in combination with other elements, such as oxygen, chlorine, and sulfur. It is found naturally in the earth's crust, soil, sediment, and many kinds of rock. Also, it may be transferred to water, groundwater, and air. The incidence of groundwater contamination in India and West Bengal was one example of contamination by naturally occurring arsenic. In addition to naturally occurring sources, arsenic can be released during its use in various commercial products such as wood preservatives, pesticides, insecticides, pigments, and semiconductor materials that are used in integrated circuits (Jones 2007). The closure of a children's playground due to leaching of arsenic from wood preservatives is one example of the environmental threat that results from anthropogenic arsenic use. Whether it is naturally occurring or produced by humans, arsenic is ubiquitous.

This dissertation follows the style of *Journal of Environmental Engineering.*

Since it is the second most common contaminant of concern at sites on the National Priority List (EPA 2002) and at sites under control of DOE (Riley et al. 1992), there is no doubt that arsenic is one of the most common inorganic environmental contaminants. Also, arsenic is ranked number one on the ATSDR/EPA priority list of hazardous substances (Chou and De Rosa 2003).

The concern about arsenic treatment is a bigger issue than ever for many municipalities, schools, and businesses, because the lower Maximum Contaminant Level (MCL) for arsenic in drinking water of 0.010 mg/L is now being enforced (EPA 2001). As a result, millions of tons of arsenic-bearing waste residuals from the drinking water treatment plants are being created. Several techniques for removing arsenic from water are available; including adsorption with activated carbon, ion exchange, precipitation (or adsorption) by iron and aluminum oxy-hydroxides, reverse osmosis, and ultra-filtration. Generally, the method of precipitation by metal oxy-hydroxides is most effective for small quantities of highly concentrated arsenic wastes (Leist and Caridi 2000). That method produces waste residuals in the form of iron oxy-hydroxides sludges that are contaminated by arsenic. Although arsenic is bound to the iron oxy-hydroxides under oxidizing conditions, the possibility exists that arsenic will be released under reducing conditions such as found in landfills (Delemos et al. 2006). Many researchers (Meng et al. 2001; Blakey 1984; Hounslow 1980; Ahmann et al. 1997) have reported that the ferric iron contained in oxy-hydroxide solids can be reduced to soluble ferrous iron under reducing conditions, which releases arsenic.

To help prevent arsenic release under reducing conditions, compounds that have a high affinity for arsenic and are stable for geological time periods should be identified for

use in treating water or soils contaminated by arsenic. Pyrite (FeS_2) is such a compound and it is suitable under reducing conditions. A major advantage of pyrite-based removal technologies is that the residuals would be sorbed arsenic, arsenian pyrite, arsenopyrite, or some arsenic sulfide solid phase, all of which are stable in anoxic landfill environments. Another advantage of pyrite-based removal technologies is that they would not require that As(III) be oxidized to As(V) in order to improve removal (EPA 2000; EPA 2002).

In this study, an analytical method for measuring arsenic species was developed. Pyrite was synthesized and applied for arsenic removal. Arsenic removal capacity by synthesized pyrite and its stability as an arsenic-pyrite solid after use in treatment was estimated.

1.2 OBJECTIVES

1. To characterize and optimize the synthesis procedure for pyrite.
2. To develop required experimental and analytical procedures.
3. To characterize removal of arsenic by synthesized pyrite.
4. To measure the stability of arsenic-pyrite solids.

1.3 RESEARCH APPROACH

To characterize and optimize a procedure to synthesize pyrite (FeS_2), the ratio of Fe/S, temperature, pH, and reaction time were investigated. Additional product except pyrite was produced, so purification of pyrite was involved. Then, synthesized and purified pyrite was verified by the technique of SEM and XRD. To develop experimental and analytical methods, a differential-pH hydride generation procedure followed by AAS

analysis was applied for arsenic species measurement. The ferrozine method using UV-spectrophotometry was applied for iron measurement (Gibbs 1976). Also, comparisons were made among known chemical equilibrium models for arsenic-pyrite system, which included the Langmuir, Freundlich, and BET isotherm models.

To characterize arsenic removal by synthesized pyrite, experimental variables, including pH, arsenic concentration, arsenic type (III, V), and contact time, were investigated under anaerobic condition. To measure the stability of residuals from pyrite-treated water, leaching experiments were conducted to evaluate the effects of arsenic type (III, V), and pH on arsenic release.

1.4 DISSERTATION ORGANIZATION

Chapter II of this dissertation presents a literature review that includes background information on properties and toxicity of arsenic, treatment methods for its removal from water, theory of arsenic adsorption, characteristics of its release from the treated wastes, and analytical method for its analysis, including Hydride Generation Atomic Absorption Spectroscopy (HGAAS), Scanning Electron Microscope (SEM), X-Ray Diffraction (XRD), and X-ray Photoelectron Spectroscopy (XPS). Information is also included on the properties of pyrite. Chapter III presents the methodology for producing and purifying pyrite, for measuring arsenic and iron, and for applying other analytical methods such as SEM, XRD, and XPS. Chapter IV presents the optimum variables for pyrite synthesis including Fe/S ratio, temperature, pH, and reaction time. Chapters V and VI present results of experiments on the capacity of synthesized pyrite to remove arsenic and the stability of arsenic-pyrite solids, respectively, and the last chapter concludes and summarizes the entire study.

CHAPTER II

BACKGROUND

2.1 THE PROPERTIES OF ARSENIC

Arsenic (As) is a metallic chemical element with a molecular weight of 74.9 and an atomic number of 33. Earth's crust is the source of arsenic, and it exists as various minerals including arsenopyrite (FeAsS), orpiment (As_2S_3), realgar (AsS), and loellingite ($FeAs_2$). Arsenic is found both in organic and inorganic forms. Organic arsenic compounds include CH_5AsO_3 (monomethylarsonic acid, MMA), $C_2H_7AsO_2$ (dimethylarsinic acid, DMA), while inorganic arsenic compounds include H_3AsO_3 (arsenous acid) and H_3AsO_4 (arsenic acid). These acids can release hydrogen ions and form a number of anionic forms of inorganic arsenic. Arsenic exists in a variety of oxidations states, such as As(-I) in arsenopyrite (FeAsS), As(II) in realgar (As_2S_2), As(III) in arsenic trioxide (As_2O_3), and As(V) in arsenic pentoxide (As_2O_5).

The most prevalent oxidation state for inorganic arsenic species in the environment are arsenite (As(III)) and arsenate (As(V)). It is important to be able to distinguish concentrations of As(III) and As(V) because of their different properties. As(III) is a carcinogen and is more toxic than As(V). The primary forms of As(III) are uncharged below pH 9.2, because the pK_a of arsenous acid is 9.2. On the other hand, the primary forms of As(V) are anionic above pH 2.2, because the first pK_a for arsenic acid is 2.2. The second and third values of pK_a on As(V) are 7.0, and 11.4. This is why As(III) is more mobile than As(V). Typically, the primary method to remove arsenic from waters is to convert As(III) to As(V), because it is easier to remove As(V) than As(III). The dominant arsenic species at each pH are presented in Fig. 2.1 and 2.2.

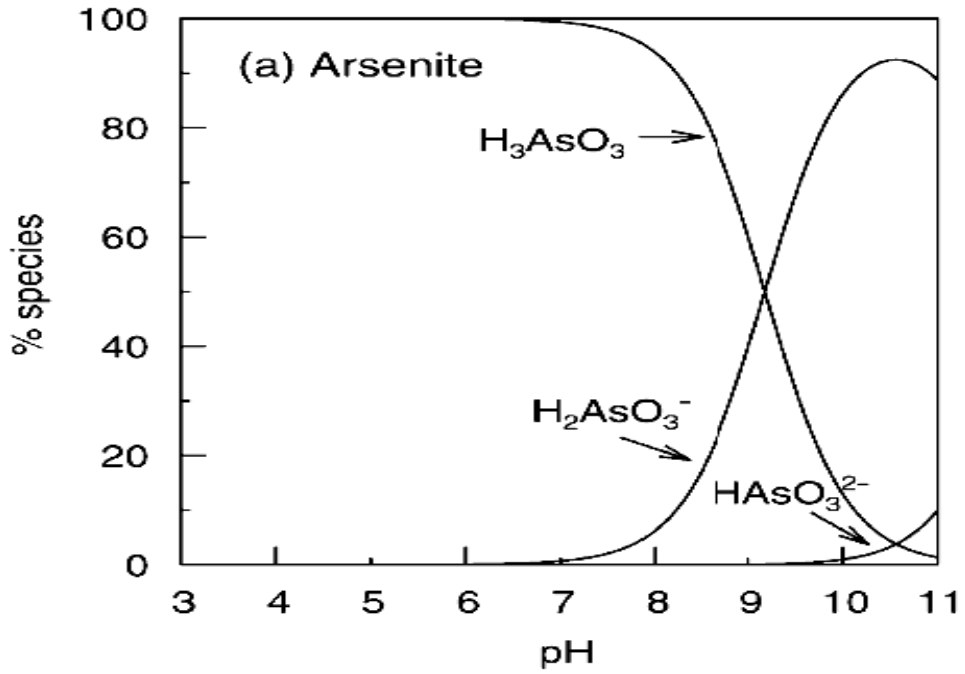

Fig. 2.1 Arsenite speciation as a function of pH

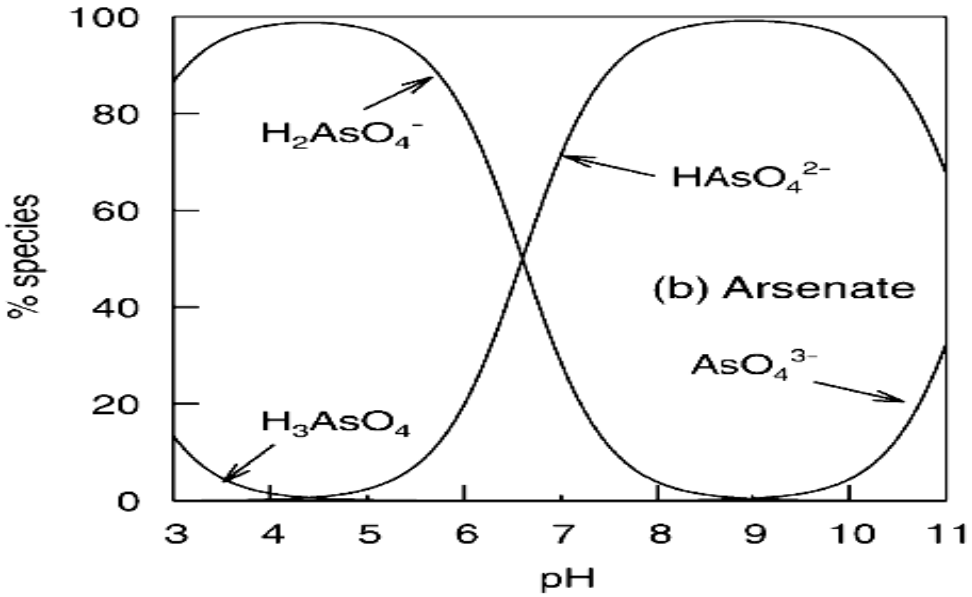

Fig. 2.2 Arsenate speciation as a function of pH (ionic strength of about 0.01M)

(Fig 2.1 and 2.2 were cited from Smedley and Kinniburgh 2002.)

The Eh-pH diagram for arsenic species is shown in Fig. 2.3. As(III) is thermodynamically stable under reduced conditions, while As(V) is prevalent under

oxidized conditions. Arsenic acid and its ionization products are of prime importance for arsenic transport under a wide range of Eh and pH.

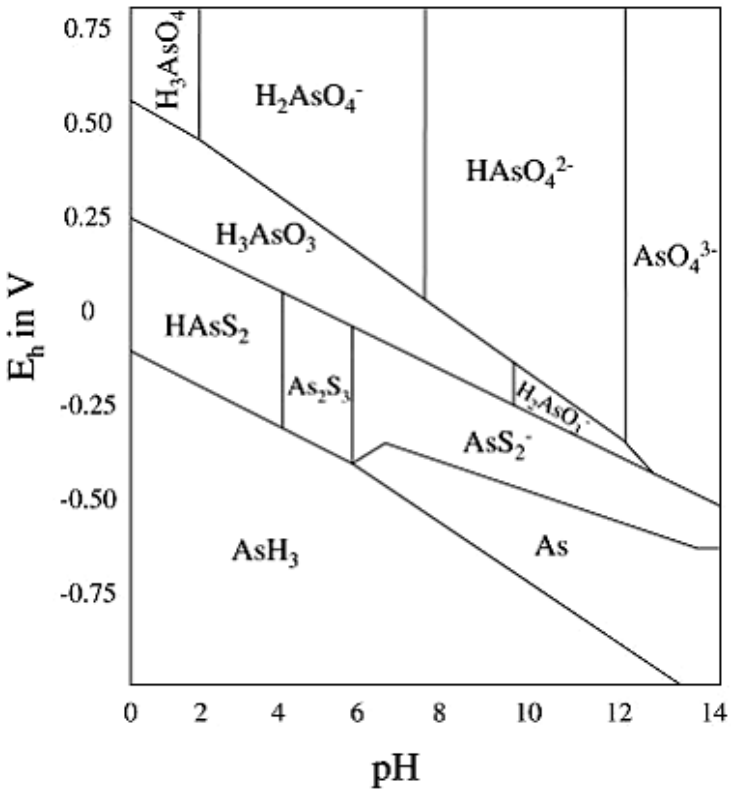

Fig. 2.3 Eh-pH diagram for As-O_2-S-H_2O system (cited from Brookins 1988)

2.2 ARSENIC TOXICITY

This section was summarized from the toxicological profile for arsenic published by the Agency for Toxic Substances and Disease Registry of the U.S. Department of Health and Human Services (ATSDR 2007). As(III) is more toxic than As(V), but both As(III) and As(V) are known human carcinogen by both the inhalation and oral routes. There are several ways for arsenic to enter our body, including through breathing, eating, or drinking the substance, or by skin contact. The degree of harmfulness of arsenic is

measured by the dose, the duration of exposure, and the nature of contact with the arsenic. The principal route of exposure to arsenic for the general population is the oral route. When consumed orally, arsenic affects virtually every organ or tissue evaluated. Oral exposure data from studies on humans showed that these lesions begin to be manifested with exposure levels of 0.002-0.02 mg As/kg/day. At these exposure levels, researchers found peripheral vascular effects, including cyanosis, gangrene, and blackfoot disease, or cardiovascular effects, including increased incidences of high blood pressure and circulatory problems. In addition to dermal, cardiovascular, and respiratory effects, oral exposure to arsenic may result in nausea, vomiting, and diarrhea. Acute, high doses of arsenic can cause confusion, hallucinations, impaired memory, and emotional lability.

The risks of lung cancer, respiratory irritation, nausea, skin effects, and neurological effects have been reported for people exposed to arsenic by inhalation. The inhalation unit cancer risk is calculated to be 0.0043 $(\mu g/m^3)^{-1}$. For dermal contact with arsenic, it is reported that the chief effect is local irritation and dermatitis, including hyperkeratinization of the skin, especially on the palms and soles.

2.3 ARSENIC TREATMENT

Several technologies are used for the treatment of arsenic in water, including precipitation/coprecipitation, membrane filtration, adsorption, ion exchange, and permeable reactive barriers. Other technologies are under investigation including iron oxide coated sand, nanofiltration, iron filings, sulfur-modified iron, and granular ferric hydroxide (EPA 2000).

Precipitation/coprecipitation has been the most frequently used method for the treatment of arsenic in groundwater, surface water, leachate, mine drainage, drinking

water, and wastewater (EPA 2002). Precipitation refers to the process of forming a solid phase that contains the contaminant by exceeding the solubility product of the solid phase, while coprecipitation is the process of incorporating a soluble contaminant into a growing solid phase via inclusion, occlusion, or adsorption (Edwards 1994). This method uses chemicals that are called a coagulant, such as ferric salts and alum to transform dissolved contaminants into an insoluble solid. Then the solid is removed from the liquid phase by clarification or filtration (EPA 2002). This method usually involves pH adjustment, and addition of a chemical oxidant along with addition of the chemical precipitant or coagulant. Fig. 2.4. presents the model of a precipitation/coprecipitation system to remove arsenic from water.

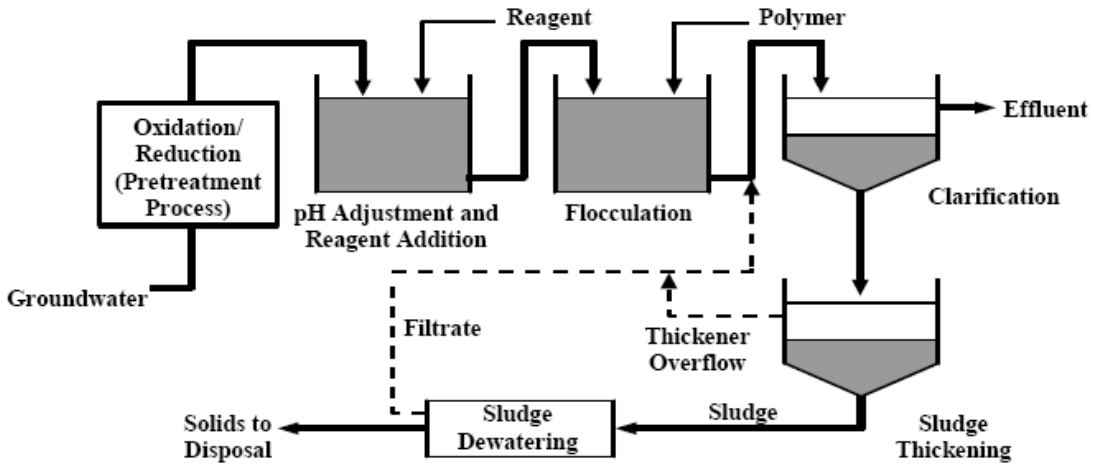

Fig. 2.4 Model of a precipitation/coprecipitation system (cited from EPA 2002)

The addition of oxidant, such as bleaching powder, permanganate, δ-MnO_2, ozone, hydrogen peroxide, or chlorine, is required prior to applying a process for arsenic removal, because As(V) is removed more efficiently than As(III). Based on bench- and pilot-tests, Cheng and et al. (1994) concluded that $FeCl_3$ is much more effective in

removing arsenic than alum, when compared on an equal-weight dosage basis. Also, Edwards (1994) compared ferric iron and alum, and found that ferric iron is more effective than alum when solution pH is greater than 7.5. A similar conclusion was reached by Hering et al., 1997, who reported that arsenic removal was adversely affected by the presence of sulfate and natural organic matter.

Membrane filtration is a pressure-driven process that separates contaminants by physical sieving or chemical diffusion across a permeable membrane. Filtration, electric repulsion, and adsorption of arsenic-contained compounds are important in determining removal. This method is used less frequently than the other techniques, because of its high cost and production of large volumes of wastewater.

Adsorption is defined as the formation of surface complexes between soluble arsenic and solid oxyhydroxide surface sites (Edwards 1994). Adsorption treatment is applying adsorption media that usually are packed into a column to adsorb contaminants as they pass through the column. Activated alumina, activated carbon, granular ferric hydroxide (Driehaus et al. 1998), iron oxide coated sand, natural materials such as zeolites (Elizalde-Gonzalez et al. 2001), and greensand are used as adsorption media for arsenic. This method is used less frequently than precipitation/coprecipitation and is most commonly used for arsenic treatment in groundwater and drinking water.

The ion exchange method is employed with resins that usually are packed into a column. Contaminant ions are removed and replaced by ions released by the exchange medium.

Permeable reactive barriers (PRBs) are being used for *in situ* treatment of groundwater. PRBs are walls containing reactive media that are installed across the path of a contaminated groundwater as shown in Fig. 2.5.

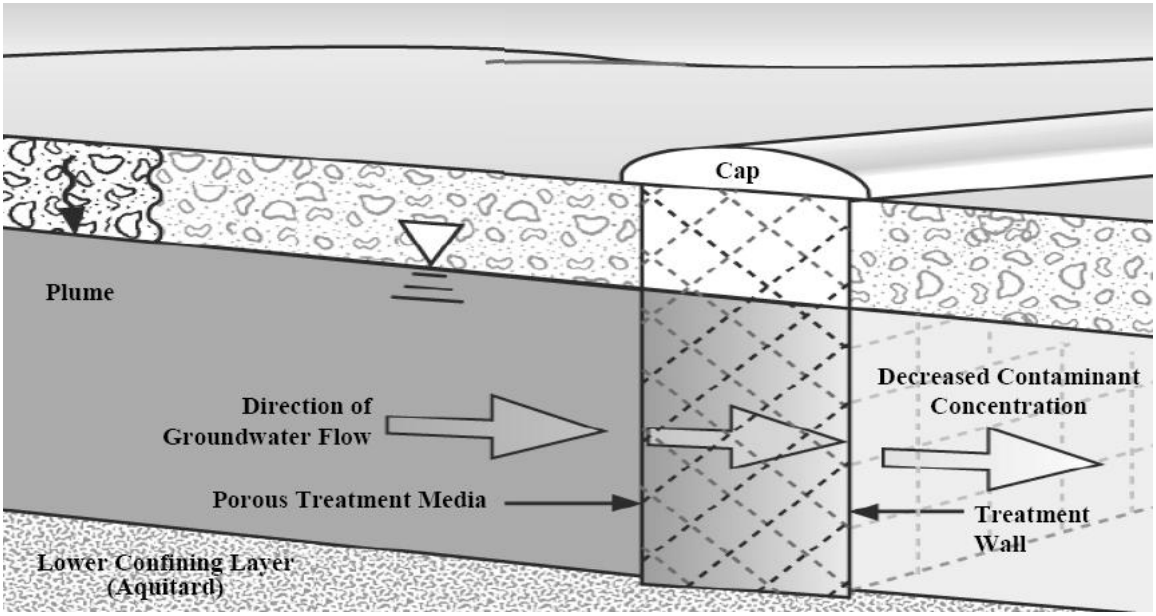

Fig. 2.5 Model of a permeable reactive barrier system (cited from EPA. 2002)

In summary, many arsenic treatment technologies are available, but none of them has been found to be a perfect solution. Selection of the most appropriate treatment technology will depend on water quality, other constituents in the water, initial arsenic concentration, arsenic species, treatment objectives, treatment system capacity, and residuals handling cost. Thus, treatment plants should attempt to meet the new standard by optimizing existing techniques or advanced new treatment methods.

2.4 ARSENIC RELEASE FROM TREATED WASTES

Arsenic can be released from solid phases by three principal mechanisms. Arsenic can be desorbed under alkaline conditions, it can be released and replaced by a

competitive ion such as phosphate, and it can be released by being reduced from As(V) to As(III) during dissolution of iron oxides (Delemos et al. 2006). Last mechanism can be divided into two parts: reduction of iron oxy-hydroxide to iron (II) and reduction of As(V) to As(III).

Arsenic is released not only in groundwater systems, such as occurred in Bangladesh and West Bengal, but also from arsenic-contaminated wastes or minerals. Iron oxy-hydroxide can release arsenic when affected by microbial activity, anoxic subsurface environments (Bose and Sharma 2002) or high pH (Jain 1999). Caronell-Barrachina and et al. (1999) reported that arsenic sulfide minerals were probably formed in the presence of high levels of sulfide under highly reducing conditions (-250 mV). No significant arsenic release was found from the arsenic sulfide while highly reducing conditions were maintained. Arsenic was released from the pyrite mine waste under moderately reducing conditions (0-100 mV), because of dissolution of iron oxy-hydroxides. Blakley (1984) reported that wastes can release arsenic under mildly reducing conditions in the pH range of 5 to 9.

Ghosh and et al. (2006 a) conducted column tests to simulate the landfill conditions with arsenic-bearing solid residuals, such as granular ferric hydroxide, compost, paper, and sludge. They detected greater arsenic release with a lower liquid to solid ratio, under anaerobic conditions, and with the use of a citric acid buffer solution (Jing et al. 2005).

Delemos and et al. (2006) investigated the relationship between arsenic release over long periods of time and the presence of organic contaminants at superfund sites

with contaminated landfills. They found that arsenic might be released under reducing environments with organic contaminant plumes.

Many researchers have assumed that a high concentration of dissolved organic carbon in landfills allows microorganisms to produce moderately reducing conditions resulting in reduction of As(V) to As(III). Furthermore, iron (oxy)hydroxides that may stabilize arsenic can suffer reductive dissolution, which releases more arsenic.

2.5 THEORY OF ARSENIC ADSORPTION

Adsorption is one of the most important chemical processes that remove arsenic from water. Other removal processes include precipitation and polymerization. Precipitation involves an increase in volume of a mineral as the result of a three-dimensional growth of the mineral's structure, while polymerization is the formation of small, soluble, multinuclear inorganic species.

Physical and chemical forces are involved in adsorption of arsenic onto the surface of minerals. Examples of physical and chemical forces involved in adsorption are electrostatic coulombic interactions and inner-sphere complexation, respectively. When a surface functional group on the surface of the mineral interacts with an ion or molecule in solution, they can produce a surface complex. Surface functional groups are identified as chemically reactive molecular units that are bound into the structure of a solid at its surface. Carboxyl, carbonyl, and phenolic molecular units are examples of important surface functional groups.

There are two types of surface complexes: outer-sphere and inner-sphere complexes. The difference between them is whether a water molecule is present between the surface functional group and the bound molecule. Outer-sphere complexes contain a

water molecule between the surface functional group and the bound molecule, while inner-sphere complexes do not contain a water molecule between them. Outer-sphere complexes involve electrostatic coulombic interactions, which leads to generally weak binding compared to inner-sphere complexes, because ionic binding is used. Outer-sphere complexes form rapidly, are reversible and are affected by the ionic strength of the aqueous phase, while inner-sphere complexes are generally irreversible and weakly affected by the ionic strength of the aqueous phase.

There are two basic types of charge that can develop on mineral surfaces: permanent and pH dependent. The permanent charge on a mineral can not be changed once the mineral is formed. Permanent charge results from the process of isomorphic substitution. Isomorphic substitution occurs when an element substitutes in the mineral structure, resulting in a net charge. For example, when Al^{3+} substitutes for Si^{4+} in the tetrahedral layer a negative charge will result. When Fe^{3+} substitutes for Mg^{2+} in the octahedral layer, a positive charge results. The pH dependent charge results from the combined influence of the mineral surface and the environment in which the mineral resides. Protonation and deprotonation of surface hydroxyl groups decide the charge of the mineral surface, so H^+ is the leading potential determining ion (pdi) in the aqueous phase. The following equations show how the pdi changes surface charge.

$$S\text{-}OH + H^+ \leftrightarrow S\text{-}OH_2^+ \quad \text{(equation 2.1)}$$

$$S\text{-}OH \leftrightarrow S\text{-}O^- + H^+ \quad \text{(equation 2.2)}$$

Many researchers have applied many kinds of materials as adsorbents to remove arsenic. Examples include activated carbon (Chen et al. 2007, Chuang et al. 2005), iron oxides and hydroxide (Deschamps et al 2005, Jessen et al. 2005, Goldberg 2002, Jain and

Loeppert 2000, Jain et al. 1999, Raven et al. 1998, Wilkie and Hering 1996) such as goethite (Ladeira et al. 2004, Grafe et al. 2001, Manning et al 1998), aluminum (hydr)oxide (Jeong et al. 2007, Beaulieu and Savage 2005) such as gibbsite (Liu et al. 2006, Ladeira et al. 2004), zeolite, kaolinite (Goldberg 2002), and zerovalent iron (Yu et al. 2006, Yuan and Lien 2006, Kanel et al. 2006, Kober et al. 2005, Manning et al 2002). Mohan and Pittman (2007) summarize the adsorbents that have been utilized for arsenic removal and include experimental conditions, surface areas, and adsorption capacities (Attached in Appendix B).

Arai et al. (2000) investigated As(III) and As(V) adsorption complexes at the aluminum oxide/water interface as a function of pH and ionic strength using spectroscopic studies. These studies suggested that As(III) forms both inner and outer-sphere complexes above pH 5.5, whereas As(V) predominantly forms inner-sphere bidentate binuclear complexes regardless of pH and ionic strength.

Also, Goldberg and Johnston (2001) investigated As(III) and As(V) adsorption on amorphous aluminum and iron oxides as a function of pH, solution ionic strength, redox state using spectroscopic methods. They found that As(III) forms both inner- and outer-sphere surface complexes on amorphous Fe oxide and outer-sphere surface complexes on amorphous Al oxide, whereas As(V) forms inner-sphere surface complexes on both amorphous Al and Fe oxide.

Waychunas et al. (1993) concluded that As(V) forms inner-sphere complexes when contacting surfaces of ferrihydrite and crystalline FeOOH polymorphs. Manning et al. (1998) determined that As(III) forms inner-sphere complexes on the surface of goethite. As(V) forms monodentate-mononuclear or bidentate-binuclear surface

complexes, as do phosphate, borate, selenite, chromate, molybdate, carbonate, and silicate (Essington, 2004).

Dixit and Hering (2003) found that As(V) sorption on amorphous iron oxide and goethite decreased with increasing pH with the highest sorption observed at pH 4. Similar results were drawn by Manning et al. (1998) for As(V) adsorption by goethite. Bowell (1994) also found that the sorption of As(V) is greater in the pH range between 4-8 when contacted with goethite, lepidocrocite, and hematite.

As(III) sorption on HFO, goethite, and magnetite showed a weaker effect of pH on sorption over the range from pH 4 to pH 10, compared with that of As(V) (Dixit and Hering 2003, Manning et al. 1998). In addition, As(III) sorption on HFO and goethite is more favorable at higher pH (7-9) and As(V) sorption is more favorable at lower pH ranges (4-6). Generally, As(III) sorption increased with increasing pH.

Only a few of researchers have studied iron sulfides, such as mackinawite (Gallegos et al. 2007, Wolthers et al. 2007, Wolthers et al. 2005, Farquhar et al. 2002) or pyrite (Zouboulis et al. 1993, Bostic and Fendorf 2003), as arsenic removing adsorbents. Zouboulis et al. (1993) used pyrite, obtained from one of chemical producing companies in Greece, as an adsorbent because its low price offered an economic benefit. They found that optimum pH values for removing As(III) were basic (pH 7-10) and were circumneutral pH (pH 3-9) for As(V). Also, more As(V) was removed than As(III) by the same amount of pyrite. Bostick and Fendorf (2003) conducted experiments with As(III) and FeS or As(III) and FeS_2 using macroscopic and spectroscopic technique. The iron sulfides were obtained from chemical producing companies. Since macroscopic data, such as adsorption isotherm data, can not explain the mechanisms that operate between

an adsorbent and an adsorbate, spectroscopic techniques were applied. X-ray absorption spectroscopy (XAS) and X-ray photoelectron spectroscopy (XPS) were examples of spectroscopic techniques used to identify the structure and oxidation state of sorbed arsenic. As(III) and FeS was observed to follow the Langmuir isotherm at low arsenic concentration, while surface precipitation occurred with elevated arsenic concentration. Whereas, As(III) and FeS_2 was observed to follow the Langmuir isotherm over the experimental condition. Surface precipitation was verified using the technique of XAS. As(III) was not removed effectively at lower pH with FeS or FeS_2, which is in contrast with behavior of most (hydr)oxide minerals. However, it is agreed with the result conducted by Zouboulis et al., 1993, that higher pHs are more suitable for removing As(III) using FeS_2. Reduction of arsenic and oxidation of both surface S and Fe(II) were shown by XAS. Also, a mineral was formed when As(III) and FeS/FeS_2 were reacted that appeared to be similar to FeAsS or As_2S_3.

2.6 THE PROPERTIES OF PYRITE

Pyrite (FeS_2) consists of one molecule of iron and two molecules of sulfur. It is used as an adsorbent removing toxic contaminants such as arsenic (Zouboulis et al. 1993; Han and Fyfe 2000; and Bostic and Fendorf 2003), cadmium (Borah and Senapati 2006), hexavalent chromium (Zouboulis et al. 1995), mercury (Ehrhardt et al. 2000; Behra et al. 2001), and molybdate (Bostic et al. 2003). There are several ways to synthesis pyrite using difference sources of iron and sulfur. Some researchers used amorphous FeS and H_2S as iron and sulfur sources, respectively (Wilkin and Barnes 1996, Butler and Rickard 2000). Various iron sources including FeOOH, $FeSO_4$, Fe_3S_4, and $FeCl_2$, and sulfur sources, including Na_2S_5, S(0), $S_4O_6^{2-}$and Na_2S, have been utilized to synthesize pyrite.

Also, heating to temperatures ranging from 100 to 300 °C has been applied to produce pyrite (Sunagawa et al., 1971, Luther, 1991, and Graham and Ohmoto, 1994). Wei and Osseo-Asare (1996) used $FeCl_3$-NaSH reaction for pyrite formation sizing micro- to nano- sized at room temperature.

The structure of pyrite is presented in Fig. 2.6. Iron is surrounded by six nearest-neighbor sulfur atoms in an octahedral environment, while one sulfur is bound to the other sulfur and three iron atoms. The octahedral symetry of pyrite is as same as that of sodium chloride.

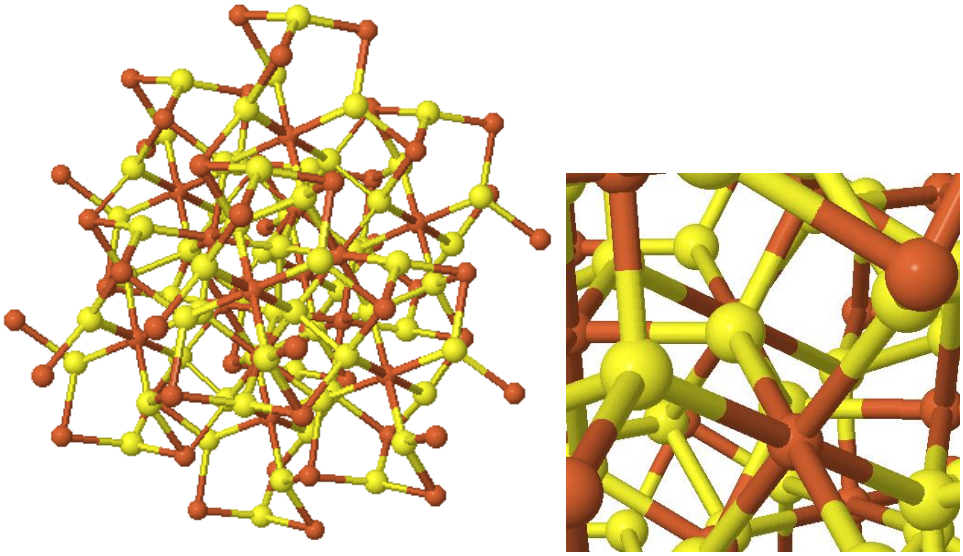

Fig. 2.6 The 3D structure of pyrite (sulfur is yellow (white in black and white), iron is brown (black in black and white))
(cited from: http://www.3dchem.com/3dmolecule.asp?ID=153)

2.7 ANALYTICAL METHOD

Several analytical techniques were used during this study, including Scanning Electron Microscopy (SEM), X-Ray Diffraction (XRD), UV/Vis spectrophotometer (UVS), Hydride Generation Atomic Absorption Spectrophotometer (HGAAS), and X-ray

Photoelectron Spectroscopy (XPS). A brief explanation on each analytical technique will be given. SEM is used to examine the surface of a sample with high resolution and to determine the particle size and shape of the sample. XRD is used to identify a crystalline phase and orientation. When an X-ray beam hits a sample and is diffracted, the distances between the planes of the atoms can be measured. The value of θ and count per second (CPS) can be drawn using Bragg's Law, which is $n\lambda = 2 d \sin\theta$. The value of *n* is the order of the diffracted beam, λ is the wavelength of the incident X-ray beam, d is the distance between adjacent planes of atoms (the d-spacing), and θ is the angle of incidence of the X-ray beam. Because the values of λ and θ can be measured, the value of d-spacing can be estimated with Bragg's Law. Each crystalline solid produces a diffractogram that contains peaks with specific position, width, and intensity. By matching the position, width, and intensity of peaks of an unknown material with information provided by JCPDS (Joint Committee on Powder Diffraction Standard), the material can be identified. XRD was used to confirm that pyrite was the material synthesized in this study.

UVS is used to measure the concentration of a compound in solution. Many molecules absorb ultraviolet or visible light. By Beer's law, the light absorbance is proportional to the path length and the concentration of the absorbing species. The concentration of iron contained in pyrite particles was measured in this study by UVS in order to estimate how much pyrite was synthesized.

HGAAS is used to measure arsenic species in solution. The technique that was used in this study was able to differentiate between As(III) and As(V) based on how pH affected formation of arsenic hydride (AsH_3) by reaction of sodium borohydride with

As(III) or As(V) (Masscheleyn et al. 1991). If the reaction occurs at low pH, both As(III) and As(V) will react to form the hydride. If the reaction occurs at moderate pH, then only As(III) will react to form the hydride. Therefore, analysis at low pH will measure total arsenic and analysis at moderate pH will measure As(III). The concentration of As(V) can be obtained by difference.

XPS is used for the chemical analysis of surfaces. A simple description of how XPS works is that it strikes a sample with x-rays that stimulate a variety of electronic processes such as photoemission of core electrons, which is the ejection of an electron from a core level by an X-ray photon of energy. The schematic of XPS and its process were presented in Fig. 2.7 and 2.8, respectively.

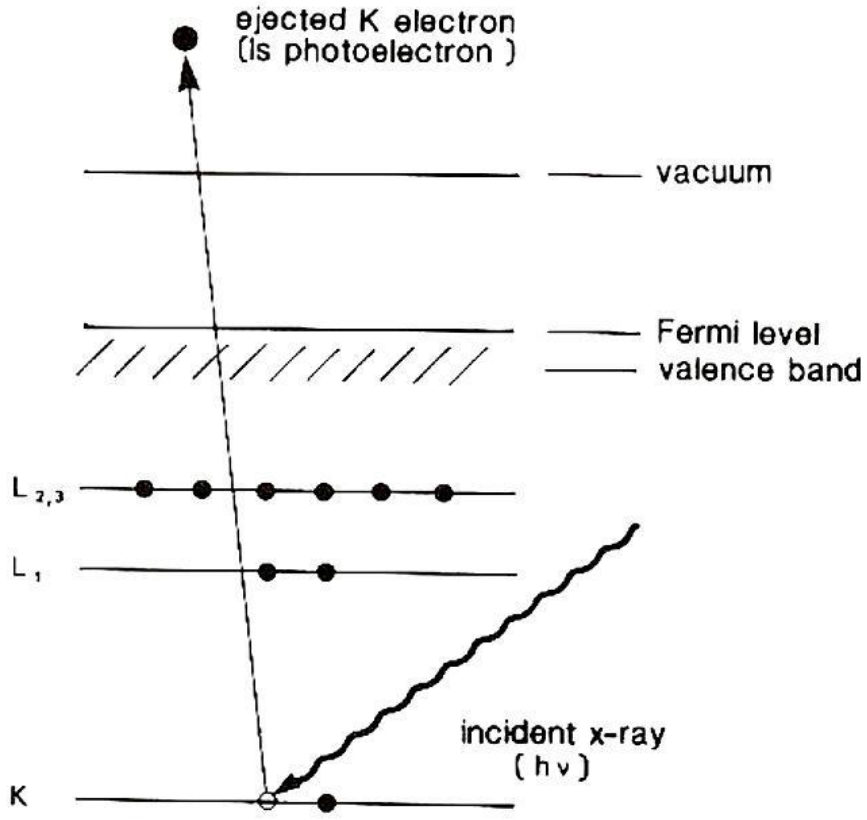

Fig. 2.7 Schematic of the XPS process, showing photoionization of an atom by the ejection of a 1s electron (cited from Watts 1990)

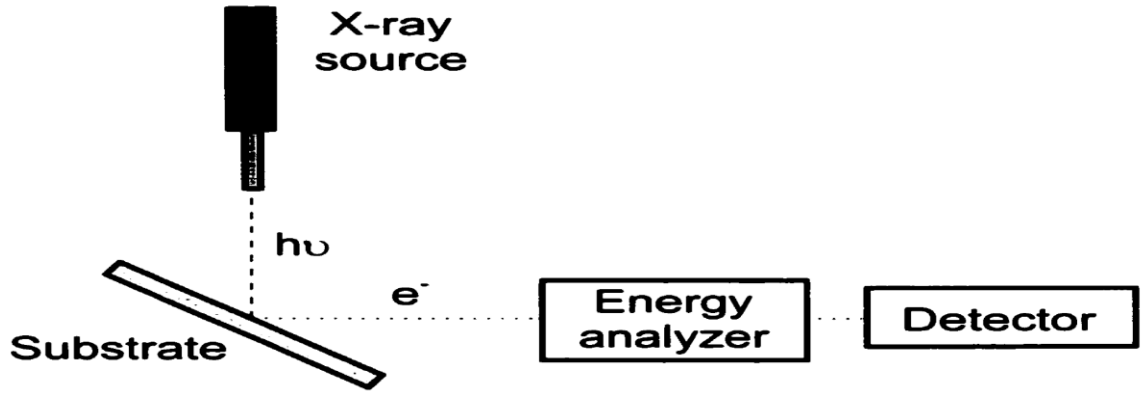

Fig. 2.8 Schematic of an x-ray photoelectron spectrometer (XPS) (cited from Baker 2002)

The emitted electrons are collected and analyzed and these data are presented as a graph of intensity versus electron energy. The kinetic energy of the emitted inner shell electrons is determined by the equation KE = hυ – BE - W (where as, hυ: photon energy, BE: Binding energy, W: the spectrometer work function, KE: the kinetic energy) (Watts 1990). The XPS technique identifies the element and its chemical state.

CHAPTER III

METHODOLOGY

3.1 SYNTHESIS AND PURIFICATION OF PYRITE

Pyrite synthesis was conducted in an anaerobic chamber. All the chemicals used in synthesizing pyrite, including $FeCl_3$, NaHS, HCl, and NaOH, were ACS certified chemicals. A 1-L volumetric flask, a 2-L volumetric flask, and a 4-L polyethylene bottle were placed in the anaerobic chamber for at least 2 hours before pyrite synthesis began, in order to prevent the presence of oxygen in the anaerobic chamber due to them. All of the aqueous media used in the synthesis was purged with nitrogen in the anaerobic chamber to remove all oxygen. More specifically, deoxygenate the aqueous media with 99.99 % grade nitrogen for 2 hours in atmosphere, and then purge it with mixed gas in an anaerobic chamber for 12 hours, which contains 95 % of nitrogen and 5 % of hydrogen.

A 2-L volume of 0.1 mol NaHS and a 1-L volume of 0.1 mol $FeCl_3$ were prepared in 1- and 2-L volumetric flasks, respectively. Each flask was added to the 4-L polyethylene bottle and mixed. This produced a solution with 6.67E-2 M of NaHS and 3.33E-2 M of $FeCl_3$. The mixture pH was adjusted to about pH 4.2 by using 0.05 M NaOH or 0.05 M HCl. After adjusting pH, the 4-L polyethylene bottle was transferred to a shaker with a heating device (Forma Scientific Inc., model 4518). The solution was mixed at 150 rpm for 24 hours at 60 ^{o}C to produce pyrite. The solids were separated by centrifugation for 15 minutes at 3210 g. The centrifuge used in this study was a Beckman model J-6 M with JS-7.5 rotor.

Iron sulfide (FeS) was another solid that was produced during pyrite synthesis, as shown by the chemical equation:

$$Fe^{3+} + 2\ HS^{-} = \frac{1}{2}\ FeS + \frac{1}{2}\ FeS_2 + 2\ H^{+} + \frac{1}{2}\ S^{2-} \quad \text{(equation 3.1)}$$

One mole of ferric iron and two moles of hydrogen sulfide make half mole of iron mono-sulfide and iron di-sulfide (pyrite), two moles of hydrogen, and half elemental sulfur. Unwanted products except pyrite should be removed or separated from the pyrite.

FeS was removed by addition of 5N HCl, which dissolved it, but did not dissolve FeS_2 (Berner, 1970). The pyrite was separated by filtration with 0.2-μm cellulose nitrate membrane filter. Elemental sulfur was removed by dissolving it with acetone and carbon disulfide (CS_4) and separating pyrite by filtration with an anodisc with pore size of 0.02 mm. The solid phase, which contained synthetic pyrite, was collected and stored in an anaerobic chamber.

3.2 ANALYTICAL PROCEDURES

3.2.1 Measurement of Arsenic

Hydride Generation Atomic Absorption Spectrometry (HGAAS) was used for the analysis of arsenic species because it is one of the most useful techniques for arsenic speciation in environmental and biological matrices (Gong et al 2002). A procedure for analyzing As(III) and As(V) was adopted that was based on the effect of pH on formation of arsenic hydride (AsH_3) by reaction of sodium borohydride with As(III) or As(V). When the reaction occurs at low pH, both As(III) and As(V) react to form the hydride. When the reaction occurs at moderate pH, only As(III) reacts to form the hydride (Aggett and Aspell 1976, Masscheleyn et al 1991). Fig. 3.1 shows experimental results that

document the effect of pH and concentration of acid on formation of the hydride from different arsenic species. Therefore, analysis at low pH will measure total arsenic and analysis at moderate pH will measure As(III). The concentration of As(V) can be obtained by difference.

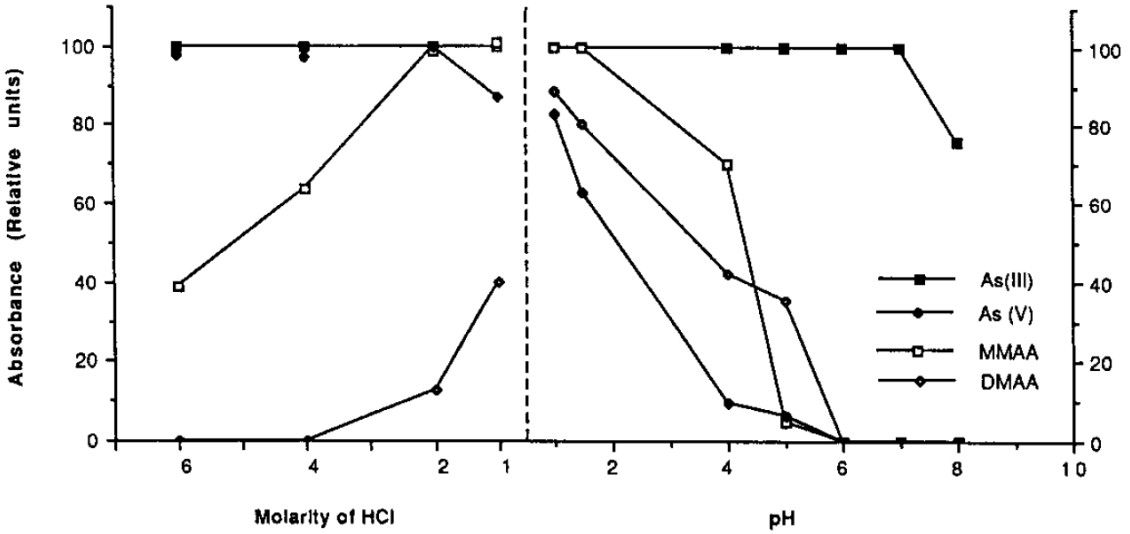

Fig. 3.1 Effect of acid concentration and pH on arsine absorption signal (50 ng/ml As solution, 4 ml of 3 % $NaBH_4$) (cited from Masscheleyn et al 1991)

This procedure, which is depicted in Fig. 3.2, is automated when using a Thermo-elemental Solar M6 Atomic Absorption Spectrophotometer and a continuous hydride generation system (Thermo Elemental model VP90).

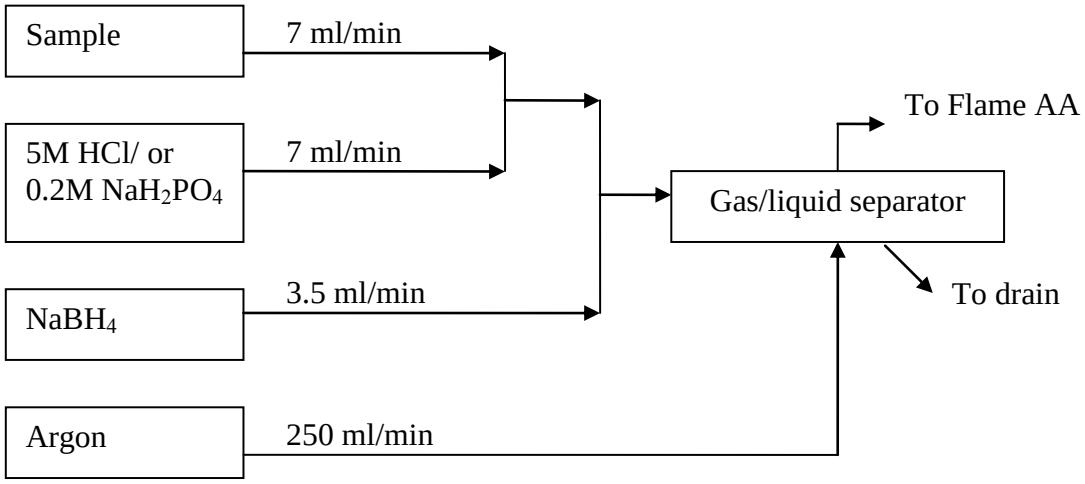

Fig. 3.2 Schematic diagram of system for arsenic analysis by hydride generation (Ref: standard method 3114C 1998)

As(III) and As(V) stock solutions were made with sodium arsenite ($AsNaO_2$) and sodium arsenate (Na_2HAsO_4), respectively. The chemicals used to produce arsenic stock solutions, including sodium arsenite and sodium arsenate, were ACS certified. Each stock solution contained 1000 ppm of arsenic and was stored in the refrigerator. The detection limit for total arsenic was found to be 0.27 ppb. The detection limit is defined as "the minimum concentration of an analyte (substance) that can be measured and reported with a 99% confidence that the analyte concentration is greater than zero" (40 CFR 136.2.f 2007). This was determined by replicate measurements of a solution with a specific concentration of arsenic. In this case, a solution of 2 ppb of arsenic was measured 11 times. The method detection limit (40 CFR 136 appendix B 2007) was calculated as the standard deviation (S=0.0985) multiplied by the value of the T test at a 99% confidence level with n=11 (T_{10}=2.764).

3.2.2 Measurement of Iron in Liquid Phase

A UV spectrophotometer (Hewlett Packard model G 1103 A) was employed to measure iron. The chemicals used in measuring iron, including standard iron (1000 ppm), ferrozine, ammonium acetate, and hydroxylamine, were ACS certified. Ferrous iron (Fe(II)) was measured by mixing an aliquot of the sample with an acid quencher solution of 0.7 M HNO_3 and then mixing with a ferrozine solution. Ferrozine solution was prepared by mixing 0.15 g of ferrozine ($C_{20}H_{14}N_4O_6S_2$) with 50 ml of a solution prepared by adding 1 drop of concentrated hydrochloric acid to 200 ml of a 10 % solution of ammonium acetate ($C_2H_7NO_2$). Since this procedure was able to measured only ferrous iron (Fe(II)), total iron (Fe(II) + Fe(III)) was measured after reducing ferric iron (Fe(III)) in the sample to ferrous iron using a solution of 10 % hydroxylamine. This procedure was used to measure how much pyrite was produced by identifying the amount of iron contained in the solids.

3.2.3 Measurement of Iron from Pyrite Solid Phase

The concentration of pyrite in a suspension can be obtained by measuring the concentration of iron from pyrite (FeS_2). The analysis procedure was initiated by separating the solids from the liquid phase by filtration with 0.2-µm cellulose membrane filters. The solid particles retained on the filter contained either FeS or FeS_2. FeS was removed by dissolving it by adding 5 M HCl. The pyrite that remained was separated by filtration using 0.2-µm cellulose membrane filters. The solid particles that remained on the filter were regarded as pyrite and they were dissolved by contact for 1 hour with concentrated HNO_3 at a temperature of around 95 °C. The amount of pyrite was determined by measuring the amount of iron in solution after dissolution, using the same

procedure discussed in the previous section for measurement of iron in liquid phase. The procedure of FeS removal and FeS_2 quantification is summarized in Fig. 3.3.

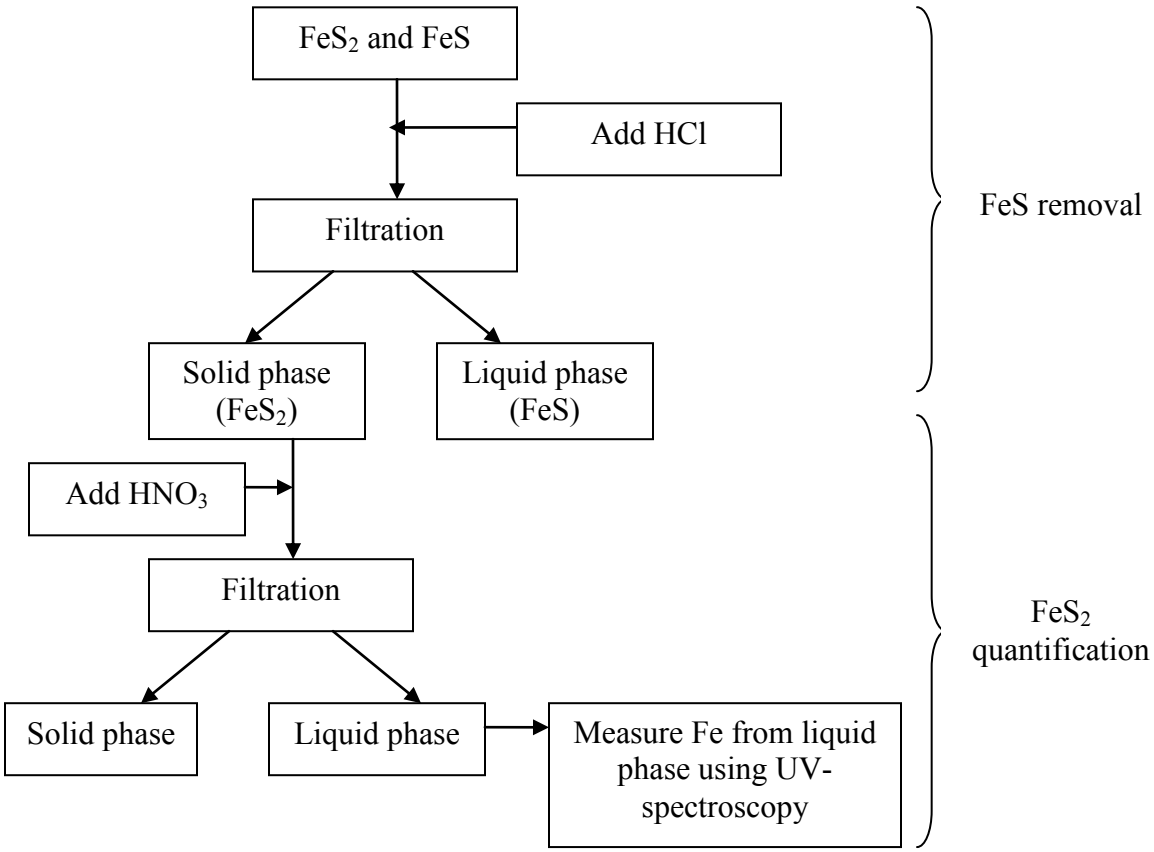

Fig. 3.3 Diagram of FeS removal and FeS_2 quantification

3.2.4 X-Ray Diffraction (XRD) Spectroscopy Analysis

XRD analyses were conducted by the department of geology at Texas A&M University. XRD patterns were recorded for Cu Kα radiation on the Rigaku model Geigerflex, operating at 40 kV and 20 mA, between 2° and 65° (2θ) with a step size of 0.05. The XRD analysis was performed to confirm that the mineral synthesized was pyrite.

3.2.5 Scanning Electron Microscopy (SEM) Analysis

SEM analysis was done in the department of biology in the Texas A&M University using a JEOL 6400 SEM in order to measure the particle size and shape of synthesized pyrite. The sample was pretreated before the analysis by coating with gold to obtain an electrically conductive surface so as to avoid charging of the surface. When an electrical charge builds up on the surface, the incident electron beam is deflected resulting in incorrect analyses.

3.2.6 X-ray Photoelectron Spectroscopy (XPS) Analysis

XPS analysis was conducted by the department of chemistry in the Texas A&M University. XPS data are collected using a Perkin-Elmer PHI 5500 spectrometer with a Mg 400 W source and a double-pass cylindrical mirror analyzer (Model 25-260). XPS was used to determine the oxidation state and chemical structure of synthesized pyrite in this study.

3.3 EXPERIMENTAL METHODS

Experimental methods were developed to synthesize pyrite with minimal reaction time and at high yield and to determine the optimum conditions for arsenic removal by synthesized pyrite including reaction time and pH. Experimental methods were also developed for experiments to determine the maximum capacity of pyrite for arsenic removal, and to measure the stability arsenic after removal by pyrite.

3.3.1 Optimizing the Synthesis Procedure for Pyrite

It is important for an adsorbent to be produced with as small a particle size as possible, in order to increase the specific surface area. Optimum conditions of pH,

reaction time, and temperature for production of pyrite at high yield were investigated in this section.

Optimum pH

In order to determine what pH values were best for pyrite synthesis, experiments were conducted in an anaerobic chamber at various pH values (pH 2.5, 3.6, 4.5, 5.6, 7, and 8). Six 100-ml solutions, containing 0.033 M $FeCl_3$ and 0.066 M NaHS, were adjusted to the designated pH using 0.05 M HCl or 0.05 M NaOH. All pH-adjusted solutions were allowed to react for 4 days before XRD analysis.

Aging Time

Experiments were conducted with various aging times, in order to determine how much time is required to synthesize pyrite. A 50-ml solution of 3.33E-2M $FeCl_3$ and a 50-ml solution of 6.67E-2M NaHS were prepared under anaerobic conditions. Their contents were added to a 120-ml polyethylene bottle to achieve final concentrations of 1.67E-2M $FeCl_3$ and 3.30E-2M NaHS. The solution pH was adjusted to pH 4.2 using 0.05 M HCl or 0.05 M NaOH. A total of eight bottles were prepared to investigate the effect of reaction time (0.1, 0.2, 0.7, 1, 2, 4, 6, 8 days). The intervals between these times were chosen to be short at the beginning of the experiment, because the reaction would occur faster at the beginning.

Temperature Effects

Seven 100-ml solution containing 3.33E-2 M $FeCl_3$ and 6.67E-2 M NaHS were placed on a heated shaker with rotational speed set to 150 rpm and temperature set to 60 °C. Samples were taken after reaction times of 0.5, 1, 2, 3, 4.5, 11, and 22 hours.

Optimum Iron and Sulfur Ratio

The yield of pyrite depended on the overall amounts of iron and sulfur added as well as their ratio. The effect of the molar ratio Fe^{3+}/HS^- on pyrite synthesis was examined in a series of experiments. Equal volumes (50 ml) of a solution of 1.67E-1 M $FeCl_3$ and a solution with various concentrations of NaHS were mixed, the pH was adjusted to pH 4.2, and the solutions were aged for 24 hours at 60 °C. Values of Fe^{3+}/HS^- of 0.400, 0.444, 0.500, 0.571, and 0.667 were investigated.

3.3.2 Determining Optimum Conditions for Arsenic Removal and Removal Capacity of Pyrite

Experiments were conducted with arsenic and pyrite to determine the optimum pH and reaction time for arsenic removal.

Kinetic Experiment

Kinetic experiments were performed with arsenic and pyrite to determine how removal of arsenic varied with time in order to choose an appropriate reaction time for removal experiments. Experiments were conducted with As(III) and As(V), because of their different properties.

As(III)

Experiments were conducted to characterize the kinetics of arsenic removal by taking a 250-ml solution containing 13.3μM As(III) and 1 g/l of pyrite and adjusting its pH to 9 using borate buffer solution in an anaerobic chamber. This solution was transferred to a rotating shaker. A number of 10-ml portions of the solution were taken at time intervals of 0, 15, 30, 45, 60, and 120 minutes. The samples were filtered using

membrane disc filters with 0.2-μm pores and the filtrate was analyzed for arsenic by application of HGAA.

As(V)

Six 20-ml solutions containing 66.7 μM As(V) and 1 g/l of pyrite were prepared under anaerobic conditions to characterize of the kinetics of arsenic removal by pyrite. After adjusting the pH of solutions to pH 7, they were transferred to a rotating shaker. Several 10-ml portions of the solutions were taken at time intervals of 0, 15, 30, 60, 720 and 1440 minutes. The sample was filtered using 0.2-μm membrane disc filters and the filtrates were analyzed for arsenic using HGAA.

pH Effects

Since pH plays a great role between toxic contaminant and environmental media, it is important to know what pH ranges are suitable for arsenic removal using pyrite. Reasonable pH values in environmental media, including low (pH 4), neutral (pH 7), and high pH (pH 9), were chosen for the experiment.

As(III)

The optimum pH for As(III) removal by pyrite was investigated. Three polyethylene bottles containing 50-ml solutions with several pH values (pH 4, 7, 9) were prepared using buffers. The buffers used to maintain pH 4, 7 and 9 were acetate, 4-morpholinepropanesulfonic acid (MOPS), and borate, respectively. The suspensions contained initial concentration of 4 g/L pyrite and 26.7 μM As(III). The suspensions were mixed on a rotating shaker for 30 minutes before samples were taken and filtered using 0.2-μm membrane disc filter. The filtrates were analyzed for arsenic using HGAA.

As(V)

The optimum pH for As(V) removal by pyrite was investigated. Three polyethylene bottles containing 20-ml solutions were prepared with several pH values (pH 4, 7, 10) that were maintained by adding different amounts of 0.05M HCl and 0.05 M NaOH. Pyrite and As(V) were added to each solution to achieve concentrations of 1 g/l and 13.3 μM, respectively. The suspensions were mixed on a rotating shaker and samples were taken after 30 minutes and filtered using 0.2-μm membrane disc filter. The filtrates were analyzed for arsenic using HGAA.

Combined Effects of Reaction Time and pH

Experiments to measure kinetics of removal of As(V) were conducted under anaerobic conditions at pH 4, 7, and 10. Nine polyethylene bottles were used for each pH condition. Each bottle held a 20-ml solution containing 13.3 μM As(V) and 1 g/l of pyrite. The solution pH was adjusted by adding 0.05 M HCl or 0.05 M NaOH before being transferred to a rotating shaker. A 20-ml portion of the solution was taken from the bottle at time intervals of 0, 15, 30, 45, 60, 90, 120, 180, and 360 minutes. These samples were filtered using membrane disc filter with 0.2-μm pores and the filtrates were analyzed for arsenic using HGAA.

Arsenic Removal Capacity of Pyrite

After acquiring the optimum conditions for arsenic removal with pyrite, experiments were conducted to evaluate removal of arsenic by pyrite under those conditions. Adsorption isotherm experiments can be conducted by varying either the amount of pyrite or the amount of arsenic. In this study, various amounts of arsenic

were contacted with a fixed amount of pyrite to obtain data. Suspensions were prepared with known amounts of arsenic and pyrite, and they were mixed for a period of time by shaking or stirring. It is important to allow arsenic and pyrite a sufficient time to react so that the system can approach steady state. However, the reaction time should not be so long that other reactions such as precipitation or dissolution are able to occur. An appropriate period of time can be determined by the kinetic experiment. After the appropriate reaction time, , liquid and solid phases were separated by filtering, and the liquid phase was analyzed for arsenic concentration.

As(III)

Removal experiments were conducted with As(III) and synthesized pyrite in the anaerobic chamber. Nineteen 50-ml solutions were prepared that contained various initial As(III) concentrations, ranging from 0.267 μM through 400 μM. The solutions were adjusted to pH 9 using a borate buffer solution. A small amount (0.05 g, 1 g/l) of pyrite was added to each solution and they all were allowed to react for 30 minutes while being mixed with a rotating shaker. Samples taken from the reactors were filtered through 0.2-μm membrane disc filters and the filtrates were analyzed for arsenic using HGAA.

As(V)

Sixteen 20-ml solutions containing 1 g/l of pyrite and various concentrations of As(V), ranging from 13.3 μM through 133 μM were prepared in an anaerobic chamber. Each solution was adjusted to pH 7 by using 0.05M HCl or 0.05 M NaOH. The solutions were added to 20-ml polyethylene bottles that were placed on a rotating mixer operated at

30 rpm. After 6 hours of reaction time, the contents of the bottles was filtered using a 0.2-µm membrane disc filter and the filtrates were analyzed for arsenic using HGAA. The experimental data for initial and final concentrations in the liquid phase was used to calculate the arsenic concentration on the solid phase by applying a material balance.

3.3.3 Determining Optimum Conditions for Stabilization of Arsenic on Pyrite

The goal of this experiment was to observe the stability of the mixture of arsenic and pyrite. After producing the mixture of arsenic and pyrite, its stability was measured by leaching experiments conducted over a range of pH from pH 4 through pH 10.

Kinetic Experiment

After arsenic is removed by pyrite, it is important to know easily it can be released. Experiments were conducted to measure effect of time on arsenic release from pyrite over a time period of 7 days.

As(III)

A mixture of arsenic and pyrite was prepared before conducting kinetic experiments on desorption of arsenic from pyrite. The mixture of arsenic and pyrite was prepared in polyethylene bottles and contained 250 ml solution with 53.4 µM As(III) and 1 g/l pyrite. The pH of the solution was adjusted to pH 9 by using a borate buffer solution and then it was placed on a shaker for 48 hours. The arsenic and pyrite mixture was separated by a 0.2-µm membrane filter and the liquid phase was analyzed for arsenic by HGAA. The solid phase was transferred to a polyethylene bottle and DI water was added into the polyethylene bottle, and pH was adjusted to 7. A set of 10-ml portions of the solution was taken at time intervals of 30, 120, 360, 720, 1440, 2880 (2 days), 5760

(4 days), and 10080 (7 days) minutes for analysis. The solution was separated by a 0.2-μm membrane filter, and the liquid phase was analyzed by HGAA.

As(V)

A mixture (250 ml) of arsenic(V) and pyrite was prepared in a polyethylene bottle and contained 53.4 μM As(V) and 1 g/l pyrite. The pH of the solution was adjusted to pH 7 by using 0.05 M HCl or 0.05 M NaOH, and it was placed on a shaker for 48 hours. The arsenic and pyrite mixture was separated by a 0.2-μm membrane filter, and the liquid phase was analyzed by HGAA. The solid phase was transferred to a polyethylene bottle and DI water was added into the polyethylene bottle, and the pH was adjusted to 7. A set of 10-ml portions of the solution was taken at time intervals of 30, 120, 360, 720, 1440, 2880 (2 days), 5760 (4 days), and 10080 (7 days) minutes. The solution was separated by a 0.2-μm membrane filter, and the liquid phase was analyzed by HGAA.

pH Effects

The Toxicity Characteristic Leaching Procedure (TCLP) was approved by EPA for the measurement of the toxicity characteristic of solid materials. However, it has been reported by some researchers to underestimate the extent of leaching of toxic compounds (Ghosh et al. 2004, Halim el al. 2005). Therefore, a leaching procedure was used that measured release at various pH values that are typical for real environments. The goal of this study is to measure the stability of arsenic on pyrite as a function of pH.

As(III)

Seven 250-ml solutions containing 1 g/l of pyrite and 53.4 μM As(III) were prepared and the pH was adjusted to pH 9 using borate buffer solution. These

suspensions were transferred to a rotating shaker and allowed to react for 48 hours. The supernatant was filtered through a 0.2-µm membrane filter and the filtrate was analyzed for arsenic concentration by HGAA. De-ionized water (DIW) was added into the bottle containing arsenic and pyrite. The pH was adjusted to different values over the range from pH 4 through pH 10 with either HCl or NaOH, and the total volume was made up to 250 ml with DIW. These mixtures were shaken at 150 rpm for 48 hours. The supernatants were filtered through 0.2-µm membrane filters and were analyzed for As concentration using HGAA.

As(V)

Seven 250-ml solutions containing 1 g/l of pyrite and 53.4 µM As(III) were prepared and the pH was adjusted to pH 7 using 0.05 M HCl or 0.05 M NaOH. These suspensions were transferred to a rotating shaker and allowed to react for 48 hours. The supernatant was filtered through a 0.2-µm membrane filter and the filtrate was analyzed for arsenic concentration by HGAA. De-ionized water (DIW) was added into the bottle containing pyrite with sorbed arsenic. The pH was adjusted to different values over the range from pH 4 through pH 10 with either HCl or NaOH, and the total volume was made up to 250 ml with DIW. These mixtures were shaken at 150 rpm for 12 hours. The supernatants were filtered through 0.2-µm membrane filters and were analyzed for As concentration using HGAA.

CHAPTER IV

CHARACTERIZE AND OPTIMIZE THE SYNTHESIS PROCEDURE FOR PYRITE

4.1 INTRODUCTION

Developing effective treatment methods using pyrite to remove arsenic from water and to stabilize arsenic in wastes requires reliable techniques for synthesizing pyrite. There are several ways to synthesize pyrite using different sources of iron and sulfur either applying heat or not. Among them, Wei and Osseo-Asare (1996) used $FeCl_3$-NaSH reaction for pyrite formation, because it is relatively straightforward and fast. Also, they produced micro- or nano-sized pyrite at room temperature. The modifications of their method were chosen in order to synthesize pyrite with smaller particle size, produce higher yield, and reduce synthesis time in this study. The effects of pH, reaction time, temperature, and ratio of ferric iron to sulfide on synthesis of pyrite are reported in this chapter and the detailed experimental procedures are presented in Chapter III.

The goal of the research described in this chapter was to develop methods for making pyrite crystals of defined size with minimal reaction time and at high yield. To verify the size of the pyrite particles and to characterize the mineral produced, analytical methods such as Scanning Electron Microscopy (SEM) and X-Ray Diffraction (XRD) were applied.

4.2 RESULTS AND DISCUSSION

The effects of various conditions (pH, aging time, temperature, iron/sulfur reaction ratio) on pyrite synthesis are summarized in this section. The synthesized pyrite

particles were characterized by XRD and SEM and results of those analyses are presented in this section.

4.2.1 Optimum pH

The results of XRD analysis on solids believed to be pyrite that were produced at pH values of 2.5, 3.6, 4.5, 5.6, 7, and 8 are presented in Fig. 4.1, 4.2, 4.3, 4.4, 4.5, and 4.6, respectively. These figures show counts per second on the y-axis and values of 2 theta (2θ) on the x-axis. Peaks associated with pyrite in these figures were determined by matching their position, width, and intensity with information provided by JCPDS (Joint Committee on Powder Diffraction Standard). JCPDS indicates that pyrite produces peaks that are associated with d-spacings of 3.13, 2.71, 2.43, 2.21, and 1.63, which correspond to values of 2 theta (2θ) of 56.34, 47.45, 40.79, 37.03, and 33.07. The peaks that were identified as being associated with pyrite are indicated with an "X" in Fig. 4.1 - 4.6.

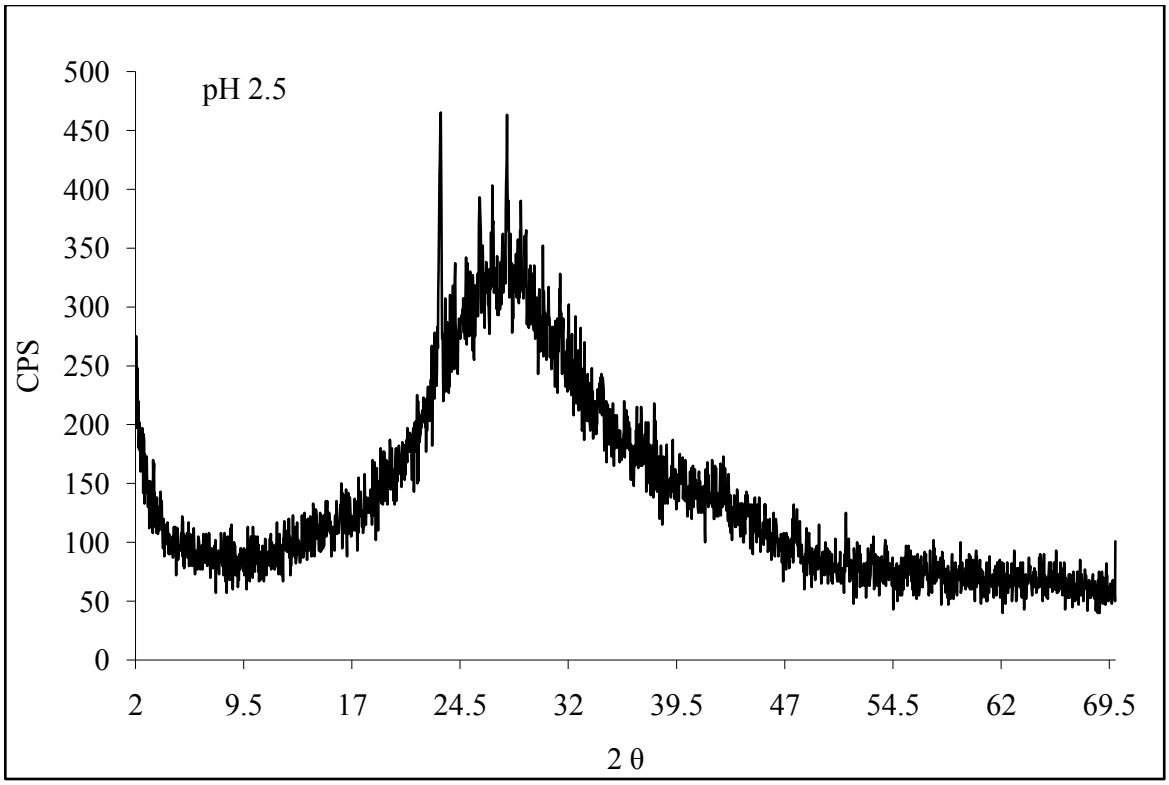

Fig. 4.1 XRD results for solid produced at pH 2.5

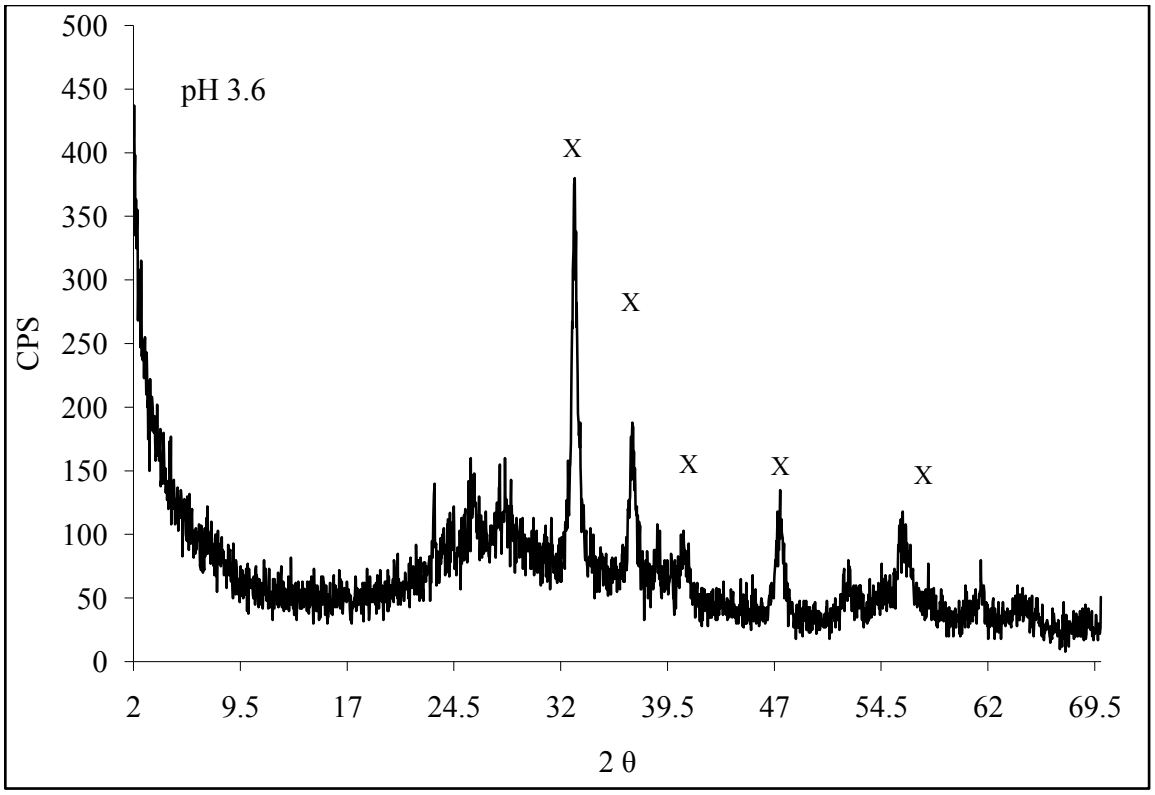

Fig. 4.2 XRD results for solid produced at pH 3.6

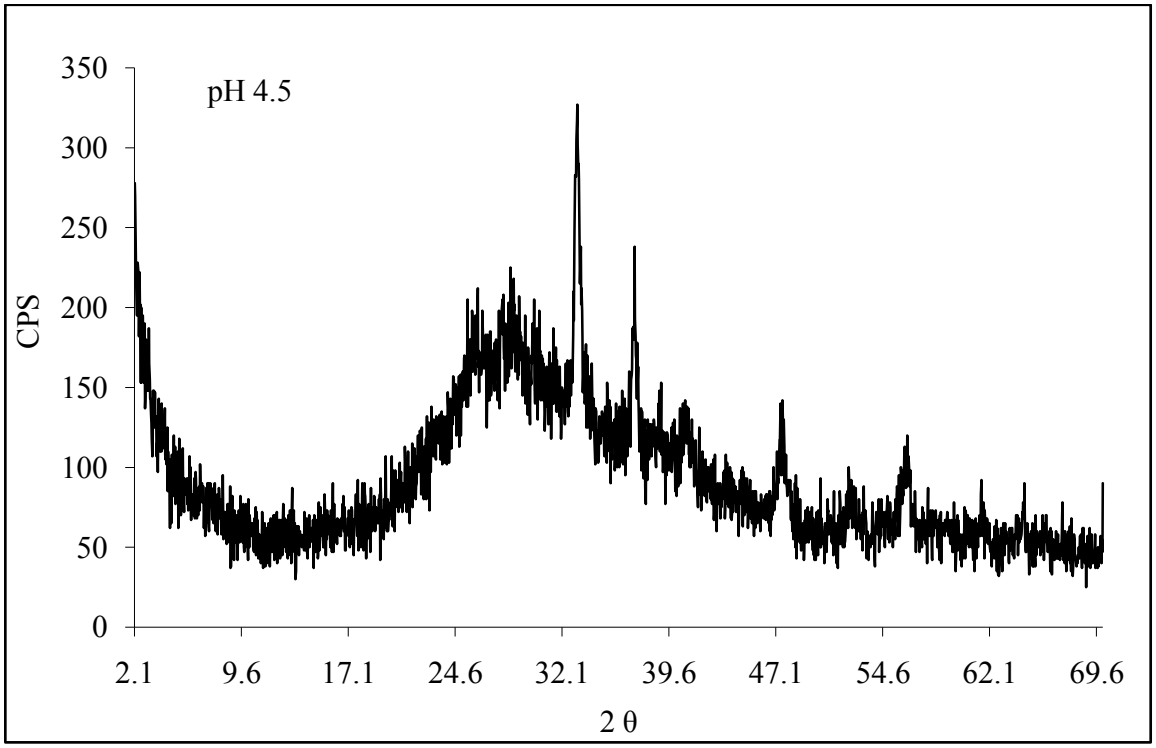

Fig. 4.3 XRD results for solid produced at pH 4.5

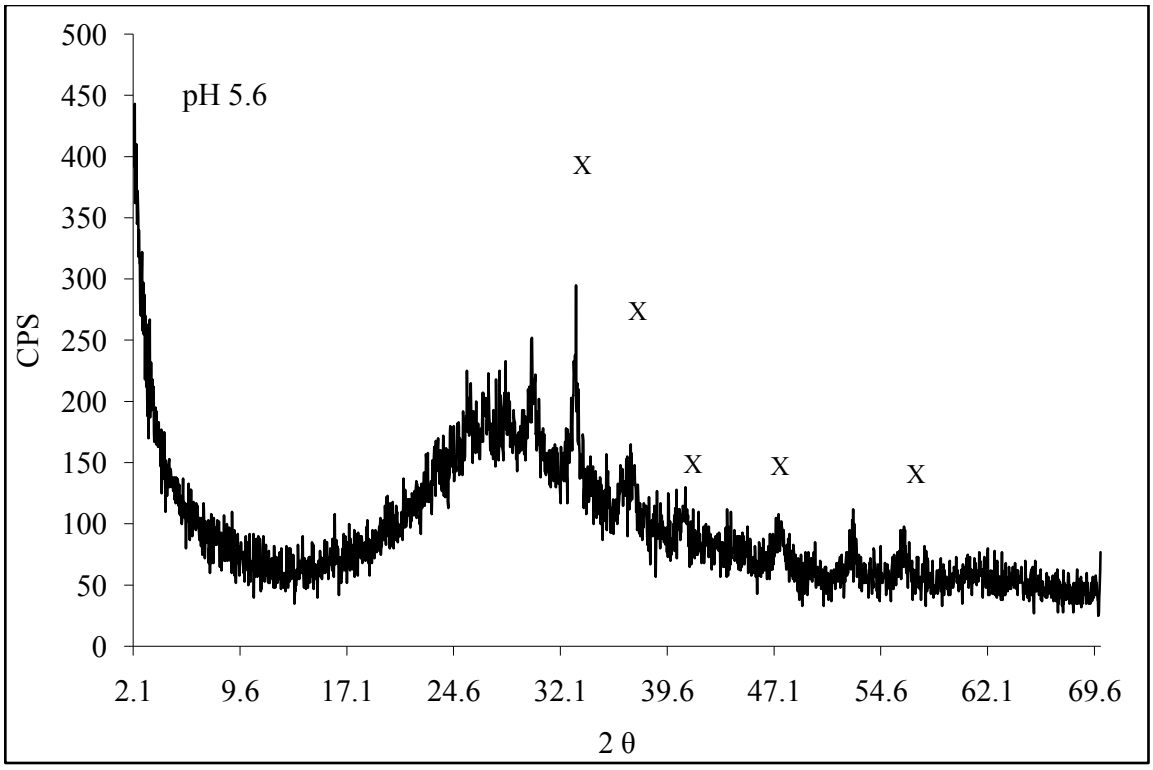

Fig. 4.4 XRD results for solid produced at pH 5.6

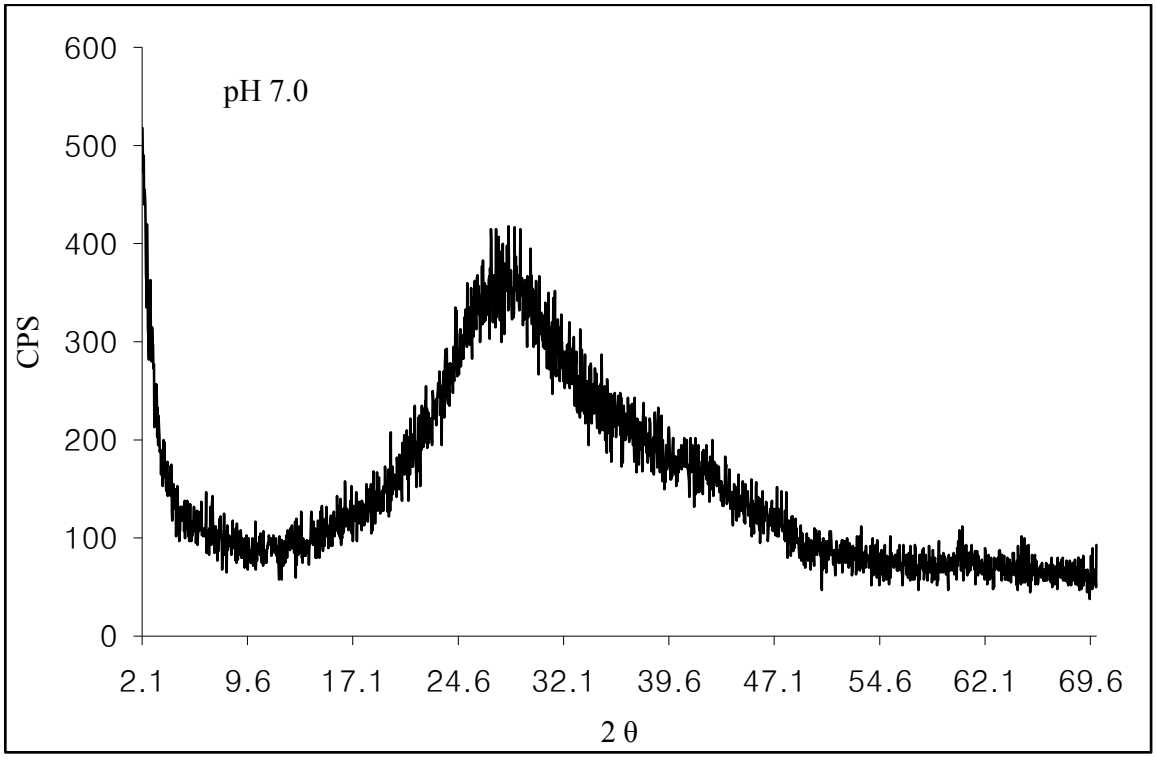

Fig. 4.5 XRD results for solid produced at pH 7.0

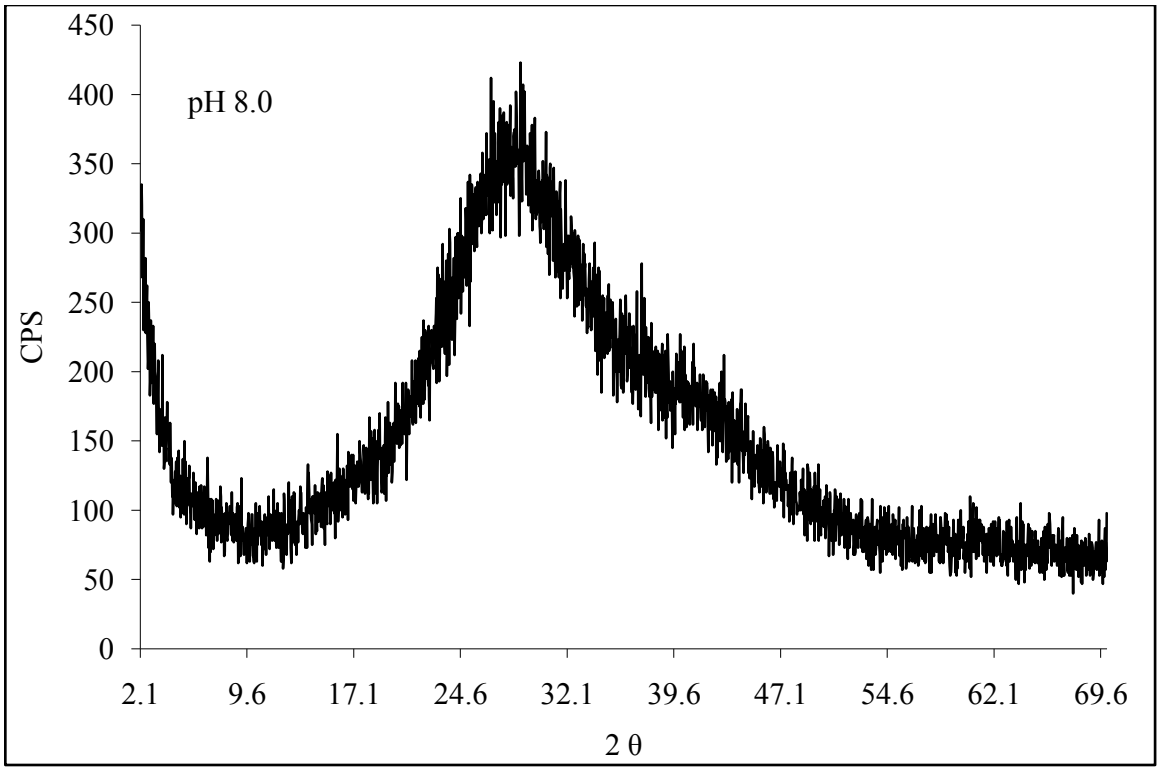

Fig. 4.6 XRD results for solid produced at pH 8.0

Based on XRD analysis results on pyrite synthesis, only pHs ranging from 3.6 through 5.6 produced pyrite. Amorphous iron sulfide can be produced except those pH ranges. Also, it was defined by the analysis of XRD in previous figures.

In general, there are two pathways to synthesize pyrite at low temperature but both begin with the formation of FeS (equation 5.1). The two pathways involve a reaction between FeS and elemental sulfur (equation 5.2a), or with polysulfides S_n^{2-} (equation 5.2b).

$Fe^{2+} + HS^- \rightarrow FeS + H^+$ (equation 5.1)

$FeS + S° \rightarrow FeS_2$ (equation 5.2a)

$FeS + S_n^{2-} \rightarrow FeS_2 + S_{n-1}^{2-}$ (equation 5.2b)

FeS and either S° or S_n^{2-} are required for pyrite formation.

The Eh-pH diagram for S-H_2O (Fig. 4.7) shows that elemental sulfur is not thermodynamically stable above pH 7. The marks as "□" in Fig. 4.7 is presented the place where pyrite formed, also the marks as "■" is the place where pyrite is not formed.

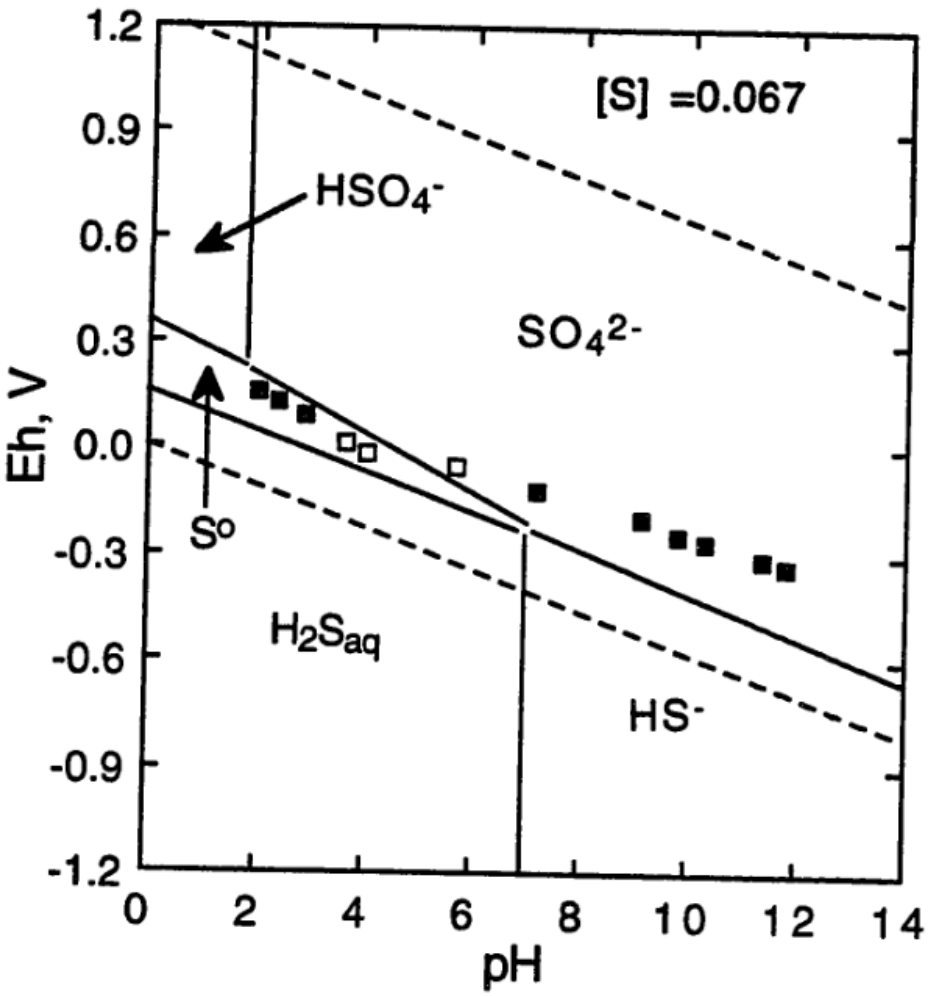

Fig. 4.7 Eh-pH diagram for S-H_2O system at 25 ºC with measured Eh, □ pyrite formed, ■ no pyrite formed (cited from Wei 1995)

Also, FeS is not thermodynamically stable below pH 3.5, which is shown in Fig. 4.8.

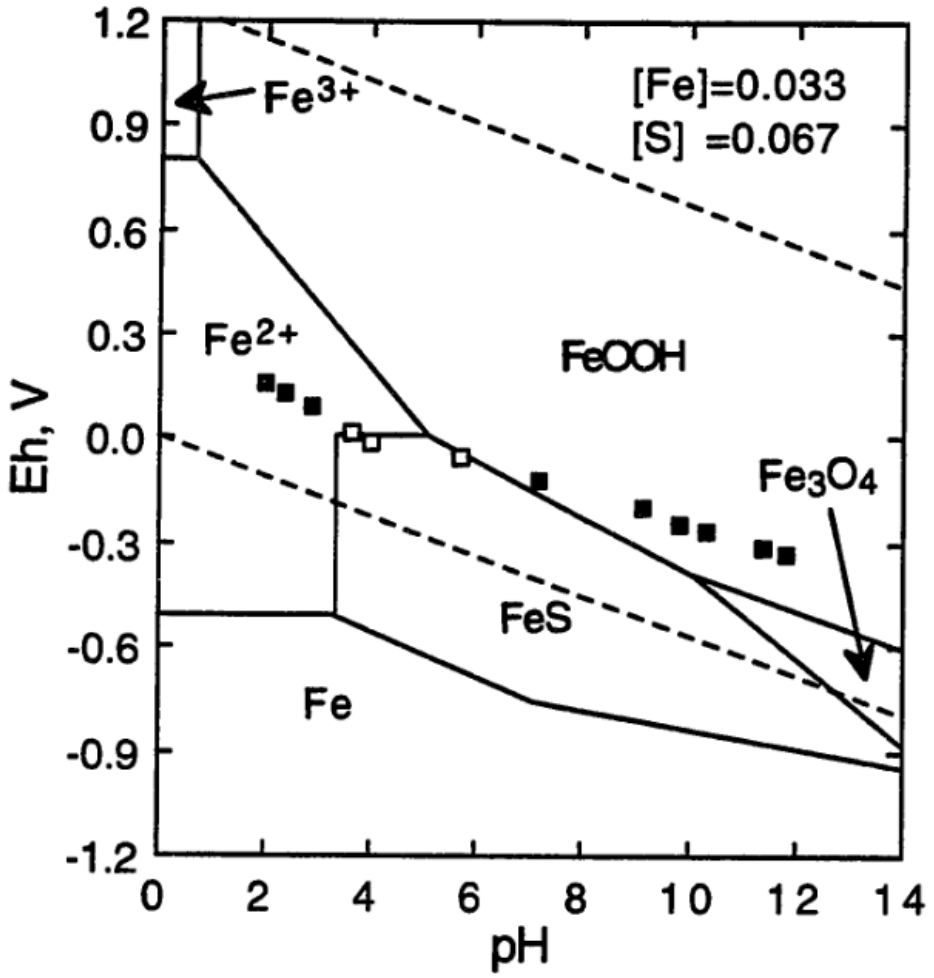

Fig. 4.8 Eh-pH diagram for Fe-S-H_2O system at 25 ºC with exclusion of FeS_2, □ pyrite formed, ■ no pyrite formed (cited from Wei 1995)

4.2.2 Aging Time

Fig. 4.9 shows the amount of pyrite produced as a function of time using the modified method of Wei and Osseo-Asare (1996). The maximum theoretical concentration of pyrite that could be produced with these reagents was 8.25E-3 M and this concentration is indicated by the line in Fig. 4.9.

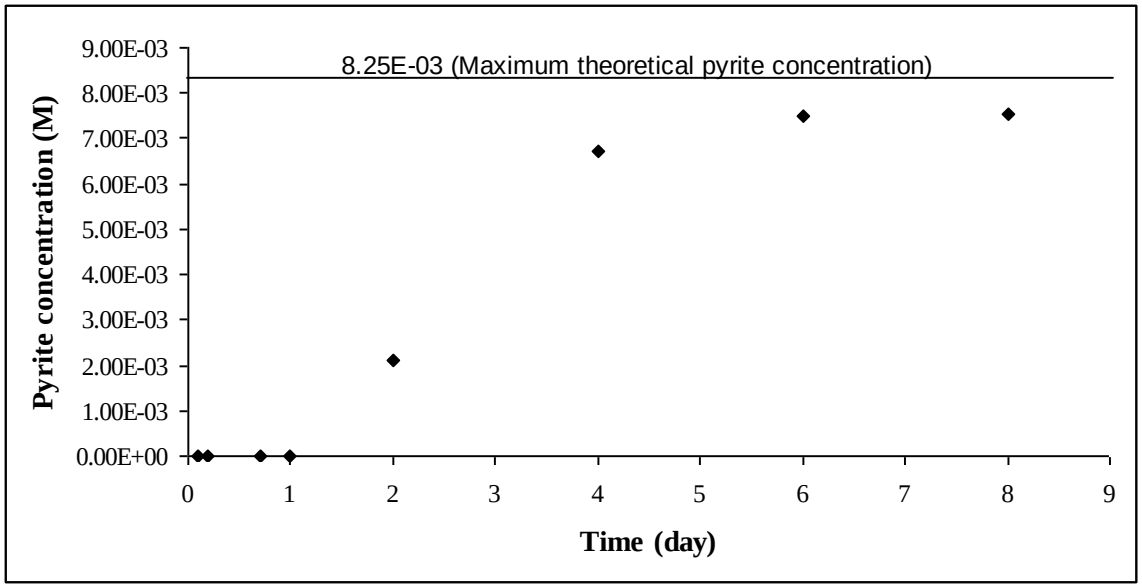

Fig. 4.9 Pyrite formation with time at room temperature

There was no pyrite produced until the reaction time exceeded 1 day. Reaction times of 2, 4, 6, 8 days yielded 26 %, 81 %, 91 %, and 91 % of the maximum theoretical pyrite production, respectively. XRD analysis showed no unique peaks in the sample after 30 minutes of aging time, so the solid phase was considered to be amorphous iron monosulfide. These results are consistent with previous research that found that pyrite was synthesized gradually from iron sulfide (Wei and Osseo-Asare 1996, Wilkin and Barnes 1996).

4.2.3 Temperature Effects

Fig. 4.10 shows pyrite production as a function of time at 60 °C. The maximum theoretical concentration of pyrite possible with these experimental conditions is 1.65E-2 M and this concentration is indicated by the line in Fig. 4.10.

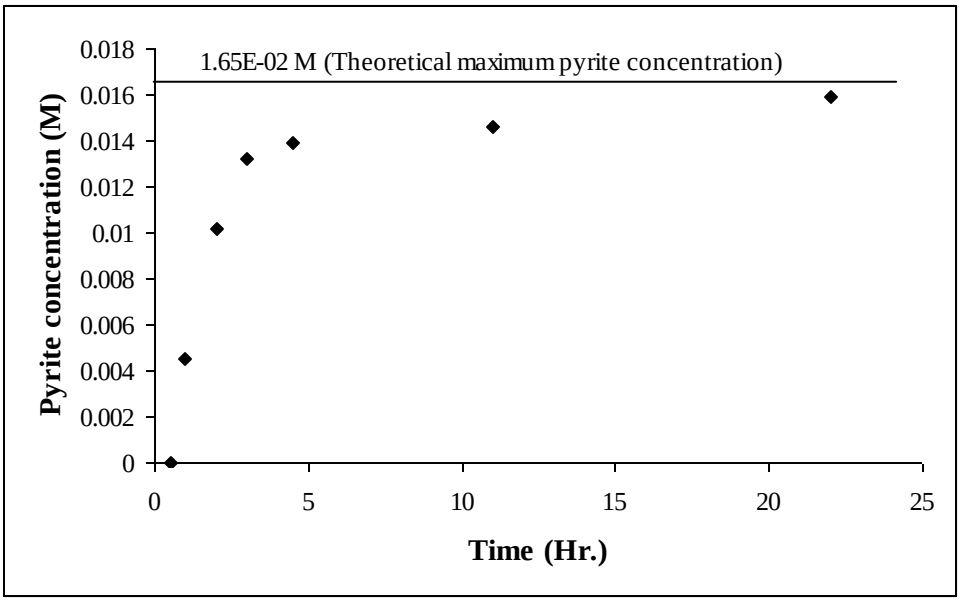

Fig. 4.10 Pyrite formation with time at 60 °C

While it took two days to produce pyrite at room temperature, it took only one hour to synthesize pyrite at 60 °C. The experiments at reaction times of one, three, and twenty-two hours yielded 27 %, 80 %, and 97 % of the theoretical maximum pyrite concentration. The role of temperature is generally assumed to increase the rate of reaction. The XRD analyses verified that the produced mineral was pyrite and SEM analyses determined the particle size and shape of the synthesized pyrite. An SEM of synthesized pyrite is presented in Fig. 4.11 and it shows that particle sizes ranged from 0.7 to 1.2 μm.

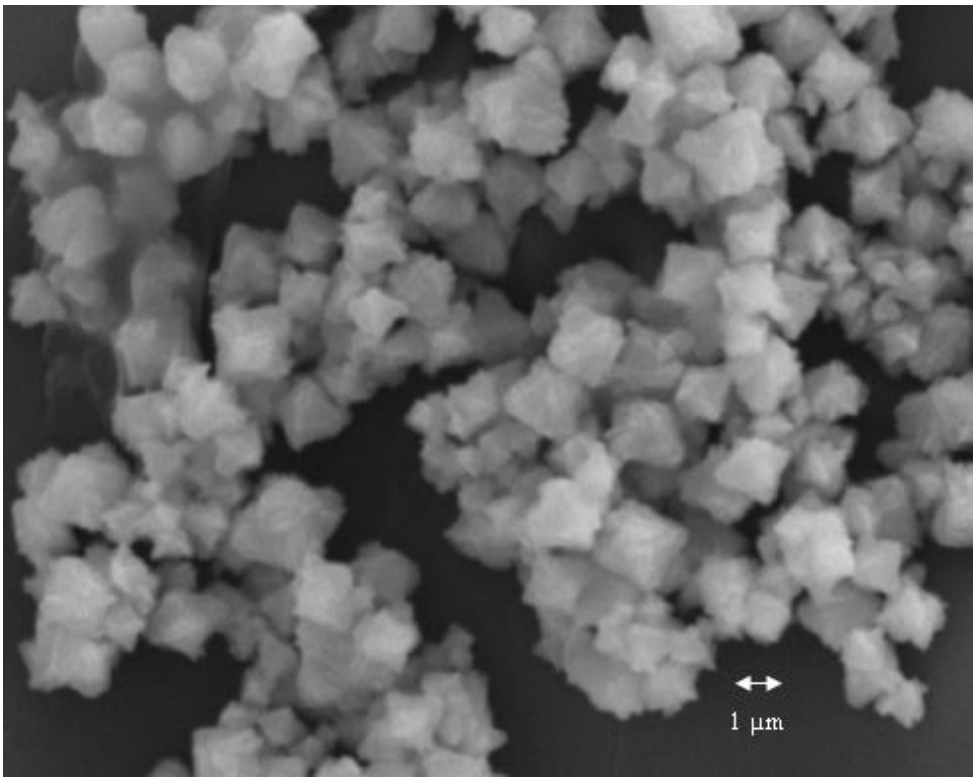

Fig. 4.11 SEM of synthesized pyrite showing size and shape

4.2.4 Stability of Synthesized Pyrite in Contact with Air

Pyrite can be oxidized when in contact with air, so an investigation of its stability in air was conducted. Pyrite was synthesized and then air dried at room temperature for 3 days. XRD analysis was performed and the results are presented in Fig. 4.12.

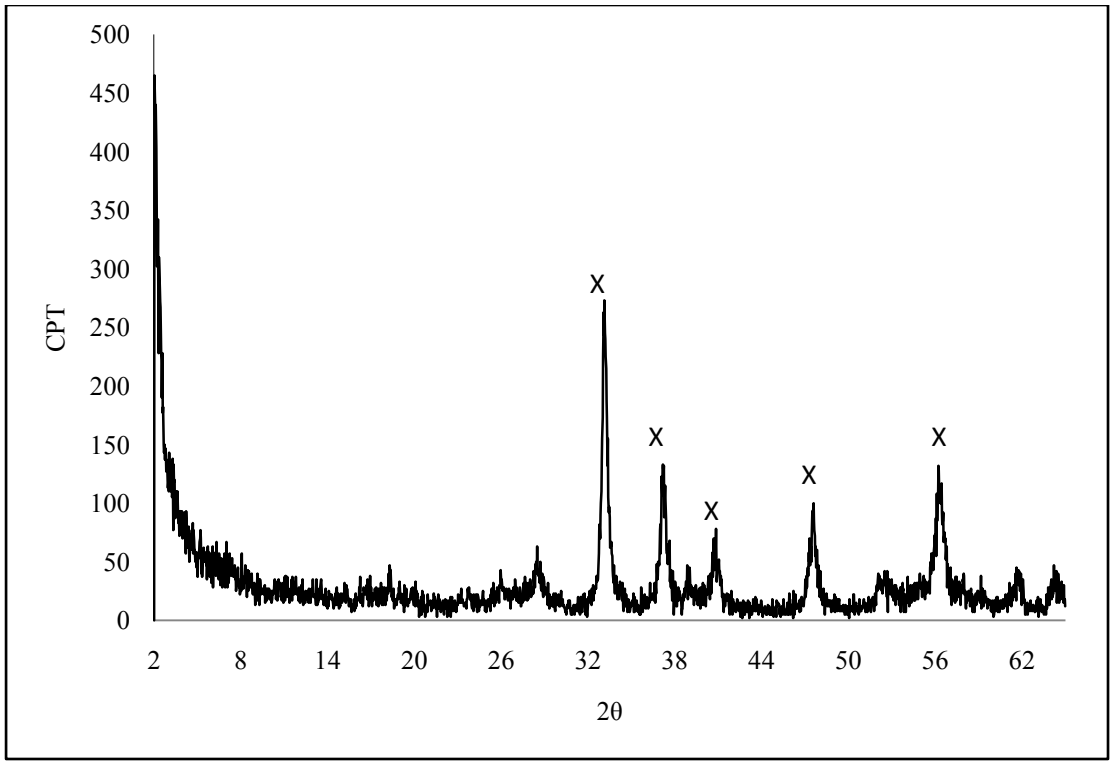

Fig. 4.12 XRD result of 3 day air dried pyrite

Fig. 4.12 shows that pyrite remained even after contact with air for 3 days. This result is in accord with Wei's experiment (1995). He found that synthesized pyrite did not change its identity after drying in air for 5 days, as measured by XRD analysis.

4.2.5 Optimum Iron and Sulfur Ratio

Table 4.1 shows the efficiency of pyrite production in these experiments.

Table 4.1 Amount of FeS_2 produced at various Fe^{3+}/HS^- ratios

Fe^{3+}/HS^- ratio	FeS_2 production (M) / HS^- (M) used
0.400	1.87E-01
0.444	1.97E-01
0.500	2.00E-01
0.571	2.01E-01
0.667	1.44E-01

The concentration of pyrite synthesized increased then decreased as Fe^{3+}/HS^- increased. However, the Fe^{3+}/HS^- values of 0.500 and 0.571 produced pyrite most efficiently in terms of the amount of HS^- used. Wei and Osseo-Asare (1996) investigated the effect of a range of Fe^{3+}/HS^- (0.25, 0.5, 0.75, and 1) on pyrite synthesis and they found that pyrite was not synthesized with ratio of 1. Unfortunately, they did not quantify the amount of pyrite produced.

CHAPTER V

CHARACTERIZE REMOVAL OF ARSENIC BY SYNTHESIZED PYRITE

5.1 INTRODUCTION

Adsorption has been used as a technique for removal of arsenic. Adsorption is the process in which a chemical substance accumulates at the common boundary of two contiguous phases. If one of the contiguous phases is a solid and the other a fluid, the solid phase is termed the adsorbent, and the matter that sticks to the solid phase is called the adsorbate. The adsorbent is the pyrite and the adsorbate is the arsenic in this study. A related process occurs when a chemical is detached from a solid phase and this process is called desorption or negative adsorption. Typical adsorption experiments are conducted in a sequence of three steps. First, the reaction between adsorbent and adsorbate is allowed to proceed for a prescribed period of time. Second, the adsorbent is separated from the liquid phase after a sufficient time passes for the removal reaction to be completed. Last, the amount of adsorbate remaining in the liquid phase is measured and the amount of adsorbate attached to the solid phase is calculated. Removal of the adsorbate by the adsorbent can be the beginning of the process. After that, chemical processes such as precipitation can occur, which can affect the total amount of material removed. In this study, synthesized pyrite was applied to remove arsenic and its capacity for arsenic removal was measured in batch adsorption experiments. The effects of pH and reaction time on arsenic removal were determined. Also, information was obtained on the characteristics of chemical species containing sulfur and iron before and after the reaction with arsenic.

5.2 RESULTS AND DISCUSSION

5.2.1 Kinetic Experiment

To determine the optimum reaction time for the removal of arsenic by pyrite, kinetic experiments with pyrite and As(III), or pyrite and As(V) were conducted. The detailed experimental procedure was described in Chapter III, but the experimental conditions are summarized in Table 5.1.

Table 5.1 Experimental conditions to determine optimum reaction time for removal of As by pyrite

	Initial As Conc. (μM)	Conc. of Pyrite (g/l)	Adjusted pH
As(III)	13.3	1	9
As(V)	66.7	1	7

As(III)

Arsenic concentration in the liquid phase as a function of time is presented in Fig. 5.1.

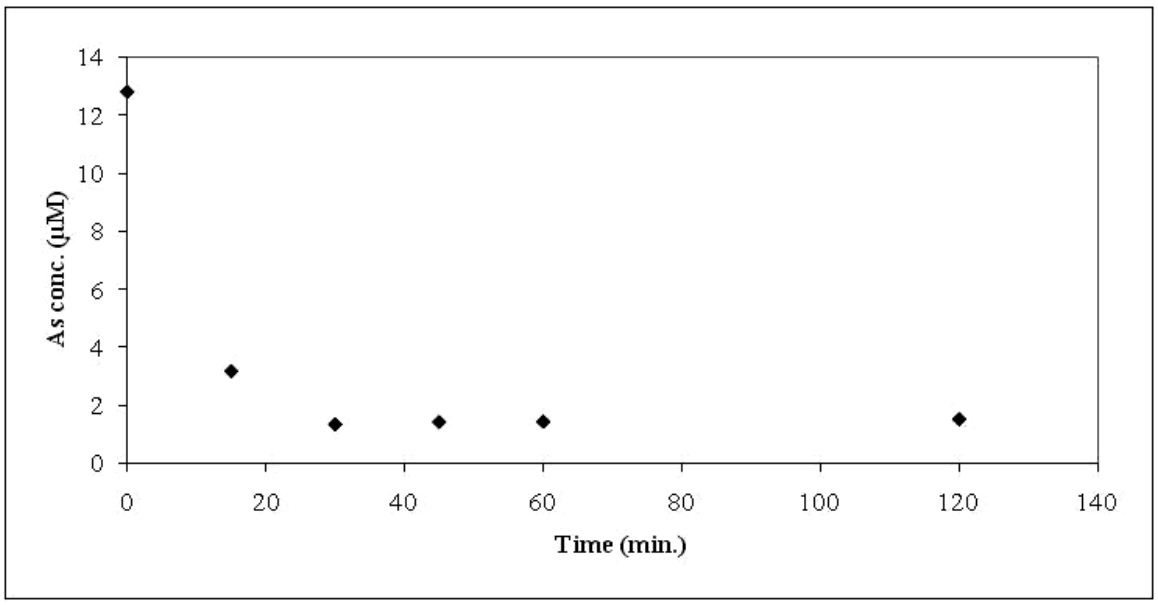

Fig. 5.1 As(III) concentration with time in presence of pyrite

The amount of arsenic in the liquid phase was constant after 30 minutes. Therefore, 30 minutes should be sufficient time for contact between As(III) and pyrite in experiments designed to evaluate initial removal. Contact times less than 30 minutes were used by most other researchers who examined removal of As(III) by pyrite (Wolthers et al. 2003, Bostick and Fendorf 2003, and Wolthers et al. 2005).

As(V)

Arsenic concentration in the liquid phase as a function of time is presented in Fig. 5.2.

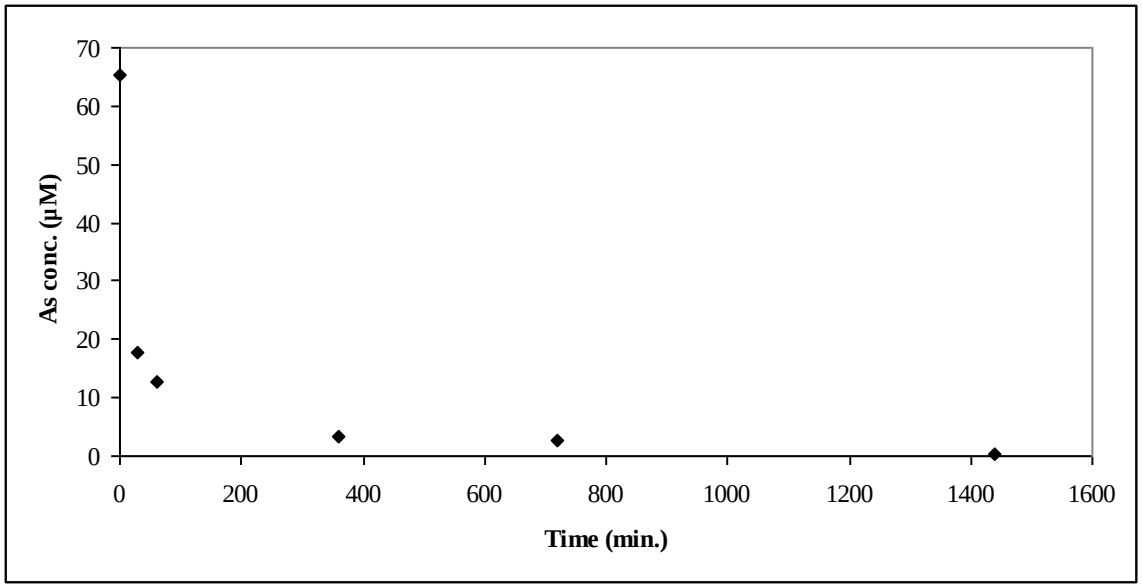

Fig. 5.2 As(V) concentration with time in presence of pyrite

Dramatic reduction of arsenic concentration in the liquid phase was observed at the beginning. More than 70 % of the initial arsenic was removed within 30 minutes, and 80 % arsenic disappeared in 60 minutes. With reaction time of 360 minutes, 95 % arsenic in the liquid phase was eliminated. The amount of arsenic in the liquid phase was constant after 360 minutes, so 360 minutes was selected as the reaction time to be used in later experiments designed to evaluate initial removal. Most researchers have used As(III) and iron sulfide when investigating removal of arsenic compounds by iron-sulfur compounds. A contact time of 30 minutes has been determined to be sufficient when experiments were conducted to evaluate As(V) removal by disordered mackinawite (Wolters et al., 2003). However, a reaction time of 360 minutes was selected for these experiments, because the kinetic experiment showed that such a time period is needed to complete the initial removal of arsenic. Generally, the amount of As removed would increase with increase of the reaction time.

5.2.2 pH Effects

Optimum pH ranges was measured for the arsenic removal using pyrite. Also, experiments to measure kinetics of removal of As(V) were performed at several pH values, including pH 4, 7, and 10. The detail experimental procedures were presented in Chapter III, but a short summary is presented in Table 5.2.

Table 5.2 Experimental conditions to determine effect of pH on removal of As by pyrite

	Initial As Conc. (μM)	Conc. of Pyrite (g/l)	Adjusted pH	Reaction time (min.)
As(III)	26.7	4	4, 7, and 9	30
As(V)	13.3	1	4, 7, and 10	30
As(V)	13.3	1	4, 7, and 10	0, 15, 30, 45, 60, 90, 120, 180, and 360

As(III)

The concentration of arsenic in the liquid phase was measured by HGAA and used to calculate the amount of arsenic removed, which is presented in Fig. 5.3. The most As(III) was removed by pyrite at pH 9.

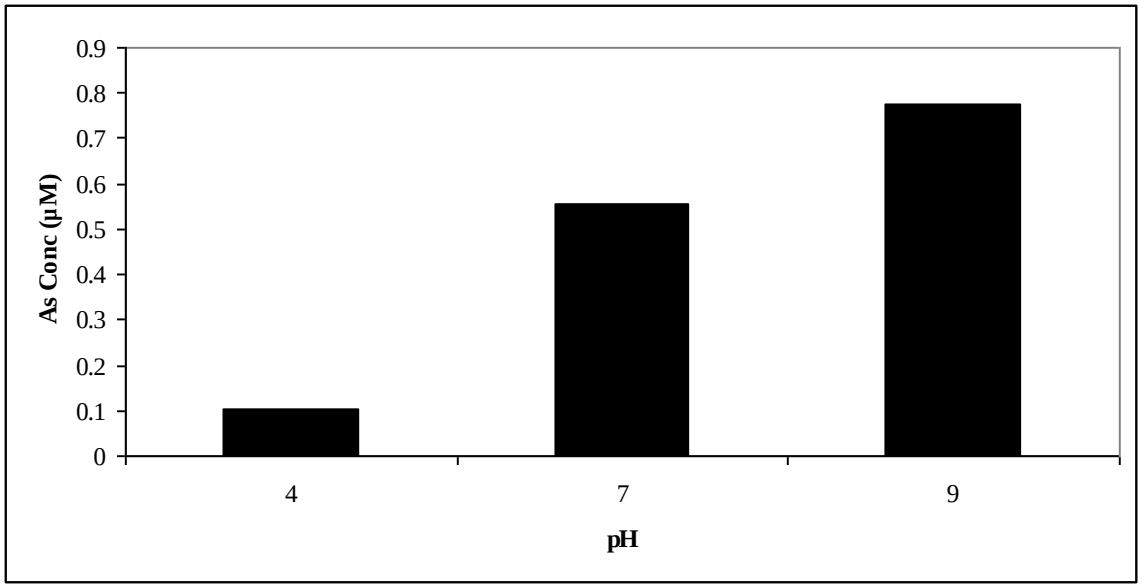

Fig. 5.3 Effects of pH on concentration of As(III) removed by pyrite

The results of experiments to evaluate the effect of pH on removal of As(III) by pyrite show that removal increases with increasing pH. Similar results were found by other researchers working with As(III) and pyrite. Bostick and Fendorf (2003) found the optimum pH for As(III) removal by pyrite was pH above 5 and Zouboulis et al. (1993) noticed that the range between pH 7 and pH 10 was the optimum. While, As(III) sorption on metal hydroxides is usually to be highest at circumneutral pH and lowest at high pH. Since As(III) is stable as neutral H_3AsO_3 at pH < 9, it can be removed in this pH range without overcoming electrostatic repulsion by the pyrite surface, which has a negative charge above pH 2 or pH 3. As pH increases over 9, the charge of As(III) changes to negative, resulting in repulsion between As(III) and pyrite. This explains why As(III) removal capacity using metal hydroxides decreases above pH 9. However, a different mechanism occurs for As(III) sorption by pyrite than by metal hydroxides.

As(V)

The concentration of arsenic in the liquid phase was measured by HGAA and was used to calculate the concentration of arsenic removed, which is presented in Fig. 5.4. The most As(V) was removed by pyrite at pH 7.

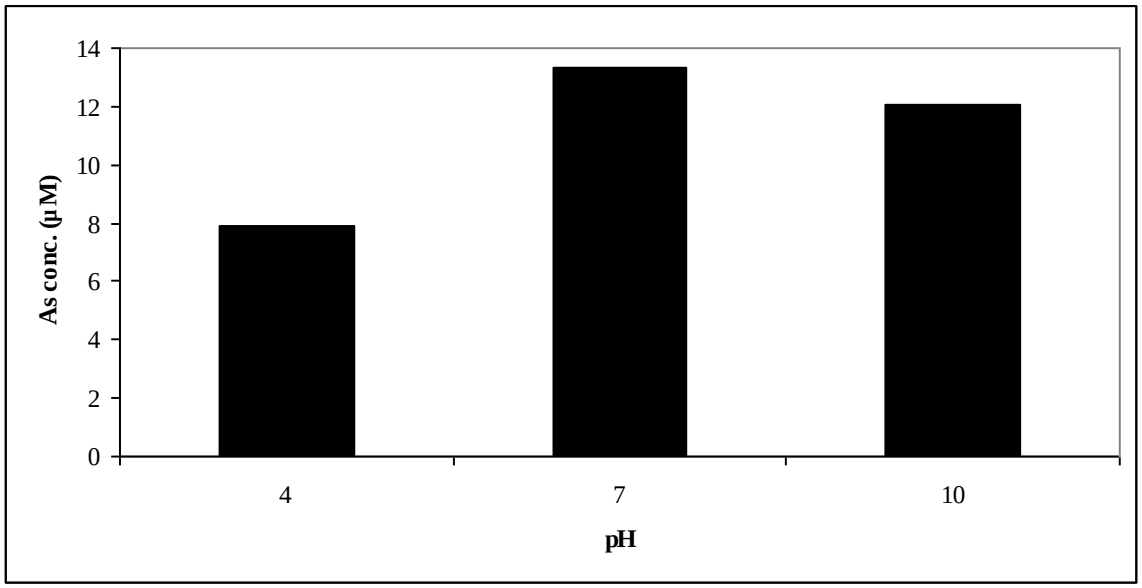

Fig. 5.4 Effects of pH on concentration of As(V) removal by pyrite

The experiments to measure the effect of pH on removal of As(V) by pyrite shows that highest arsenic removal occurs at circumneutral pH and lowest at low pH. Similar results were found by Zouboulis et al. (1993), who reported high As(V) removal in the region from pH 3 through pH 9. As(V) sorption on metal hydroxides is usually found to decrease as pH increases. As the pH increases above the pH_{zpc}, which is usually above pH 8 for iron hydroxide, the decreased percentage removal of As(V) is attributed to the increased electrostatic repulsion between the surface of the metal hydroxide and anionic As(V) species. However, the effect of pH on removal of As(V) by pyrite show in Fig. 5.4 cannot be explained by electrostatic forces so a different mechanism occurs for As(V) sorption by pyrite than by metal hydroxides.

Kinetics of As(V) removal at several pH values

Arsenic concentrations in liquid phase were measured with time at several pH values and they are presented in Fig. 5.5. At pH 4, the concentration of arsenic in the liquid phase decreased continuously, but some arsenic was detected after 360 minutes. The pH remained constant at pH 4 until the end of the experiment (360 minutes).

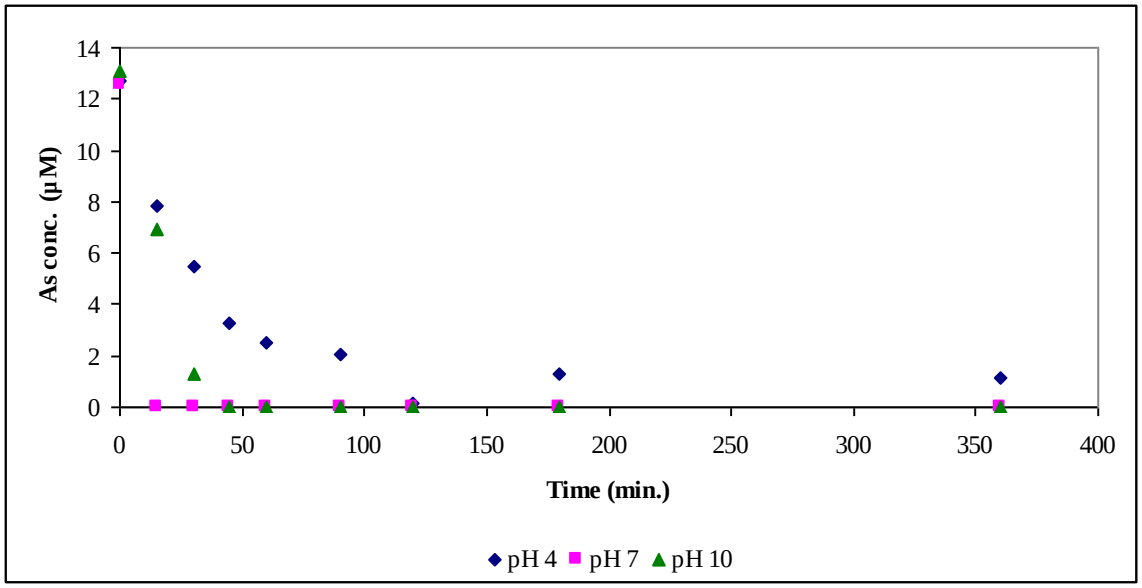

Fig. 5.5 The concentration of arsenic in the liquid phase at several pH conditions

At pH 7, arsenic in liquid phase was reduced to a negligible concentration before the first sampling time (15 minutes). However, the solution pH was not constant over time. The pH decreased from pH 7 to pH 6.3 after 20 minutes, to pH 5.5 after 60 minutes, and to pH 5.1 after 360 minutes. At pH 10, the concentration of arsenic in the liquid phase decreased continuously and no arsenic was below the detection limit after the 45 minutes. The pH decreased continuously from pH 9 to pH 4.5 after 180 minutes and remained at pH 4.5 from 180 through 360 minutes. This confirms the result observed in

previous experiments (Fig. 5.4) that the optimum pH for removal of As(V) is pH 7, compared with pH 4 and 10.

5.2.3 Removal Experiments

Adsorption experiments were conducted with arsenic and pyrite to determine the relationship between the concentration of arsenic in the liquid phase and the concentration of arsenic in pyrite after specified reaction times. Also, the maximum capacity of pyrite for removal of arsenic was determined from results of this study. The experimental conditions for these experiments were presented in Chapter III, but they are summarized in Table 5. 3.

Table 5.3 Experimental conditions for determining the effect of initial arsenic concentration on removal of arsenic by pyrite

	Initial As Conc. (μM) range	Conc. of Pyrite addition (g/l)	Adjusted pH	Reaction time (min.)
As(III)	0.267-400	1	9	30
As(V)	13.3-133	1	7	360

As(III)

Various concentrations of As(III) ranging from 0.267 through 400 μM were reacted with a pyrite concentration of 1 g/l for 30 minutes at pH 9. Experimental data and several model isotherms are presented in Fig. 5.6. Arsenic concentration in the solid phase is shown as q_e and arsenic concentration in the liquid phase is shown as C.

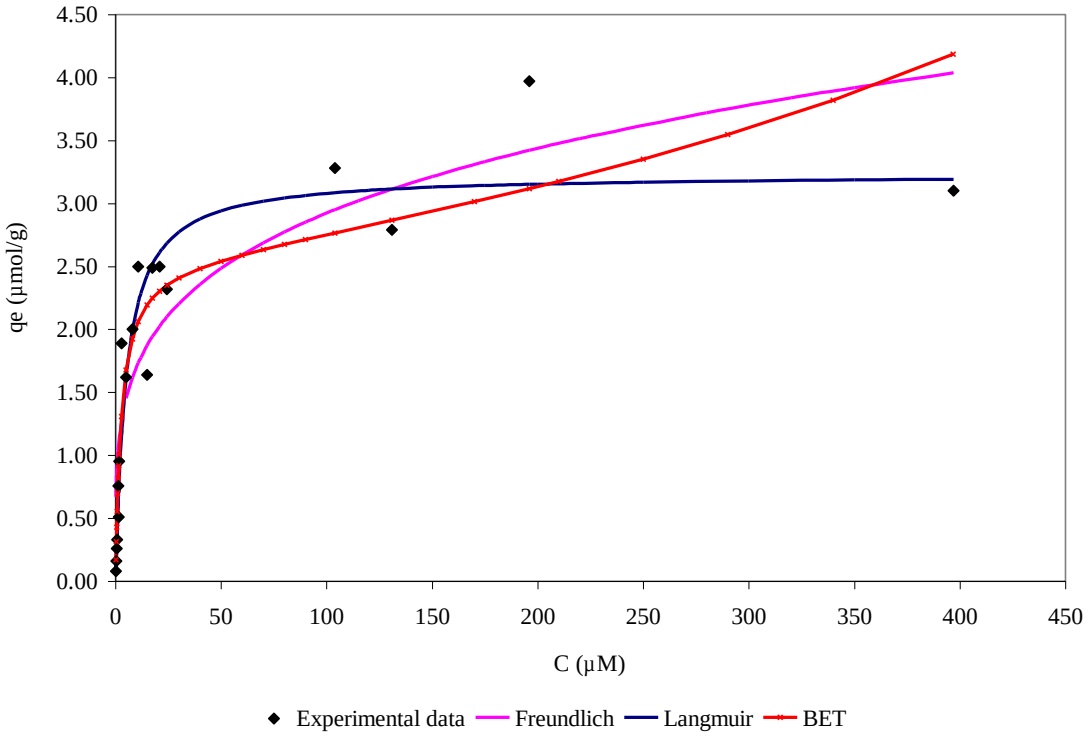

Fig. 5.6 Experimental data and model equations fit to solid and liquid phase concentrations for As(III) and pyrite

Several models that are typically used to describe adsorption equilibrium were applied to fit this data. These include the Langmuir model ($q_e = \frac{q_{max} * b * C}{1 + b * C}$, where q_{max} is the maximum sorption capacity of the adsorbent, b is the equilibrium constant, C is the concentration of the adsorbate in the liquid phase), the Freundlich model ($q_e = k_f * C^{1/n}$), and the BET model ($q_e = \frac{q_{max} * k_b * C}{(C_s - C) * (1 + \frac{(K_b - 1) * C}{C_s})}$).

The Solver tool from the MS Excel was utilized to conduct a non-linear regression to choose values of coefficients in the model equations. Solver chooses values of coefficients that gave the lowest value of the sum of squared residuals, i.e. the difference between measurements and model predictions. The values of the model

coefficients and the sum of squares for the regressions are presented in table 5.4. The Langmuir model has the lowest sum of squares, which indicates that it fits the experimental data best. However, there was not a great difference in the values of the sum of squares among the different models. So, the Langmuir model is not clearly the best model.

Table 5.4 Values of coefficients and the sum of squares for different models describing data for As(III) and pyrite

Model isotherms		Sum of squares
Langmuir	$q_e = \frac{3.23 * 0.201 * C}{1 + 0.201 * C}$	2.30
Freundlich	$q_e = 0.993 * C^{1/4.27}$	5.09
BET	$q_e = \frac{2.53 * 379 * C}{(C_s - C) * (1 + \frac{(379 - 1) * C}{C_s})}$	3.40

Bostick and Fendorf (2003) conducted adsorption experiments for removal of As(III) by FeS (troilite) and FeS_2 (pyrite). Maximum solid phase concentrations of As(III) were found to be 14, and 231 μmol/g for FeS and FeS_2, respectively. The adsorption maximum with FeS_2 is much higher than that for FeS. As(III) sorption with FeS showed a Langmuir isotherm at low As concentration (up 20 μM), but followed a BET isotherm at higher As concentration. However, As(III) removed by pyrite followed the Langmuir isotherm up to 250 μM As. The maximum solid phase concentration of As(III) on pyrite measured in this research (3.23 μmol/g) is much lower than that reported by Bostick and Fendorf. This difference in maximum solid phase concentration could be due to differences in surface areas of pyrite. The surface area of pyrite used by Bostick and

Fendorf was reported to be 41 m^2/g. The surface area of pyrite used in this study is believed to be 4.1 m^2/g, based on the work by Wei (1995). This assumption was made because the procedures used in this study to produce pyrite are the same as those used by Wei in terms of the source of iron ($FeCl_3$), source of sulfur (NaHS), preparation in an anaerobic chamber, and the ratio of iron to sulfur (1:2). Since the surface area is larger for smaller particles, the sorption capacity for smaller particles is expected to be higher than for larger particles.

Macroscopic data, such as adsorption isotherm data, cannot explain the mechanisms that operate between an adsorbent and an adsorbate. Therefore, spectroscopic techniques have been applied by Bostick and Fendorf (2003). X-ray absorption spectroscopy (XAS) and X-ray photoelectron spectroscopy (XPS) are examples of spectroscopic techniques used to identify the structure and oxidation state of sorbed arsenic. They used the technique of XAS to verify that surface precipitation was occurring. Reduction of arsenic and oxidation of both surface S and Fe(II) were shown by XAS. Also, a mineral was formed when As(III) and FeS/FeS_2 were reacted that appeared to be similar to FeAsS or As_2S_3.

Data from experiments for removal of As(III) with synthesized disordered mackinawite (FeS) followed the Freundlich isotherm ($q_e = 0.026 * C_e^{0.98}$) at pH 7.4 (Wolthers 2005). Gallegos et al (2007) characterized pH dependent (pH 5, 7, and 9) uptake behavior when mackinawite (FeS) reacts with As(III), and they identified solid phase products formed using spectroscopic techniques. They reported reduction of As(III) to a lower valence state at pH 5 and 7 over the entire range of initial As(III) concentrations (5E-5 M through 5E-4 M) and at pH 9 at only a higher initial As(III)

concentration (5E-4M), but not at a lower initial As(III) concentration (5E-5M). They attributed this to an insufficient concentration of As(III). They suggested that a realgar-like precipitate was produced when mackinawite reacted with As(III).

As shown above, only a few researchers have studied iron sulfides as adsorbents for removal of arsenic. Generally, they agree that As(III) is reduced and forms a precipitate when it reacts with iron sulfides. Several models are able to describe experimental data for removal of As(III) by pyrite at lower As(III) concentrations. If As(III) is reduced and forms a precipitate on the surface, then more As may be removed from the liquid phase, resulting in data that would follow a BET-like isotherm model.

As(V)

Pyrite at a concentration of 1 g/l and As(V) at concentrations ranging from 13.3 through 133 μM were reacted for 360 minutes at pH 7. Fig. 5.7 shows arsenic concentration in solution (C), and arsenic concentration in solid phase (q_e) and several isotherm models.

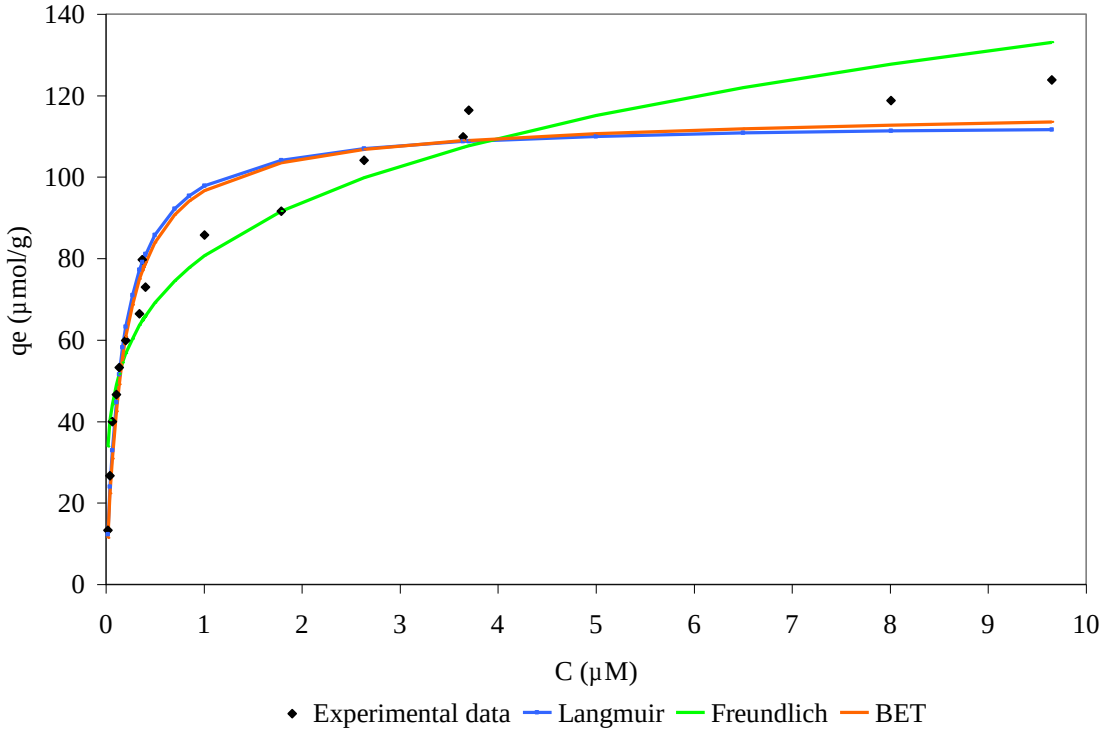

Fig. 5.7 Experimental data and model equations fit to solid and liquid phase concentration for As(V) and pyrite

The Langmuir, Freundlich, and BET models were compared for their ability to fit the measured data and the sum of squares was used to measure the goodness of fit. The values of coefficients in the isotherm models and the sum of squares are presented in table 5.5. Although, the BET isotherm had the lowest sum of squares, it is hard to conclude that the BET is a much better model, because the value of sum of squares for the Langmuir model was almost identical. Values of coefficients and the sum of squares for different models describing data for As(III) and pyrite are presented in Table 5.5.

Table 5.5 Values of coefficients and the sum of squares for different models describing data for As(V) and pyrite

Model isotherms		Sum of squares
Langmuir	$q_e = \frac{114 * 6.18 * C}{1 + 6.18 * C}$	833
Freundlich	$q_e = 80.6 * C^{1/4.52}$	1210
BET	$q_e = \frac{113 * 2837 * C}{(C_s - C) * (1 + \frac{(2837 - 1) * C}{C_s})}$	726

The capacity of pyrite for arsenic removal depends on the oxidation state of the arsenic species being removed. The capacity for removal of As(III) was 3.23 μmol/g, while the capacity of pyrite for As(V) removal was 113 μmol/g, which is approximately 35 times higher. As(III) was removed most effectively at pH 9 and As(V) was removed most effectively at pH 7.

Zouboulis et al. (1993) removed arsenic with pyrite that was obtained from a chemical producing company in Greece, because its low price offered an economic benefit. They found that optimum pH values for removing As(III) were basic (pH 7-9) and circumneutral pH for As(V). Also, more As(V) was removed than As(III) by the same amount of pyrite.

XPS analysis was conducted to determine the chemical oxidation state or chemical form of species on the surface of pyrite after contact with As(V). Pyrite that had not been contacted with As and pyrite that had been contacted with As(V) for a period of 2.5 days were analyzed by XPS. The sulfur 2p spectra for both samples is presented in Fig. 5.8. Results for pyrite that was not contacted with As is shown as a

solid line (pyrite w/o As) and results for pyrite that had been contacted with As(V) is shown as a dotted line (pyrite w/As for 2.5 days).

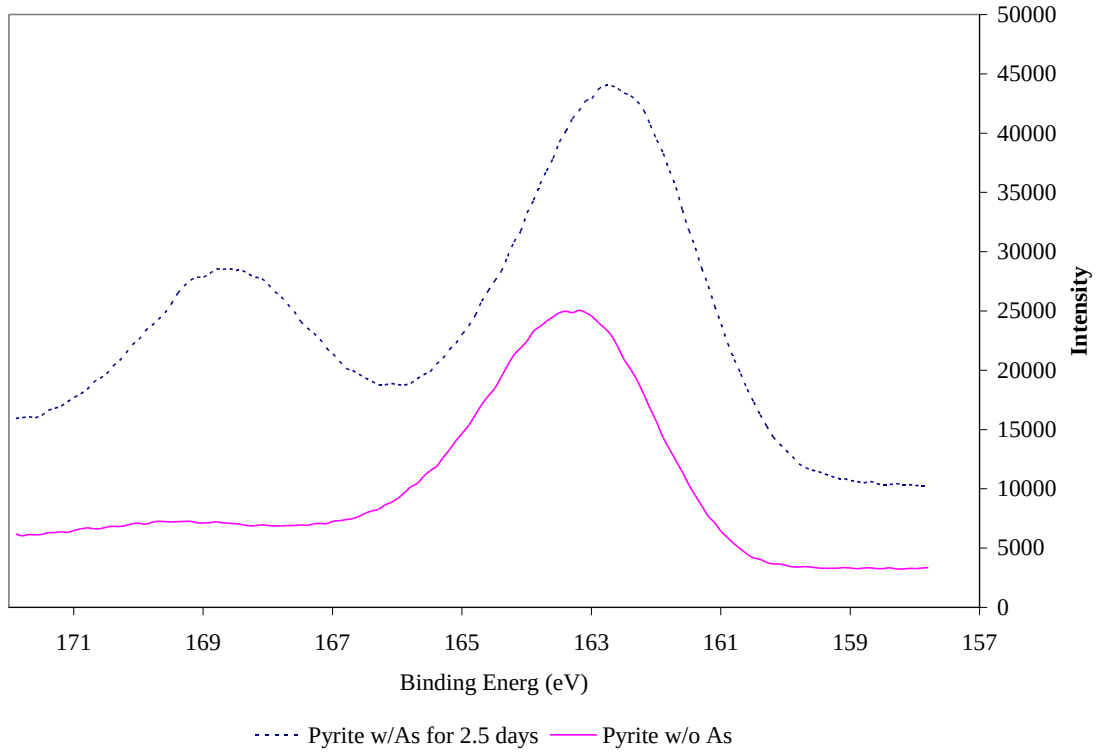

Fig. 5.8 The sulfur 2p spectra of pyrite not contacted with As and pyrite contacted with As(V) for 2.5 days

Pyrite that was not contacted with As will be identified as pristine pyrite and pyrite that was contacted with pyrite will be identified as As-pyrite. The S 2p spectra contains principal peaks at 163.3 eV for pristine pyrite and peaks at 168.59 and 162.69 eV for As-pyrite. The peak for pristine pyrite is found at a slightly higher binding energy than that of bulk pyrite measured by other researchers. Bostic and Fendorf (2002) reported this peak at 162.6 eV; Buckley and Woods (1984) found it at 162.1 eV and Nesbitt et al. (1995) reported it at 162.2 eV. However, As-pyrite shows an additional peak at 168.59 eV, which was identified as sulfate (SO_4^{2-}) by other researchers. Bostic and Fendorf (2002) found it at 169.0 eV; Nesbitt et al. (1995) reported it at 168.4 eV; and

Costa et al. (2002) measured it at 168.0 eV. The existence of sulfate indicates that sulfur in pyrite was oxidized by reaction with As(V). The Fe 2p spectra are presented in Fig. 5.9, with a dotted line used for As-pyrite and a solid line for pristine pyrite.

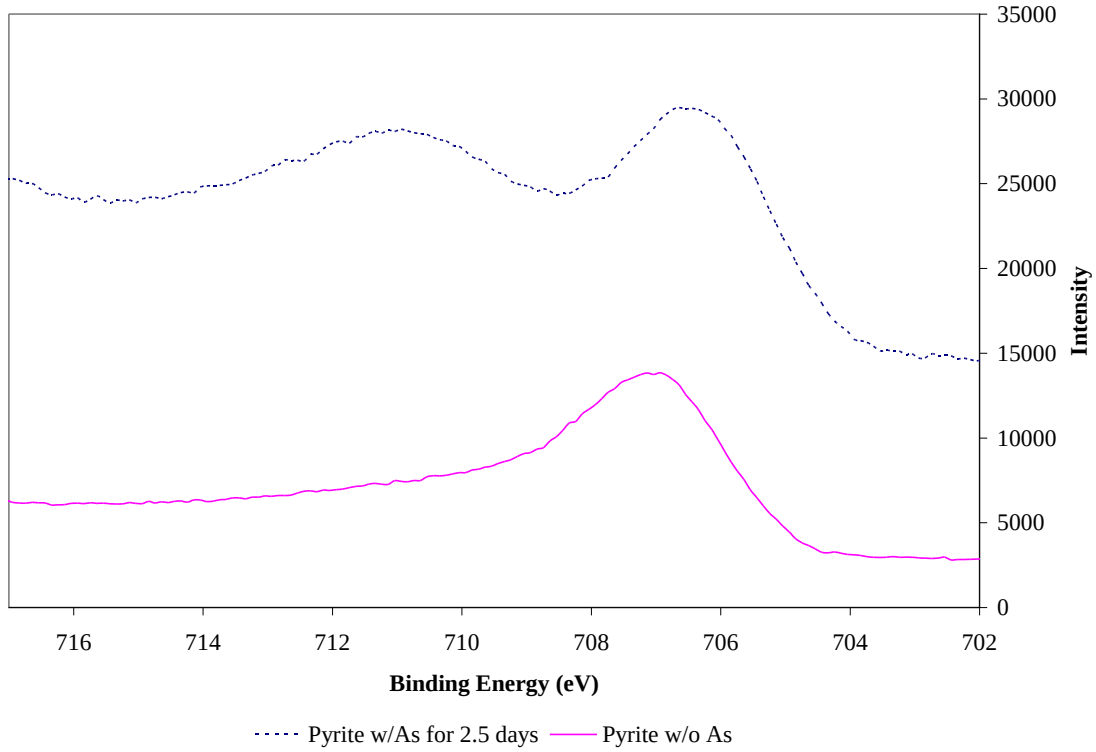

Fig. 5.9 The Fe 2p spectra of pyrite not contacted with As and pyrite contacted with As(V) for 2.5 days

The Fe 2p spectra contain principal peaks at 706.84 eV for pristine pyrite and 706.34 eV and 710.84 eV for As-pyrite. The peak from the pristine pyrite has been identified as being associated with pyrite by other researchers (Buckley and Woods 1984, Mycroft et al. 1990, Pratt et al. 1998, and Nesbitt and Muir 1994), who report the peak at slightly different locations (707.0 eV). In addition, As-pyrite showed an additional peak at 710.84 eV. Second peaks have also been reported by other researchers. Bostic and Fendorf (2002) as well as Costa et al. (2002) identified an additional peak as being associated with Fe(III)-OH and reported it to be located at 711.2 and 709.6 eV,

respectively. Bostic and Fendorf (2002), Nesbitt and Muir (1998), and Nesbitt et al. (1995) identified another peak as being associated with Fe(III)-As-S and located it at 709.2, 710.78 and 710.78 eV, respectively. It is hard to conclude whether the additional peak is due to Fe(III)-OH or Fe(III)-As-S, based on the peak location. However, it can be inferred the iron was oxidized by the reaction of As(V) with the surface, because the binding energy increased .

CHAPTER VI

STABILITY OF ARSENIC-PYRITE SOLIDS

6.1 INTRODUCTION

It is important to remove arsenic from arsenic contaminated water and wastewater. However, it is much more important that arsenic not be released from residual materials produced by the treatment systems. Recent studies show that there is high probability that arsenic can be leached from wastes under anoxic conditions or extreme pH (Jain et al. 1999, Bose and Sharma 2002, Bennett & Dudas 2003, Mohapatra et al. 2005, Kocar et al. 2006, Al-Abed et al. 2007, Copeland et al. 2007). How strongly arsenic is bound to pyrite is investigated in this chapter. This part of the project measured the ability of products produced by treatment of arsenic contaminated water to resist release of arsenic in leaching tests with wide ranges of pH. The amount of arsenic that was leached from the wastes was measured using two procedures. One procedure conducted the leach test at the natural pH of the waste and evaluated the effect of time, while the other procedure evaluated the effect of pH.

6.2 RESULTS AND DISCUSSION

A detailed description of experimental procedures used to develop data presented in this section is presented in Chapter III. The goal of this study was to determine what would be the effects of time and pH on release of arsenic from pyrite that had removed arsenic from solution. Experiments were conduced with both As(III) and As(V).

6.2.1 Kinetic Experiments

This section presents results of experiments to determine the effect of time on release of arsenic by pyrite. Two types of experiments were conducted. The first produced arsenic-contaminated pyrite and the second evaluated release of arsenic from those solids. Removal experiments were conducted at pH 9 with As(III) and pH 7 with As(V), based on previous experimental results (chapter V). Table 6.1 summarizes other experimental conditions for removal and release experiments.

Table 6.1 Experimental conditions for determining effects of time on arsenic release

	As species	Initial As conc. (μM)	Pyrite conc. (g/l)	pH	Reaction Time (min.)
Removal	As(III)	53.4	1	9	2880
	As(V)	53.4	1	7	2880
Release	As(III)			7	30, 120, 360, 720, 1440, 2880, 5760, and 10080
	As(V)			7	30, 120, 360, 720, 1440, 2880, 5760, and 10080

As(III)

The concentration of As(III) in the liquid phase after the reaction with pyrite for a period of 2880 minutes was measured as 31.2 μM, which means that 22.2 μM of arsenic was transferred to the solid phase, resulting in a solid phase concentration of 22.2 μmol/g. After arsenic removal, the pH of the suspension was adjusted to pH 7 and samples were taken for analysis at the time intervals of 30, 120, 360, 720, 1440, 2880 (2 days), 5760 (4 days), and 10080 (7 days). The concentration of arsenic in the solid phase as a function of time is shown in Fig. 6.1.

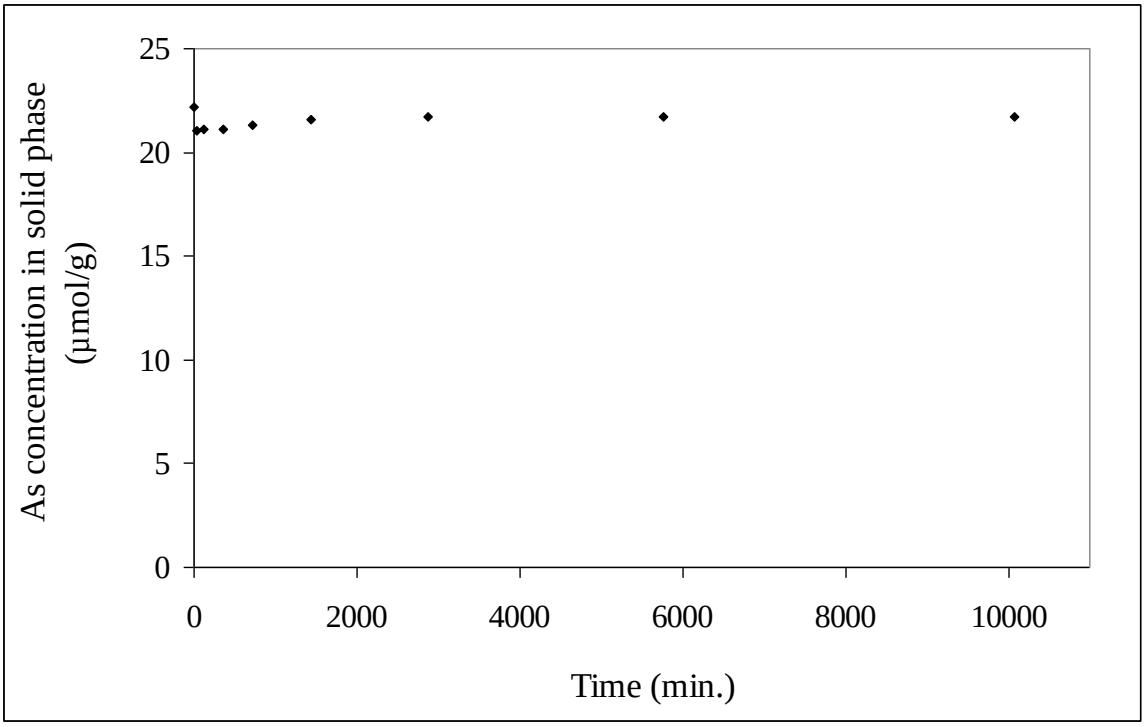

Fig. 6.1 Desorption kinetic experiment with As(III)-pyrite solid

Little arsenic was leached from the arsenic-pyrite solid, resulting in between 96 to 98 % of arsenic remaining on the solid. The arsenic concentration changed very little from the first measurement (30 min) to the last one (10,080 min). A reaction time of 2880 min was chosen for experiments to evaluate the effect of pH on release.

As(V)

The concentration of As(V) in the liquid phase after the reaction with pyrite for the period of 2880 minutes was measured as 0.15 µM, which means that 53.2 µM of arsenic was transferred to the solid phase, resulting in a solid phase concentration of 53.2 µmol/g. The pH of the suspension was adjusted to pH 7, and samples were taken for analysis at time intervals of 30, 120, 360, 720, 1440, 2880 (2 days), 5760 (4 days), and

10080 (7 days). Fig. 6.2 shows the concentrations of arsenic in the solid phase as a function of time.

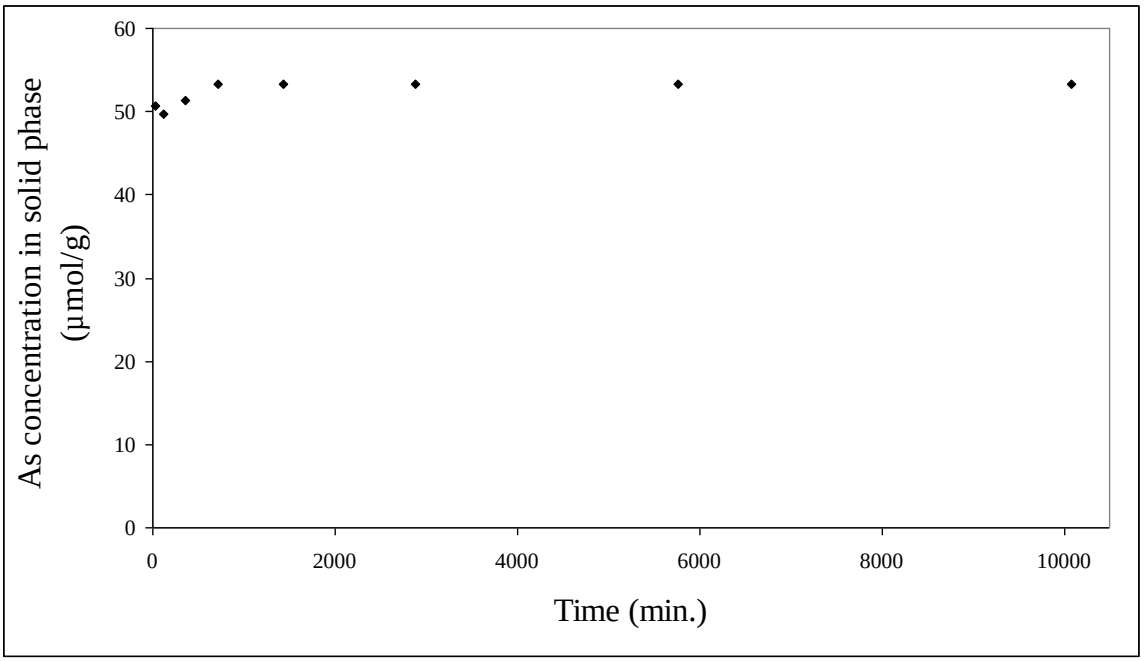

Fig. 6.2 Desorption kinetic experiment with As(V)-pyrite solid

Little arsenic leached from the arsenic-pyrite solid, resulting in between 93% to 100 % remaining on the solid. Also, there was little difference in the amount leached after 720 min. A reaction time of 1440 min. was chosen for experiments to evaluate the effect of pH on leaching.

6.2.2 pH Effects

This section presents results of experiments to evaluate the effect of pH on arsenic release from pyrite. The experimental conditions were as same as those used in the kinetic experiment, except pH was varied over a range from pH 4 through pH 10. Measurements were made over at time period of 2880 minutes for As(III) and 1440 minutes for As(V).

As(III)

The initial arsenic concentrations in the solid phase were 35.4 µmol/g. The initial and final concentrations in the liquid phase were used with a material balance to calculate the amount of arsenic remaining on the solid phase and these results are presented in Fig. 6.3.

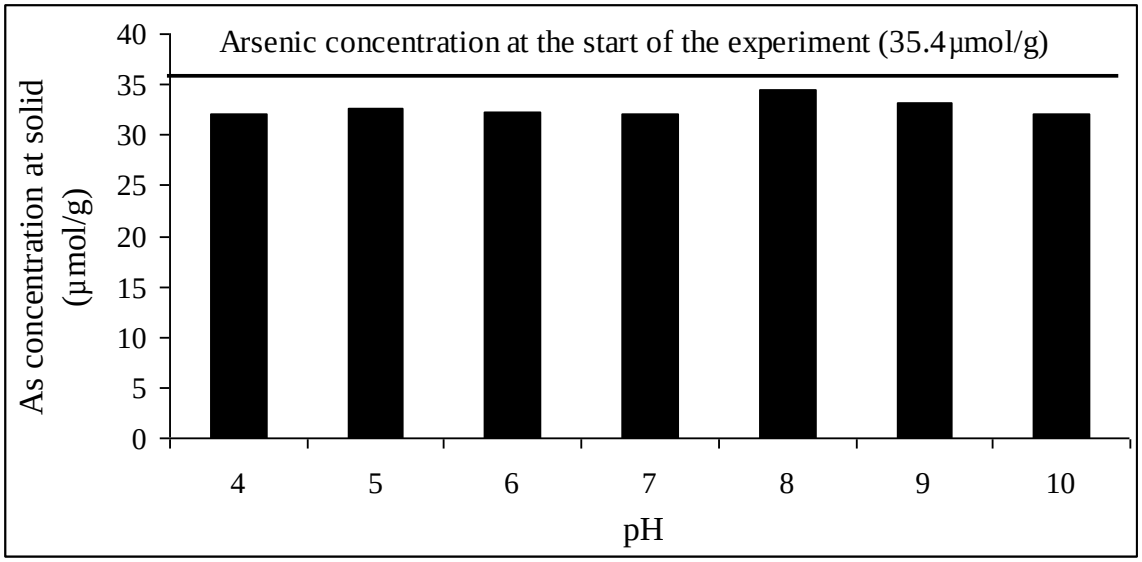

Fig. 6.3 As(III) concentration on the solid phase over a range of pH after leaching

The concentrations of arsenic in the solid phase ranged from 32.0 to 34.4 µmol/g, which means that only a small percentage of arsenic (2.82 to 9.60 %) was released. Also, there was only a small effect of pH on arsenic release. Experiments to determine an As(III) adsorption envelope on goethite (α-FeOOH) were conducted by Manning et al. (1998) and they found that little change was caused by changes in pH. To determine how As(III) was bound to the surface of α-FeOOH, they used the technique of EXAFS, which showed that As(III) forms an inner-sphere, bidentate binuclear bridging complex with As-O and As-Fe. Also, they concluded that both pH and As(III) surface coverage had only minor influence on the As-Fe interatomic distance and coordination number. It is

hard to confirm that As(III) forms an inner-sphere complex with pyrite, because the surface analysis of As(III) on pyrite was not conducted. However, it is possible to conclude that strong binding between As(III) and pyrite prevents the release of As(III) regardless of pH conditions, if As(III) and pyrite interact the same as do As(III) and α-FeOOH.

Bostick and Fendorf (2003) conducted research on As(III) sorption by pyrite and they found that after As(III) sorbed on the pyrite, an arsenopyrite-like mineral was formed, which was identified by X-ray absorption spectroscopy. When As(III) was sorbed on pyrite in the natural environment, stable minerals such as arsenopyrite (Bostick and Fendorf, 2003) or arsenian pyrite (Wolthers et al. 2005) were formed.

As(III) sorption experiments were conducted with sediments from a sulfidic estuarine marsh and the structure of As(III) retained on the solids was measured using X-ray absorption spectroscopy by Bostick et al. (2004). The samples were a mixture of quartz, feldspars, and organic matter. Pyrite was also detected in the samples using XRD, and most of the iron was present as an iron sulfide identified as mackinawite. They found that As(III) sorption increased gradually over the entire pH range and much of As(III) had undergone significant structural changes during sorption, going from oxygen coordination in As(III) to sulfur coordination on the sediments. After As(III) sorbed onto iron sulfide samples, an arsenopyrite-like (FeAsS) mineral was formed and its conversion to orpiment (As_2S_3) was shown using EXAFS over 21 days.

Results from the experiment on the effect of pH on removal of As(III) by pyrite led to the conclusion that reaction of As(III) and pyrite would form environmentally

stable minerals, such as arsenopyrite or orpiment, and this precipitates would not release arsenic over the entire pH range (pH 4 – pH 10).

As(V)

The initial arsenic concentrations in the solid phase were 28.9 µmol/g. The initial and final arsenic concentrations in the solution were used with a material balance to calculate the amount of arsenic remaining on the solid phase and these results are presented in Fig. 6.4.

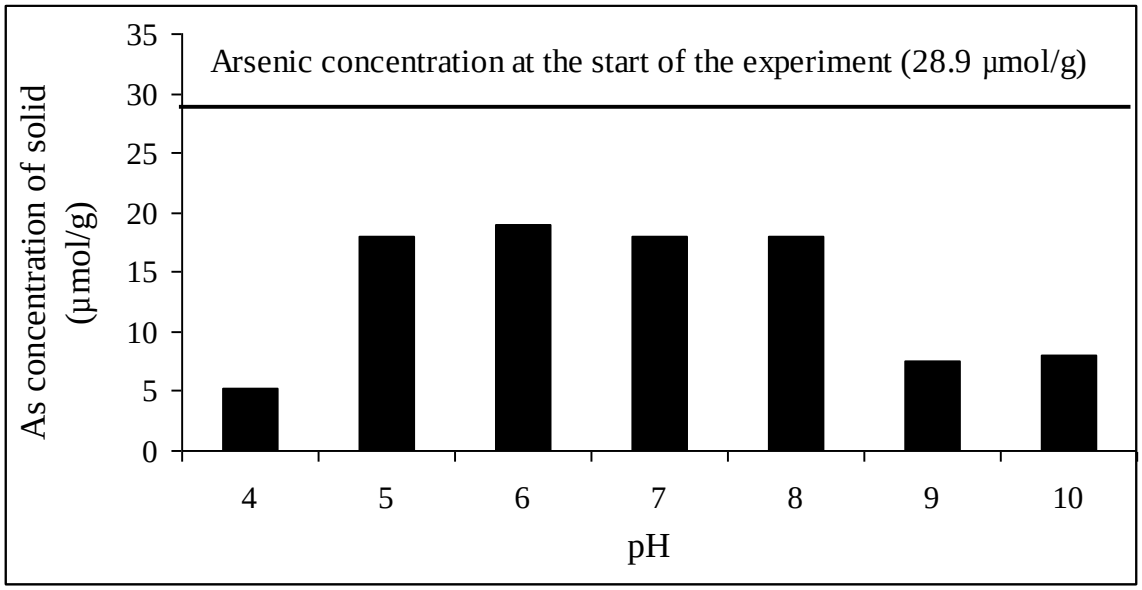

Fig. 6.4 As(V) concentration on the solid phase over a range of pH after leaching

The concentrations of arsenic in the solid phase ranged widely, from 5.22 to 19.0 µmol/g, with the highest concentration at pH 6 and lowest at pH 4. The percentage of arsenic remaining on the solid phase ranged from 21.4 % to 77.9 %. There were low levels of release in the range of pH from pH 5 through pH 8, while higher arsenic release was observed at pH 4, pH 9, and pH 10. These results are consistent with those of Copeland et al (2007), who reported the amounts of arsenic released from solids and

sediments collected by flushing a drinking water distribution system. They found that arsenic release was greatly affected by pH and increased with increasing pH over the range pH 7 to pH 9.

More As(V) was released from pyrite than As(III), which shows that As(V)-pyrite solids are less stable than As(III)-pyrite solids. There are some effects of pH on release of arsenic(V), while there was little effect of pH on release of arsenic(III).

As(III) might be interacting with different sites on the pyrite surface than does As(V). As(III) might contact with pyrite by forming an inner-sphere complex, then forms arsenopyrite like minerals, while As(V) might contact with pyrite at different sites or in different ways. The attraction between As(V) and pyrite cannot be an electrostatic coulombic interaction, because the point of zero charge (PZC) for pyrite is 2.3 and As(V) is present in species ($HAsO^{2-}_4$ and $H_2AsO_4^-$) with a negative charge for pH above 2.2. If outer-sphere complexes between As(V) and pyrite are to form, the zero point of charge for pyrite should be high enough to give a positively charged surface at the pH values used in experiments. A positively charged surface would attract the negatively charged As(V) ions and this attraction would exist at all pH values above pH 2.2. However, the pH_{zpc} for pyrite was determined to be 2.3 (Wei 1995), which means that pyrite would have a negative charge under all experimental conditions. Therefore, coulombic interactions can not explain the attraction of As(V) for the surface of pyrite. However, As(III) and As(V) both could form inner-sphere complexes on the pyrite surface, but with different bond strengths. Many researchers (Luo et al. 2006, Pena et al. 2006, Manning et al. 2002, Farquhar et al. 2002, Manning et al. 1998, and Sparks 1995) have found that

As(V) forms inner-sphere complexes, including monodentate-mononuclear and bidentate-binuclear surface complexes.

CHAPTER VII

CONCLUSIONS AND SUMMARY

7.1 CHARACTERIZE AND OPTIMIZE THE SYNTHESIS PROCEDURE FOR PYRITE (CHAPTER IV)

It is important to produce pyrite to remove arsenic from water and to stabilize arsenic in wastes, but it is more critical to make pyrite with smaller particle size, higher yield, and shorter synthesis time. Many methods are available to synthesize pyrite using different sources of iron and sulfur. $FeCl_3$ and NaHS were selected, because the procedure using them is relatively straightforward and fast.

The effects of pH, reaction time, temperature, and ratio of ferric iron to sulfide on synthesis of pyrite were investigated. After reacting and mixing solutions containing $FeCl_3$ and NaHS under the anaerobic conditions, pyrite was produced only in solutions with pH ranging from pH 3.6 to pH 5.6. Also, it took more than 2 days to start pyrite synthesis after the solutions of $FeCl_3$ and NaHS were mixed. Moreover, it took more than 6 days to reach maximum theoretical pyrite concentration. However, it took only one hour to start synthesizing pyrite at 60 °C. Also, it took less than one day to reach the theoretical maximum pyrite concentration. It is generally assumed that the rate of reaction is increased with temperature increase. In order to increase the yield of pyrite, the optimum Fe^{3+}/HS^- values of 0.500 and 0.571 were selected based on the amounts of HS^- used.

The solid phase produced using the conditions described above was verified to be pyrite by XRD. The stability of pyrite in air was measured by putting the synthesized

pyrite in air at room temperature for 3 days. XRD analysis verified that the remaining solid phase did not change from being pyrite.

7.2 CHARACTERIZE REMOVAL OF ARSENIC BY SYNTHESIZED PYRITE (CHAPTER V)

Kinetics of the removal of arsenic by pyrite was determined to estimate the optimum contact time with arsenic and pyrite. Reaction times of 30 and 360 minutes were selected for As(III) and pyrite, and As(V) and pyrite, respectively, because the kinetic experiment showed that removal of arsenic by sorption was almost complete during those periods.

Optimum pH for removal of As(III) by pyrite was pH 9, while optimum pH for removal of As(V) by pyrite was pH 7. Experiments to measure arsenic removal by pyrite with optimal reaction time and pH were performed with each arsenic species. The maximum solid phase concentration of As(III) on pyrite was 3.23 μmol/g. Arsenic removal capacity on pyrite was not as great as other adsorbents, but a potential advantage of using pyrite is that it is stable for geological time periods under reducing conditions, so that it helps prevent release of arsenic. A few researchers have studied iron sulfides as adsorbents for arsenic and they agree that As(III) is reduced after removal from solution and forms a precipitate when it reacts with iron sulfides.

The maximum solid phase concentration of As(V) on pyrite was 113 μmol/g. XPS analysis of pyrite that had not been contacted with As, and pyrite that had been contacted with As(V) for a period of 2.5 days (As-pyrite) showed that both iron and sulfur on As-pyrite were oxidized. This was indicated in XPS spectra by the presence of

an additional peak associated with SO_4^{2-} and peaks associated with either Fe(III)-OH or Fe(III)-As-S.

7.3 STABILITY OF ARSENIC-PYRITE SOLIDS (CHAPTER VI)

Most of the arsenic, whether As(III) or As(V), that had been removed by pyrite remained on the pyrite during period of the stability experiments (7 days). The stability experiment with As(III)-pyrite showed that less than 10% of arsenic was released from the As(III)-pyrite regardless of pH over the range examined (pH 4 – pH 10). These results indicate that after reacting with pyrite, As(III) forms environmentally stable minerals, such as arsenopyrite or orpiment.

The stability experiment with As(V)-pyrite showed that there were low levels of release in the range of pH from pH 5 through pH 8, while higher arsenic release was observed at pH 4, pH 9, and pH 10. The percentage of arsenic remaining on the solid phase varied from 21.4 % to 77.9 %.

More As(V) was released from pyrite than As(III), which shows that As(V)-pyrite solids are less stable than As(III)-pyrite solids. There is some effect of pH on release of arsenic(V), while there was little effect of pH on release of arsenic(III). As(III) might contact with pyrite by forming an inner-sphere complex, followed by formation of arsenopyrite-like minerals, while As(V) might contact with pyrite at different sites or in different ways.

REFERENCES

Aggett, J. and A. C. Aspell (1976). "Determination of arsenic(III) and total arsenic by atomic-absorption spectroscopy." *Analyst* 101(1202): 341-347.

Ahmann, D., Krumholz, L. R., Hemond, H. F., Lovley, D. R., and Morel, F. M. M. (1997). "Microbial mobilization of arsenic from sediments of the Aberjona Watershed." *Environ. Sci. Technol.*, 31(10), 2923-2930.

Al-Abed, S. R., Jegadeesan, G., Purandare, J., and Allen, D. (2007). "Arsenic release from iron rich mineral processing waste: Influence of pH and redox potential." *Chemosphere*, 66(4), 775-782.

Arai, Y., Elzinga, E. J., and Sparks, D. L. (2001). "X-ray absorption spectroscopic investigation of arsenite and arsenate adsorption at the aluminum oxide-water interface." *J. Colloid Interface Sci.*, 235(1), 80-88.

ATSDR (Agency for Toxic Substances and Disease Registry) (2007). Toxicological Profile for Arsenic. U. S. Dept. of. Health and Human Services. Atlanta, GA.

Baker, W. (2002). "Electrochemical and spectroscopic studies of novel electroactive nanostrutures." Ph.D. Dissertation, Texas A & M University, College Station.

Beaulieu, B. T. and K. S. Savage (2005). "Arsenate adsorption structures on aluminum oxide and phyllosilicate mineral sufaces in smelter-impacted soils." *Environmental Science & Technology* 39(10): 3571-3579.

Behra, P., Bonnissel-Gissinger, P., Alnot, M., Revel, R., and Ehrhardt, J. J. (2001). "XPS and XAS study of the sorption of Hg(II) onto pyrite." *Langmuir*, 17(13), 3970-3979.

Bennett, B. and M. J. Dudas (2003). "Release of arsenic and molybdenum by reductive dissolution of iron oxides in a soil with enriched levels of native arsenic." *Journal of Environmental Engineering and Science* 2(4): 265-272.

Berner, R. A. (1970). "Sedimentary pyrite formation." *American Journal of Science* 268(1): 1-23.

Blakey, N. C. (1984). "Behavior of arsenical wastes codisposed with domestic solid-wastes." *Journal Water Pollution Control Federation* 56(1): 69-75.

Borah, D. and K. Senapati (2006). "Adsorption of Cd(II) from aqueous solution onto pyrite." *Fuel* 85(12-13): 1929-1934.

Bose, P. and A. Sharma (2002). "Role of iron in controlling speciation and mobilization

of arsenic in subsurface environment." *Water Research* 36(19): 4916-4926.

Bostick, B. C., Chen, C., and Fendorf, S. (2004). "Arsenite retention mechanisms within estuarine sediments of Pescadero, CA." *Environ. Sci. Technol.*, 38(12), 3299-3304.

Bostick, B. C. and S. Fendorf (2003). "Arsenite sorption on troilite (FeS) and pyrite (FeS2)." *Geochimica Et Cosmochimica Acta* 67(5): 909-921.

Bowell, R. J. (1994). "Sorption of arsenic by iron-oxides and oxyhydroxides in soils." *Applied Geochemistry* 9(3): 279-286.

Brookins, D. G. (1988). *Eh-pH Diagrams for Geochemistry*. Springer-Verlag Berlin, New York.

Buckley, A. N. and R. Woods (1984). "An x-ray photoelectron spectroscopic study of the oxidation of galena." *Applied Surface Science* 17(4): 401-414.

Butler, I. B. and D. Rickard (2000). "Framboidal pyrite formation via the oxidation of iron (II) monosulfide by hydrogen sulphide." *Geochimica Et Cosmochimica Acta* 64(15): 2665-2672.

Chen, W. F., Parette, R., Zou, J. Y., Cannon, F. S., and Dempsey, B. A. (2007). "Arsenic removal by iron-modified activated carbon." *Water Res.*, 41(9), 1851-1858.

Cheng, R. C., Wang, H. C., and Beuhler, M. D. (1994). "Enhanced coagulation for arsenic removal." *J. Am. Water Work Assoc.*, 86(9), 79-90.

Chou, C. and C. T. De Rosa (2003). "Case studies - arsenic." *International Journal of Hygiene and Environmental Health* 206(4-5): 381-386.

Chuang, C. L., Fan, M., Xu, M., Brown, R. C., Sung, S., Saha, B., and Huang, C. P. (2005). "Adsorption of arsenic(V) by activated carbon prepared from oat hulls." *Chemosphere*, 61(4), 478-483.

Copeland, R. C., Lytle, D. A., and Dionysiou, D. D. (2007). "Desorption of arsenic from drinking water distribution system solids." *Environ. Monit. Assess.*, 127(1-3), 523-535.

Costa, M. C., do Rego, A. M. B., and Abrantes, L. M. (2002). "Characterization of a natural and an electro-oxidized arsenopyrite: a study on electrochemical and X-ray photoelectron spectroscopy." *Int. J. Miner. Process.*, 65(2), 83-108.

deLemos, J. L., Bostick, B. C., Renshaw, C. E., Sturup, S., and Feng, X. H. (2006). "Landfill-stimulated iron reduction and arsenic release at the Coakley Superfund Site (NH)." *Environ. Sci. Technol.*, 40(1), 67-73.

Deschamps, E., Ciminelli, V. S. T., and Holl, W. H. (2005). "Removal of As(III) and As(V) from water using a natural Fe and Mn enriched sample." *Water Res.*, 39(20), 5212-5220.

Dixit, S. and J. G. Hering (2003). "Comparison of arsenic(V) and arsenic(III) sorption onto iron oxide minerals: Implications for arsenic mobility." *Environmental Science & Technology* 37(18): 4182-4189.

Driehaus, W., Jekel, M., and Hildebrandt, U. (1998). "Granular ferric hydroxide - a new adsorbent for the removal of arsenic from natural water." *J. Water Serv. Res. Technol.-Aqua*, 47(1), 30-35.

Edwards, M. (1994). "Chemistry of arsenic removal during coagulation and Fe-Mn oxidation." *Journal American Water Works Association* 86(9): 64-78.

Ehrhardt, J. J., Behra, P., Bonnissel-Gissinger, P., and Alnot, M. (2000). "XPS study of the sorption of Hg(II) onto pyrite FeS2." John Wiley & Sons Ltd, 269-272.

Elizalde-Gonzalez, M. P., Mattusch, J., and Wennrich, R. (2001). "Application of natural zeolites for preconcentration of arsenic species in water samples." Royal Soc Chemistry, 22-26.

EPA (2000). "Technologies and costs for removal of arsenic from drinking water." EPA, Washington, DC.

EPA (2001). "National primary drinking water regulations; arsenic and clarificaitons to compliance and new source contaminants monitoring." 66. EPA, Washington, DC.

EPA (2002). "Arsenic treatment technologies for soil, waste, and water." EPA, Washington, DC.

Essington, M. E. (2004). *Soil and Water Chemistry*, CRC Press, Boca Raton, Florida.

Farquhar, M. L., Charnock, J. M., Livens, F. R., and Vaughan, D. J. (2002). "Mechanisms of arsenic uptake from aqueous solution by interaction with goethite, lepidocrocite, mackinawite, and pyrite: An X-ray absorption spectroscopy study." *Environ. Sci. Technol.*, 36(8), 1757-1762.

Gallegos, T. J., Hyun, S. P., and Hayes, K. F. (2007). "Spectroscopic investigation of the uptake of arsenite from solution by synthetic mackinawite." *Environ. Sci. Technol.*, 41(22), 7781-7786.

Ghosh, A., Mukiibi, M., and Ela, W. (2004). "TCLP underestimates leaching of arsenic from solid residuals under landfill conditions." *Environ. Sci. Technol.*, 38(17), 4677-4682.

Ghosh, A., Mukiibi, M., Saez, A. E., and Ela, W. P. (2006). "Leaching of arsenic from granular ferric hydroxide residuals under mature landfill conditions." *Environ. Sci. Technol.*, 40(19), 6070-6075.

Goldberg, S. (2002). "Competitive adsorption of arsenate and arsenite on oxides and clay minerals." *Soil Science Society of America Journal* 66(2): 413-421.

Goldberg, S. and C. T. Johnston (2001). "Mechanisms of arsenic adsorption on amorphous oxides evaluated using macroscopic measurements, vibrational spectroscopy, and surface complexation modeling." *Journal of Colloid and Interface Science* 234(1): 204-216.

Gong, Z. L., Lu, X. F., Ma, M. S., Watt, C., and Le, X. C. (2002). "Arsenic speciation analysis." *Talanta*, 58(1), 77-96.

Grafe, M., Eick, M. J., and Grossl, P. R. (2001). "Adsorption of arsenate (V) and arsenite (III) on goethite in the presence and absence of dissolved organic carbon." *Soil Sci. Soc. Am. J.*, 65(6), 1680-1687.

Graham, U. M. and H. Ohmoto (1994). "Experimental-study of formation mechanism of hydrothermal pyrite." *Geochimica Et Cosmochimica Acta* 58(10): 2187-2202.

Halim, C. E., Scott, J. A., Amal, R., Short, S. A., Beydoun, D., Low, G., and Cattle, J. (2005). "Evaluating the applicability of regulatory leaching tests for assessing the hazards of Pb-contaminated soils." *Journal of Hazardous Materials*, 120(1-3), 101-111.

Han, J. T. and W. S. Fyfe (2000). "Arsenic removal from water by iron-sulphide minerals." *Chinese Science Bulletin* 45(15): 1430-1434.

Hering, J. G., Chen, P. Y., Wilkie, J. A., and Elimelech, M. (1997). "Arsenic removal from drinking water during coagulation." *J. Environ. Eng.-ASCE*, 123(8), 800-807.

Hounslow, A. W. (1980). "Groundwater geochemistry – arsenic in landfills." *Ground Water* 18(4): 331-333.

Jain, A. and R. H. Loeppert (2000). "Effect of competing anions on the adsorption of arsenate and arsenite by ferrihydrite." *Journal of Environmental Quality* 29(5): 1422-1430.

Jain, A., Raven, K. P., and Loeppert, R. H. (1999). "Arsenite and arsenate adsorption on ferrihydrite: Surface charge reduction and net OH- release stoichiometry." *Environ. Sci. Technol.*, 33(8), 1179-1184.

Jeong, Y., Fan, M., Singh, S., Chuang, C. L., Saha, B., and van Leeuwen, H. (2007). "Evaluation of iron oxide and aluminum oxide as potential arsenic(V)

adsorbents." *Chem. Eng. Process.*, 46(10), 1030-1039.

Jessen, S., Larsen, F., Koch, C. B., and Arvin, E. (2005). "Sorption and desorption of arsenic to ferrihydrite in a sand filter." *Environ. Sci. Technol.*, 39(20), 8045-8051.

Jing, C. Y., Liu, S. Q., Patel, M., and Meng, X. G. (2005). "Arsenic leachability in water treatment adsorbents." *Environ. Sci. Technol.*, 39(14), 5481-5487.

Jones, F. T. (2007). "A broad view of arsenic." *Poultry Science* 86(1): 2-14.

Kanel, S. R., Greneche, J. M., and Choi, H. (2006). "Arsenic(V) removal kom groundwater using nano scale zero-valent iron as a colloidal reactive barrier material." *Environ. Sci. Technol.*, 40(6), 2045-2050.

Kober, R., Welter, E., Ebert, M., and Dahmke, A. (2005). "Removal of arsenic from groundwater by zerovalent iron and the role of sulfide." *Environ. Sci. Technol.*, 39(20), 8038-8044.

Kocar, B. D., Herbel, M. J., Tufano, K. J., and Fendorf, S. (2006). "Contrasting effects of dissimilatory iron(III) and arsenic(V) reduction on arsenic retention and transport." *Environ. Sci. Technol.*, 40(21), 6715-6721.

Ladeira, A. C. Q. and V. S. T. Ciminelli (2004). "Adsorption and desorption of arsenic on an oxisol and its constituents." *Water Research* 38(8): 2087-2094.

Leist, M., Casey, R. J., and Caridi, D. (2000). "The management of arsenic wastes: problems and prospects." *Journal of Hazardous Materials*, 76(1), 125-138.

Liu, Y. T., Wang, M. K., Chen, T. Y., Chiang, P. N., Huang, P. M., and Lee, J. F. (2006). "Arsenate sorption on lithium/aluminum layered double hydroxide intercalated by chloride and on gibbsite: Sorption isotherms, envelopes, and spectroscopic studies." *Environ. Sci. Technol.*, 40(24), 7784-7789.

Luo, L., Zhang, S. Z., Shan, X. Q., Jiang, W., Zhu, Y. G., Liu, T., Xie, Y. N., and McLaren, R. G. (2006). "Arsenate sorption on two Chinese red soils evaluated with macroscopic measurements and extended X-ray absorption fine-structure spectroscopy." *Environ. Toxicol. Chem.*, 25(12), 3118-3124.

Luther, G. W. (1991). "Pyrite synthesis via polysulfide compounds." *Geochimica Et Cosmochimica Acta* 55(10): 2839-2849.

Mandal, B. K. and K. T. Suzuki (2002). "Arsenic round the world: a review." *Talanta* 58(1): 201-235.

Manning, B. A., Fendorf, S. E., and Goldberg, S. (1998). "Surface structures and stability of arsenic(III) on goethite: Spectroscopic evidence for inner-sphere complexes."

Environ. Sci. Technol., 32(16), 2383-2388.

Manning, B. A., Hunt, M. L., Amrhein, C., and Yarmoff, J. A. (2002). "Arsenic(III) and Arsenic(V) reactions with zerovalent iron corrosion products." *Environ. Sci. Technol.*, 36(24), 5455-5461.

Masscheleyn, P. H., Delaune, R. D., and Patrick, W. H. (1991). "A hydride generation atomic-absorption technique for arsenic speciation." *J. Environ. Qual.*, 20(1), 96-100.

Meng, X. G., Korfiatis, G. P., Jing, C. Y., and Christodoulatos, C. (2001). "Redox transformations of arsenic and iron in water treatment sludge during aging and TCLP extraction." *Environ. Sci. Technol.*, 35(17), 3476-3481.

Mohan, D. and C. U. Pittman (2007). "Arsenic removal from water/wastewater using adsorbents - a critical review." *Journal of Hazardous Materials* 142(1-2): 1-53.

Mohapatra, D., Singh, P., Zhang, W., and Pullammanappallil, P. (2005). "The effect of citrate, oxalate, acetate, silicate and phosphate on stability of synthetic arsenic-loaded ferrihydrite and Al-ferrihydrite." *Journal of Hazardous Materials*, 124(1-3), 95-100.

Mycroft, J. R., Bancroft, G. M., McIntyre, N. S., Lorimer, J. W., and Hill, I. R. (1990). "Detection of sulfur and polysulfides on electrochemically oxidized pyrite surfaces by x-ray photoelectron-spectroscopy and raman-spectroscopy." *J. Electroanal. Chem.*, 292(1-2), 139-152.

Nesbitt, H. W. and I. J. Muir (1998). "Oxidation states and speciation of secondary products on pyrite and arsenopyrite reacted with mine waste waters and air." *Mineralogy and Petrology* 62(1-2): 123-144.

Nesbitt, H. W., Muir, L. J., and Pratt, A. R. (1995). "Oxidation of arsenopyrite by air and air-saturated distilled water, and implications for mechanism of oxidation." *Geochimica Et Cosmochimica Acta* 59(9): 1773-1786.

Nesbitt, H. W. and I. J. Muir (1994). "X-ray photoelectron spectroscopic study of a pristine pyrite surface reacted with water-vapor and air." *Geochimica Et Cosmochimica Acta* 58(21): 4667-4679.

Pena, M., Meng, X. G., Korfiatis, G. P., and Jing, C. Y. (2006). "Adsorption mechanism of arsenic on nanocrystalline titanium dioxide." *Environ. Sci. Technol.*, 40(4), 1257-1262.

Pratt, A. R., McIntyre, N. S., and Splinter, S. J. (1998). "Deconvolution of pyrite marcasite and arsenopyrite XPS spectra using the maximum entropy method." *Surf. Sci.*, 396(1-3), 266-272.

Raven, K. P., Jain, A., and Loeppert, R. H. (1998). "Arsenite and arsenate adsorption on ferrihydrite: Kinetics, equilibrium, and adsorption envelopes." *Environ. Sci. Technol.*, 32(3), 344-349.

Riley, R. G. and J. M. Zachara. (1992). "Chemical contaminants on DOE lands and selection of contaminant mixtures for subsurface science research." *DOE/ER-0547T*, Department of Energy, Washington, DC.

Smedley, P. L. and D. G. Kinniburgh (2002). "A review of the source, behaviour and distribution of arsenic in natural waters." *Applied Geochemistry* 17(5): 517-568.

Sparks, D. (1995). *Environmental Soil Chemistry*, Academic Press, INC, San Diego, California.

Sunagawa, I., Y. Endo, and N. Nakai (1971). "Hydrothermal synthesis of framboidal pyrite." *Journal of the Society of Mining Geologists of Japan*(2): 10-14.

Watts, J. F. (1990). *An introduction to surface analysis by electron spectr*oscopy, Oxford Science Publications, New York.

Waychunas, G. A., Rea, B. A., Fuller, C. C., and Davis, J. A. (1993). "Surface-chemistry of ferrihydrite .1. exafs studies of the geometry of coprecipitated and adsorbed arsenate." *Geochim. Cosmochim. Acta*, 57(10), 2251-2269.

Wei, D. W. (1995). "Particulate pyrite in aqueous solution: synthesis, ferrous bisulfide complexation, and semiconductor electrochemistry." The Pennsylvania State University, University Park, Ph.D. dissertation.

Wei, D. W. and K. OsseoAsare (1996). "Particulate pyrite formation by the Fe3+/HS-reaction in aqueous solutions: Effects of solution composition." *Colloids and Surfaces a-Physicochemical and Engineering Aspects* 118(1-2): 51-61.

Wilkie, J. A. and J. G. Hering (1996). "Adsorption of arsenic onto hydrous ferric oxide: Effects of adsorbate/adsorbent ratios and co-occurring solutes." *Colloids and Surfaces a-Physicochemical and Engineering Aspects* 107: 97-110.

Wilkin, R. T. and H. L. Barnes (1996). "Pyrite formation by reactions of iron monosulfides with dissolved inorganic and organic sulfur species." *Geochimica Et Cosmochimica Acta* 60(21): 4167-4179.

Wolthers, M., Butler, I. B., and Rickard, D. (2007). "Influence of arsenic on iron sulfide transformations." *Chem. Geol.*, 236(3-4), 217-227.

Wolthers, M., Butler, I. B., Rickard, D., and Mason, P. R. D. (2005). "Arsenic uptake by pyrite at ambient environmental conditions: A continuous-flow experiment."

Amer Chemical Soc, 60-76.

Wolthers, M., Charlet, L., and van der Weijden, C. H. (2003). "Arsenic sorption onto disordered mackinawite as a control on the mobility of arsenic in the ambient sulphidic environment." E D P Sciences, 1377-1380.

Yu, X. Y., Amrhein, C., Zhang, Y. Q., and Matsumoto, M. R. (2006). "Factors influencing arsenite removal by zero-valent iron." *J. Environ. Eng.-ASCE*, 132(11), 1459-1469.

Zouboulis, A. I., Kydros, K. A., and Matis, K. A. (1993). "Arsenic (III) and arsenic (V) removal from solutions by pyrite fines." *Sep. Sci. Technol.*, 28(15-16), 2449-2463.

Zouboulis, A. I., Kydros, K. A., and Matis, K. A. (1995). "Removal of hexavalent chromium anions from solutions by pyrite fines." *Water Res.*, 29(7), 1755-1760.

APPENDIX A

TABULATED DATA

1. Pyrite formation with time at room temperature

Time (day)	Pyrite concentration (M)
0.1	0
0.2	0
0.7	0
1	0
2	2.12E-03
4	6.71E-03
6	7.51E-03
8	7.52E-03

2. Pyrite formation with time at 60 ºC

Time (Hr.)	Pyrite concentration (M)
0.5	0.00E+00
1	4.49E-03
2	1.02E-02
3	1.32E-02
4.5	1.39E-02
11	1.46E-02
22	1.59E-02

3. As(III) concentration with time in presence of pyrite

Time (min.)	Arsenic concentration (μM)
0	1.28E+01
15	3.19E+00
30	1.36E+00
45	1.44E+00
60	1.45E+00
120	1.53E+00

4. As(V) concentration with time in presence of pyrite

Time (min.)	Arsenic concentration (μM)
0	6.53E+01
30	1.78E+01
60	1.26E+01
360	3.34E+00
720	2.52E+00
1440	2.40E-01

5. The concentration of arsenic in the liquid phase at several pH conditions

	pH 4	pH 7	pH 10
Time (min.)	As concentration (μM)	As concentration (μM)	As concentration (μM)
0	1.27E+01	1.25E+01	1.31E+01
15	7.86E+00	0.00E+00	6.95E+00
30	5.47E+00	0.00E+00	1.29E+00
45	3.28E+00	0.00E+00	0.00E+00
60	2.52E+00	0.00E+00	0.00E+00
90	2.08E+00	0.00E+00	0.00E+00
120	1.20E-01	0.00E+00	0.00E+00
180	1.29E+00	0.00E+00	0.00E+00
360	1.12E+00	0.00E+00	0.00E+00

6. Experimental data and model equations fit to solid and liquid phase concentration for As(III) and pyrite

	Experimental	Langmuir	Freundlich	BET
C (µmol/l)	Arsenic concentration (µmol/g)	Arsenic concentration (µmol/g)	Arsenic concentration (µmol/g)	Arsenic concentration (µmol/g)
1.88E-01	7.93E-02	1.18E-01	6.71E-01	1.69E-01
3.75E-01	1.59E-01	2.27E-01	7.89E-01	3.16E-01
5.40E-01	2.60E-01	3.17E-01	8.59E-01	4.31E-01
7.36E-01	3.31E-01	4.17E-01	9.24E-01	5.54E-01
1.49E+00	5.10E-01	7.46E-01	1.09E+00	9.17E-01
1.25E+00	7.56E-01	6.50E-01	1.05E+00	8.17E-01
1.72E+00	9.52E-01	8.31E-01	1.13E+00	1.00E+00
2.79E+00	1.89E+00	1.16E+00	1.26E+00	1.31E+00
5.06E+00	1.62E+00	1.63E+00	1.45E+00	1.68E+00
8.01E+00	2.00E+00	2.00E+00	1.62E+00	1.93E+00
1.08E+01	2.50E+00	2.21E+00	1.73E+00	2.06E+00
1.50E+01	1.64E+00	2.43E+00	1.87E+00	2.19E+00
1.75E+01	2.49E+00	2.52E+00	1.94E+00	2.25E+00
2.09E+01	2.50E+00	2.61E+00	2.02E+00	2.30E+00
2.44E+01	2.32E+00	2.69E+00	2.10E+00	2.35E+00
1.04E+02	3.28E+00	3.09E+00	2.95E+00	2.77E+00
1.31E+02	2.79E+00	3.11E+00	3.11E+00	2.87E+00
1.96E+02	3.97E+00	3.15E+00	3.42E+00	3.12E+00
3.97E+02	3.10E+00	3.19E+00	4.04E+00	4.19E+00

7. Experimental data and model equations fit to solid and liquid phase concentration for As(V) and pyrite

	Experimental	Langmuir	Freundlich	BET
C (μM)	Arsenic concentration (μmol/g)	Arsenic concentration (μmol/g)	Arsenic concentration (μmol/g)	Arsenic concentration (μmol/g)
1.96E-02	1.33E+01	1.23E+01	3.38E+01	1.14E+01
4.32E-02	2.67E+01	2.39E+01	4.02E+01	2.23E+01
6.59E-02	4.00E+01	3.29E+01	4.42E+01	3.09E+01
1.05E-01	4.66E+01	4.48E+01	4.90E+01	4.24E+01
1.35E-01	5.33E+01	5.16E+01	5.17E+01	4.91E+01
2.04E-01	5.99E+01	6.33E+01	5.67E+01	6.08E+01
3.44E-01	6.64E+01	7.72E+01	6.36E+01	7.50E+01
4.05E-01	7.30E+01	8.11E+01	6.60E+01	7.90E+01
3.72E-01	7.97E+01	7.92E+01	6.48E+01	7.70E+01
1.01E+00	8.57E+01	9.78E+01	8.07E+01	9.67E+01
1.79E+00	9.16E+01	1.04E+02	9.17E+01	1.04E+02
2.63E+00	1.04E+02	1.07E+02	9.99E+01	1.07E+02
3.64E+00	1.10E+02	1.09E+02	1.07E+02	1.09E+02
3.70E+00	1.16E+02	1.09E+02	1.08E+02	1.09E+02
8.01E+00	1.19E+02	1.11E+02	1.28E+02	1.13E+02
9.65E+00	1.24E+02	1.12E+02	1.33E+02	1.14E+02

8. Desorption kinetic experiment with As(III)-pyrite solid

Time (min.)	As concentration (μM)
0	2.22E+01
30	2.10E+01
120	2.11E+01
360	2.11E+01
720	2.13E+01
1440	2.16E+01
2880	2.17E+01
5760	2.17E+01
10080	2.17E+01

9. Desorption kinetic experiment with As(V)-pyrite solid

Time (min.)	As concentration (μM)
30	5.06E+01
120	4.97E+01
360	5.14E+01
720	5.32E+01
1440	5.32E+01
2880	5.32E+01
5760	5.32E+01
10080	5.32E+01

APPENDIX B

Table 5. Comparative evaluation of activated carbons and various low-cost adsorbents for arsenic removal

(cited from: Mohan and Pittman, 2007)

Table 5
Comparative evaluation of activated carbons and various low-cost adsorbents for arsenic removal

Adsorbent	Type of water	pH	Concentration/ range	Surface area ($m^2\ g^{-1}$)	Temperature (°C)	Model used to calculate adsorption capacity	Capacity (mg/g)		References
							As(III)	As(V)	
Iron oxide coated sand IOCS	Tap	–	100 μg/L	–	22 ± 2	Langmuir	0.136	–	[151]
Iron oxide coated sand	Drinking	7.6	100 μg/L	10.6	22 ± 2	Langmuir	0.041	0.043	[231]
Iron oxide coated sand, IOCS-2	Tap	7.6	100 μg/L	–	22 ± 2	Freundlich	–	0.008	[148]
Iron oxide coated sand (IOCS)	Natural (dose 0.5–1.20 g/100 mL); 5 h		325 μg/L	5.1	–	Langmuir	–	0.018	[152]
Ferrihydrite (FH)	Natural (dose 0.02–0.09 g/100 mL); 5 h		325 μg/L	141	–	Langmuir	–	0.25	
Iron oxide uncoated sand	Drinking (dose 20 g/L); 2 h	7.5	100–800 μg/L	–	27 ± 2	Langmuir	0.006	–	[129,130]
Iron oxide coated sand	Drinking (dose 20 g/L); 2 h	7.5	100–800 μg/L	–	27 ± 2	Langmuir	0.028	–	
$Al_2O_3/Fe(OH)_3$	Drinking (63.3 g in 50 ML; 100 g in 80 ML)	8.2–8.9	0.05 mg/L	–	–	Breakthrough capacity	–	0.09	[591]
La(III) impregnated silica gel	–	–	–	–	–	–	–	8.85	[529]
Y(III) impregnated alumina	–	–	–	–	–	–	–	14.45	[530]
Pure alumina							–	13.64	
La(III) impregnated alumina							–	12.88	
Basic yttrium carbonate	Drinking	9.8–10.5 for As(III) and 7.5–9.0 for As(V)	5.0–0.20 mmol/L for As(III) and 10–60 mmol/L for As(V)	28.6	20, 30, 40	Langmuir	305.8, 356.8, 428.1	352.6, 428.1, 483.4	[313]
Activated alumina	–	–	–	–	–	–	–	11–24	[10]
Waste Fe(III)/Cr(III)	Aqueous solution (dose 500 mg/50 ML; 5 h)	4.0	20–100 mg/L	–	32	Langmuir	–	11.02	[127]
Activated carbon (Draco)	–	–	–	–		–		3.75	[82]
Char carbon	Aqueous solution	2–3	157–737 for As(V) and 193–992 for As(III)	36.48	25	–	89.0	34.46	[76]
Activated carbon	Aqueous solution	6.4–7.5	157–737 for As(V) and 193–992 for As(III)	43.40	25	–	29.9	30.48	
Activated Bauxsol (AB)	Water (dose: 5 g/L)	4.5	7.03–220.9 Mm for As(V); 2.04–156.7 Mm for As(III)	130	23 ± 1	Langmuir	0.541	7.642	[115,116]
Bauxsol	Water (dose: 5 g/L)	4.5	0.80–32.00 Mm	–	23 ± 1	Langmuir	–	1.081	
Bauxsol-coated sand (BCS)	De-ionized/Tap	4.5	0.54–20.34 mg/L	7.56	Ambient	Langmuir	–	3.32	[117]

Table 5 (*Continued*)

AB-coated sand (ABCS)	De-ionized/Tap	7.1	0.54–20.34 mg/L	47.29	Ambient	Langmuir	–	1.64	
Seawater-neutralized red mud (Bauxsol)	De-ionized/Tap (dose: 5 g/L)	7.3	0.80–32.00 Mm	–	30	Langmuir	–	1.081	[592]
Red mud (RRM)	Water (dose: 20 g/L)	7.25 for As(III); 3.50 for As(V)	33.37–400.4 μmol/L	–	25	Langmuir	0.663	0.514	[112]
Red mud (ARM)	Aqueous solution (dose: 20 g/L)	7.25 for As(III); 3.50 for As(V)	33.37–400.4 μmol/L	–	25	Langmuir	0.884	0.941	
Bead cellulose loaded with iron oxyhydroxide (BCF)	Ground water	7.0	1–100 mmol/L	–	25 ± 0.5	Langmuir	99.6	33.2	[338]
Activated alumina	Drinking water	7.6	1 mg/L	370	25	Langmuir	0.180	–	[198]
Activated alumina (AA)	Drinking water	7.6	–	365	25	Langmuir	–		[209]
Iron oxide-impregnated activated alumina (IOIAA)	Drinking water	12	–	200	25	Langmuir	–		
MnO_2 (MO1)	Drinking water	7.9	<1 mg/L	17	25	Langmuir	–	0.172	[195]
Monoclinic hydrous zirconium oxide (Zr resin)	Drinking water	9–10 for As(III); 4–6 for As(V)	1×10^{-3} M	373	25	Langmuir	112.4	89.90	[315]
Zr resin	Drinking water	8.0 for As(III); 4.5 for As(V)	0–5 mmol/L	–	25	Langmuir	79.42	53.94	[314]
Iron(III)-loaded chelating resin	Aqueous solution	9.0 for As(III); 3.5 for As(V)	–	–	25	Langmuir	62.93	55.44	[305]
TiO_2	Drinking water	7.00	–	330	25	Langmuir	59.93	37.46	[217]
TiO_2 (Hombikat UV 1000)	Drinking water	4.0	<0.0015 M	334	22	Langmuir	22.70	22.47	[220]
TiO_2 (Degussa P25)	Drinking water	4.0	<0.0015 M	55	22	Langmuir	3.45	4.65	
HFO	Drinking water	9.0	0–60 mg/L	200	22	–	28.0	7.0	[251]
Goethite	Drinking water	9.0	0–60 mg/L	39	22	–	22.0	4.0	
$Fe_x(OH)_y$-Montm	Drinking water	9.0	0–60 mg/L	165	22	–	13.0	4.0	
Ti_xH_y-Montm	Drinking water	9.0	0–60 mg/L	229	22	–	13.0	3.0	
$FePO_4$ (amorphous)	Drinking water	7–9 for As(III); 6–6.7 for As(V)	0.5–100 mg/L	53.6	20	–	21	10	[276]
$FePO_4$ (crystalline)	Drinking water	7–9 for As(III); 6–6.7 for As(V)	0.5–100 mg/L	35.9	20	–	16	9	
MnO_2-loaded resin	Drinking water	7–8.5	3–150 mg/L	–	22	–	53	22	[531,532]
Iron(III) oxide-loaded melted slag (IOLMS)	Wastewaters	2.5	20–300 mg/L	196	20	–	2.9–30.1	18.8–78.5	[123]
TiO_2	Ground water	7.0	0.4–80 mg/L	251	25	Langmuir	32.4	41.0	[222,291,292]
Activated carbon (AC) produced from oat hulls	Drinking water	5.0	25–200 μg/L	522	24	Langmuir	–	3.08	[77]
Zirconium(IV)-loaded chelating resin (Zr-LDA)	Spring water	9.0 for As(III) and 4.0 for As(V)	–	7.3	25	Langmuir	49.15	88.73	[317]

Table 5 (*Continued*)

Adsorbent	Type of water	pH	Concentration/ range	Surface area ($m^2 g^{-1}$)	Temperature (°C)	Model used to calculate adsorption capacity	Capacity (mg/g)		References
							As(III)	As(V)	
Methylated biomass	Surface and ground water	6.5	0.5–2.5 Mm	6.5	30	–	–	3.75	[354]
Granular ferric hydroxide (GFH)	Surface and ground water	7.0	–	226–252	24	Freundlich	–	0.004	[234]
Zirconium(IV)-loaded phosphoric chelate adsorbent	NA	2.0	5 Mm	–	25	Column capacity	–	149.9	[319]
Oxisol	Wastewater (soil liner to be used in tailings dams at a sulfidic gold ore plant)	5.5	10–1000 mg/L	35.7	25	Langmuir	2.60	3.20	[269]
Gibbsite	Wastewater (soil liner to be used in tailings dams at a sulfidic gold ore plant)	5.5	10–1000 mg/L	13.5	25	Langmuir	3.30	4.60	
Goethite	Wastewater (soil liner to be used in tailings dams at a sulfidic gold ore plant)	5.5	10–1000 mg/L	12.7	25	Langmuir	7.50	12.5	
Kaolinite	Wastewater (soil liner to be used in tailings dams at a sulfidic gold ore plant)	5.5	10–1000 mg/L	8.5	25	Langmuir	–	<0.23	
Untreated GAC	Drinking water	4.7	0.10–30.0 mg/L	600–1000	25	Langmuir	–	0.038	[75]
GAC-Fe (0.05 M)	Drinking water	4.7	0.10–30.0 mg/L	600–1000	25	Langmuir	–	2.96	
GAC-Fe–O_2 (0.05 M)	Drinking water	4.7	0.10–30.0 mg/L	600–1000	25	Langmuir	–	1.92	
GAC-Fe–H_2O_2 (0.05 M)	Drinking water	4.7	0.10–30.0 mg/L	600–1000	25	Langmuir	–	3.94	
GAC-Fe–NaClO (0.05 M)	Drinking water	4.7	0.10–30.0 mg/L	600–1000	25	Langmuir	–	6.57	
Zirconium-loaded activated carbon (Zr-AC)	Drinking water	8–9	5–100 mg/L	–	25	Column capacity	–	2.8	[79]
Absorptionsmittel (AM3)	Drinking water	8–9	5–100 mg/L	–	25	Column capacity	–	2	
Granular ferric hydroxide (GIH)	Drinking water	8–9	5–100 mg/L	–	25	Column capacity	–	2.3	
Granular ferric hydroxide (GIH)							–	8.5	[233]
Ferrihydrite			0.267–26.7 mmol/L				266.5	111.02	[235]
Activated alumina grains	Drinking water	7.00 for As(III) and 5.2 for As(V)	0.79–4.90 mg/L for As(III) and 2.85–11.5 mg/L for As(V)	116–118	25	Langmuir	3.48	15.9	[203]
Activated carbon	Wastewater (copper electrorefineries)	–	300 mg/L	1000	25	–	–	2860	[67]
Activated carbon	–	–	–	–	–	–	–	25	[68]
Coconut husk carbon	Industrial wastewater	12.0	50–600 mg/L	206	30	Langmuir	146.30		[84]
Coconut shell carbon with 3% ash	Wastewater (processing of complex sulfide ore)	5.0	0–200 mg/L	1150–1250	25	Langmuir	–	2.4	[69]

Table 5 (*Continued*)

Peat-based extruded carbon with 5% ash		5.0	0–200 mg/L	975	25	Langmuir	–	4.9	
Coal-based carbon with 5–6% ash		5.0	0–200 mg/L	1050–1200	25	Langmuir	–	4.09	
Orange juice residue	Wastewater	7–11 for As(III) and 2–6 for As(V)	–	–	30	Langmuir	70.43	67.43	[339]
Phosphorylated crosslinked orange juice residue (POJR1)	Wastewater	2–6	–	–	30	Langmuir	–	39.71	[341]
Phosphorylated crosslinked orange juice residue (POJR2)	Wastewater	2–6	–	–	30	Langmuir	–	70.43	
Phosphorylated crosslinked orange waste (POW)	Wastewater	10 for As(III) and 3 for As(VI)	–	1.75	30	Langmuir	68.18	68.18	[340]
Alumina	Drinking water	6.5	0.133–1.33 mmol/L	768	25	Langmuir	–	8.99	[299]
Al_{10}SBA-15	Drinking water	6.5	0.133–1.33 mmol/L	343	25	Langmuir	–	20.98	
Fe_{10}SBA-15	Drinking water	6.5	0.133–1.33 mmol/L	–	25	Langmuir	–	12.74	
Ferrihydrite	–	7.0	0–150 mg/L	–	–	Langmuir	–	68.75	[237]
Goethite	–	7.0	0–38 mg/L	–	–	Langmuir	–	442.8	
Biomass	–	2.0	1–10 mg/L	–	28	Langmuir	13.17	–	[355]
Nanoscale zero-valent iron (NZVI)	Ground water	7.0	–	37.2	35	Langmuir	2.47	–	[294]
Cu-EDA-Si (calcined mesoporous silica)	Ground water	–	1–100 mg/L	–	–	–	–	140.0	[298]
Fe/NN-MCM-41	Drinking	6.0	~0–1500 mg/L	310	25	–	–	119.8	[301]
Co/NN-MCM-41	Drinking	6.0	~0–1500 mg/L	580	25	–	–	51.70	
Ni/NN-MCM-41	Drinking	6.0	~0–1500 mg/L	284	25	–	–	38.96	
Cu/NN-MCM-41	Drinking	6.0	~0–1500 mg/L	588	25	–	–	23.97	
Fe/NN-MCM-48	Drinking	6.0	~0–1500 mg/L	352	25	–	–	187.3	
Co/NN-MCM-48	Drinking	6.0	~0–1500 mg/L	634	25	–	–	74.92	
Ni/NN-MCM-48	Drinking	6.0	~0–1500 mg/L	305	25	–	–	64.43	
Cu/NN-MCM-48	Drinking	6.0	~0–1500 mg/L	635	25	–	–	37.46	
Alginate bead (doped and coated with iron)	Drinking	7.0	50 μg/L	–	25	Column capacity	–	0.014	[310]
Uncalcined LDHs	Wastewater (power-plant effluent streams)	4.2–5.4	20–200 mg/L	47	25	Langmuir	–	4.55	[273]
Calcined LDHs	Wastewater (power-plant effluent streams)	4.2–5.4	20–200 mg/L	198	25	Langmuir	–	5.61	
Chitosan	Wastewater	4.0	400 mg/L	–	25	–	–	58	[333]
Dry water hyacinth plant leaf							–	0.34	[359]
Akaganeite β-FeO(OH) nanocrystals	Water/wastewater	7.5	5–20 mg/L	330	25	Langmuir	–	141.3	[242]
Mixed rare earth oxide	Water/wastewater	6.5	50 mg/L	6.75	29	Langmuir	–	2.95	[261]
Fresh biomass	Ground water	6.0	50–2500 mg/L	–	30	Langmuir	128.1	–	[345]

Table 5 (*Continued*)

Adsorbent	Type of water	pH	Concentration/ range	Surface area ($m^2\ g^{-1}$)	Temperature (°C)	Model used to calculate adsorption capacity	Capacity (mg/g)		References
							As(III)	As(V)	
Immobilized biomass	Ground water	6.0	50–2500 mg/L	–	30	Langmuir	704.1	–	
Manganese ore	Ground water	6.3 for As(III) and 6.5 for As(V)	–	–	–	Langmuir	0.53	15.38	[135]
Polymetallic sea nodule	Ground water/tubewell water	6.0 for As(III); 2.0 for As(V)	0–0.7 mg/L for As(III); 0–1.0 mg/L for As(V)	–	–	Langmuir	0.69	2.85	[270]
Portland cement	Drinking water	4–5	0.2 mg/L	15.38	30	Langmuir		3.98	[262]
Iron oxide coated cement (IOCC)	Drinking water	~7	0.5–10.0 mg/L	–	35	Langmuir	–	6.43	[263]
Iron oxide coated cement (IOCC)	Drinking water	~7	0.7–13.5 mg/L	–	35	Langmuir	0.67	–	[264]
ZMA (Sonora)	Ground water	4.0	0.1–4 mg/L	279	22	Langmuir	0.0048	0.1	[180,181]
ZME (Oaxaca)	Ground water	4.0	0.1–4 mg/L	51	22	Langmuir	0.0028	0.025	
ZMS (San Luis Potosi)	Groundwater	4.0	0.1–4 mg/L	22	22	Langmuir	0.017	0.1	
ZMT (Puebla)	Ground water	4.0	0.1–4 mg/L	28	22	Langmuir	0.003	0.05	
ZH	Groundwater	4.0	0.1–4 mg/L	–	22	Langmuir	0.002	0.006	
Shirasu-zeolite (SZP_1)	Drinking water	3–10	1.3 Mm	15.6	24	Freundlich	–	65.93	[182]
Aluminum-loaded Shirasu-zeolite (Al-SZP_1')	Drinking water	3–10	1.3 Mm	–	24	Freundlich	–	10.49	
Sulfate-modified iron oxide-coated sand (SMIOCS)	Drinking water	4–10	0.5–3.5 mg/L	3.74	27	Langmuir	–	0.13 (pH 4), 0.12 (pH 7), 0.08 (pH 10)	[154]
Modified iron oxide-coated sand (SMIOCS)	Drinking water	7.2	0.5–3.5 mg/L	2.9–7.9	50	Langmuir	0.14	–	[153]
Tea fungal biomass	Ground water	7.20	1.3 for As(III) and 0.9 mg/L for As(V)	–	30	Freundlich	1.11	4.95	[349]
$FeCl_3$ treated tea fungal biomass	Ground water	7.20	1.3 for As(III) and 0.9 mg/L for As(V)	–	30	Freundlich	5.4	10.26	
Penicillium purpurogenum	–	5.0	10–750 mg/L	–	20	Langmuir	35.6	–	[348]
Human hairs	Drinking water	–	90–360 μg/L	–	22	Langmuir	–	0.012	[372]
Nanostructured akaganeite	–	7.5	5–20 mg/L	330	25	Langmuir	–	1.80	[240]
Activated carbon	–	–	–	–	–	–	–	20	[593]
Chitosan/chitin mixture	–	–	–	–	–	–	–	0.13 μequiv. As/g	[334]
Chrome sludge waste	–	–	–	–	–		–	21	[360]
Hematite	Water/wastewater	4.2	133.49 μmol/L	14.40	30	Langmuir	–	0.20	[134]
Feldspar	Water/wastewater	4.2	133.49 μmol/L	10.25	30	Langmuir	–	0.18	

Table 5 (*Continued*)

Aluminum-loaded coral limestones (Al-CL)	Drinking water	2–11	2.0–5.0 mg/L	–	24–25	Freundlich	–	0.15	[160]
Amine-modified coconut coir							–	6.44	[302]
Fe(III) alginate gel	–	4.0	0–10 mg/L	–	–	–	–	352	[307]
Poly(ethylene mercaptoacetimide) (PEM)	–	8.0 for As(III) and 2.0 for As(V)	–	–	24	Langmuir	31.56	112.7	[322]
Olivier soil	Soil	5–6	5–100 mg/L	–	25	Langmuir	–	0.42	[139]
Sharkey soil	Soil	5–6	5–100 mg/L	–	25	Langmuir	–	0.74	
Windsor soil	Soil	5–6	5–100 mg/L	–	25	Langmuir	–	0.55	
Mycan (*P. chrysogenum*)	Wastewater	3.0	1–300 mg/L	–	25	Langmuir	–	24.52	[353]
Mycan/HDTMA	Wastewater	3.0	1–300 mg/L	–	25	Langmuir	–	57.85	
Mycan/magnafloc	Wastewater	3.0	1–300 mg/L	–	25	Langmuir	–	56.08	
Mycan/DA	Wastewater	3.0	1–300 mg/L	–	25	Langmuir	–	33.31	
Cu(II)-Dow2N resin							–	44.00	[304]
Zr(IV)-loaded phosphoric acid chelating resin (RGP)	River/sea water	1.14	2.5 mmol/L	29.2	–	Column capacity	–	49.0	[320]
Molebdate-impregnated chitosan gel beads (MCCB)							–	200	[335]
Iron hydroxide coated alumina	Drinking water	6.62–6.74 for As(III) 7.15–7.2 for AS(V)	0.1–1.8 mmol/L	95.7	25	Langmuir	7.64	36.64	[215]
Ferric chloride impregnated silica gel	–	–	–	–	–	–	≤5.24	≤5.24	[277]
Titanium dioxide-loaded Amberlite XAD-7 resin	Drinking water/wastewater	1–5 for As(V) and 5–10 for As(III)	0–5 mmol/L	209	25	Langmuir	9.74	4.72	[323]
Iron(III)-loaded chelating resin							–	60.0	[311]
Water lettuce (*Pistia stratiotes* L.).	–	–	–	–	–	–	–	1.43	[346]
Penicillium purpurogenum	–	5.0	10–750 mg/L	–	20	Langmuir	35.6	–	[347]
GAC	Drinking/wastewater	7.0	1 mg/L	1.065	20–23	–	0.09	4.5	[86]
Fe(III) oxide-impregnated GAC	Drinking/wastewater	7.0	1 mg/L	840	20–23	–	4.50	4.5	
Iron(III) oxide with polyacrylamide	–	–	–	–	–	–	–	43.0	[533]
Humic acid	–	–	–	–	–	–	–	7.9	[534]
Activated alumina	Drinking water/ground water	7.0	50 mg/m^3	195	25	Langmuir	–	9.20	[535]

Table 5 (*Continued*)

Adsorbent	Type of water	pH	Concentration/ range	Surface area ($m^2\ g^{-1}$)	Temperature (°C)	Model used to calculate adsorption capacity	Capacity (mg/g)		References
							As(III)	As(V)	
Activated carbons from olive pulp and olive stone, carbon A	Drinking water	7.0	5–20 mg/L	1030	25	Langmuir	1.393	–	[95]
Activated carbons from olive pulp and olive stone, carbon B	Drinking water	7.0	5–20 mg/L	1850	25	Langmuir	0.855	–	
Activated carbons from olive pulp, olive stone, carbon C	Drinking water	7.0	5–20 mg/L	1610	25	Langmuir	0.738	–	
Activated carbons from olive pulp, olive stone, carbon D	Drinking water	7.0	5–20 mg/L	732	25	Langmuir	0.210	–	
Synthetic hydrotalcite	Ground water	7.0	400 mg/L	–	25	Langmuir	–	105	[275]
L. nigrescens	Copper smelting wastewaters	2.5	50–600 mg/L	–	25	Langmuir	–	45.2	[405,350]
Goethite	–	5.0	5–25	103	29	Langmuir	–	~5	[170]
cFeMn	Drinking water	3.0	100 μg/L to 100 mg/L	–	25	–	14.7	8.5	[594]
Drinking water treatment residuals (WTRs)	Drinking water	6.0–6.5	375–3000 mg/L	–	23	Freundlich	~15	~15	[133]
Pisolite	River water	6.5	50 mg/L	61.4	25	–	–	1.29	[136]
Activated pisolite	River water	6.5	50 mg/L	90.45	25	–	–	3.17	
Modified calcined bauxite	Ground water	~7.0	0.5–8.0 mg/L	–	25	Langmuir	–	1.57	[119]
Modified calcined bauxite	Ground water	6–8	0.5–8.0 mg/L	–	25	Freundlich	1.37	–	[122]
Coconut coir pith anion exchanger (CP-AE)	Ground water/industrial effluents	7.0	5.0–100 mg/L	175	20	Langmuir	–	13.57	[324]
		7.0	5.0–100 mg/L	175	30	Langmuir	–	12.51	
		7.0	5.0–100 mg/L	175	40	Langmuir	–	11.67	
		7.0	5.0–100 mg/L	175	50	Langmuir	–	10.42	
Hybrid (polymer/inorganic) fibrous sorbent (FIBAN-As)	Drinking water	7.7	–	–	20	Langmuir	75.67	81.66	[254]
Pine wood char	Drinking water	3.5	10–100 μg/L	2.73	25	Langmuir	0.0012	–	[103]
Oak wood char	Drinking water	3.5	10–100 μg/L	2.04	25	Langmuir	0.006	–	
Oak bark char	Drinking water	3.5	10–100 μg/L	25.4	25	Langmuir	0.0074	–	
Pine bark char	Drinking water	3.5	10–100 μg/L	1.88	25	Langmuir	12	–	

VITA

Jin Kun Song was born in Seoul, South Korea. He completed his Bachelor of Science degree from Soongsil University in Seoul, S. Korea and Master of Engineering degree from the University of Florida in 1999 and 2002, respectively. He completed his Ph.D. degree from Texas A&M University in 2008. His email address is jinkunbell@gmail.com and his permanent address is P.O Box 12129 College Station, TX 77842 U.S.A.